ENGINEERING VIRUS RESISTANT TRANSGENIC CASSAVA : THE DESIGN OF LONG HAIRPIN RNA CONSTRUCTS AGAINST SOUTH AFRICAN CASSAVA MOSAIC VIRUS

Johan Harmse

A research report, submitted to the School of Molecular and Cell Biology, Faculty of Science, University of the Witwatersrand, Johannesburg, in partial fulfillment of the requirements for the degree of Master of Science.

Johannesburg, 2007

Declaration

I declare that the work "**Engineering virus resistant transgenic cassava : The design of long hairpin RNA constructs against SACMV**" is my own original work, and that all my sources have been indicated by complete references. It has not been submitted before for any degree or examination at another university. This is being submitted in partial fulfillment of the degree "Master of Science" at the University of the Witwatersrand, Johannesburg, South Africa.

_____

Johan Harmse
7 September 2007

ABSTRACT

Cassava is currently the second most important source of carbohydrates on the African continent. In the last two decades, cassava crops have been severely affected by outbreaks of cassava mosaic disease (CMD). *South African cassava mosaic virus* (SACMV) has been associated with CMD outbreaks in the Mpumalanga province. Advances in post-transcriptional gene silencing (PTGS) technology have provided promising new strategies for the engineering of virus resistance in plants. Inverted repeat (IR) constructs are currently the most potent inducers of PTGS, however, these constructs are inherently unstable. The purpose of this study was to develop IR constructs with an improved stability for the efficient induction of PTGS in plants. Two mismatched inverted repeat constructs, one targeting the SACMV BC1 open reading frame, the other targeting the *Maize streak virus* (MSV) AC1 open reading frame, were successfully created. Sodium bisulfite was used to deaminate cytosine residues on the sense arm of the constructs. The resulting number of GT mismatches was seemingly sufficient to stabilize the linear conformation of the IR constructs, as they were efficiently propagated by *E.coli* DH5α, and subsequently behaved like linear DNA molecules. Furthermore, it was found that the number of mismatches on the BC1 construct (17.5%) was ideal, as the subsequent stability of the predicted RNA hairpin was not affected. Due to the higher number of mismatches on the AC1 construct (23.5%), it was found that the loop region of the RNA hairpin was marginally destabilized. Despite this, long stretches of stable dsRNA were still produced from the AC1 IR construct, and is likely to induce PTGS. Interestingly, it was observed that the mismatched IR constructs, although still replicated in *E.coli*, were marginally destabilized in *Agrobacterium*. Therefore, it was deduced that the stability of a mismatched IR construct may be influenced by the particular intracellular environment of an organism. Due to the recalcitrance of cassava to transformation, a model plant system, *Nicotiana benthamiana,* was used to screen constructs for toxicity, stability, and efficiency of PTGS induction. *Agrobacterium*-mediated transformation and regeneration of *N. benthamiana* was optimized, and 86% transformation efficiency was achieved when using leaf disk explants. It was found that the addition of an ethylene scrubber, potassium permanganate, substantially increased the rate of regeneration by reducing the frequency of hyperhydritic plants. Transgene

integration was confirmed by PCR amplification of the *hptII* gene in the T-DNA region. Transgene expression was confirmed by screening for GUS and GFP reporter genes. No toxic responses to the transgene have been observed thus far. Studies are currently underway to confirm the stability of the mismatched IR constructs in *N. benthamiana.* PAGE Northern blotting is being done, as the detection of siRNAs derived from the transgene will confirm that constructs are functional. In addition, infectivity assays are underway to determine the efficacy of BC1 knockdown by a stably integrated construct. Due to the enhanced stability of mismatched IR constructs, they may be an appealing alternative to currently available intron-spliced, or exact matched hairpin systems.

Acknowledgements

Above all, I would like to thank my parents for their endless encouragement, friendship and support. Their presence and involvement in my life has been a privilege, one that I am deeply grateful for.

I am equally grateful to my supervisor, Professor Christine Rey, for her constant support and enthusiasm. Her dedication to my development as a researcher has truly made this a rewarding experience.

I am deeply indebted to Dr Marco Weinberg from the Department of Molecular Medicine and Haematology at the University of the Witwatersrand. His mentoring has been invaluable to my research, and without his brilliant concepts this project would not have been possible. In addition, I owe thanks to Professor Patrick Arbuthnot and his team in the HBV laboratory. Their hospitality and willingness to help was greatly appreciated. In particular, I would like to thank Sam, Justin, and Liam for offering their help and advice.

The ladies from the cassava biotechnology team were a constant source of encouragement, advice, and entertainment. I would like to thank Chezlyn, Claudia, Erica, Farhahna, Imah, and Sarah, as they have all kindly offered advice or assistance at various times during this project.

Thank you to Dr Dionne Sheppard and Professor Ed Rybicki from the University of Cape Town for kindly entrusting me with one of their *Maize streak virus* clones.

I would like to acknowledge the University of the Witwatersrand and the National Research Foundation for financial support, and a travel grant which enabled me to attend The Keystone Symposium on RNAi and target validation in Colorado.

Finally, I express gratitude to all of my friends and siblings who have been there for me.

LIST OF FIGURES

List of abbreviations

ACMV	*African cassava mosaic virus*
BYDV	*Barley yellow dwarf virus*
CHS	Chalcone synthase
CIAT	Centro International de Agricultura Tropica
CMD	Cassava Mosaic Disease
CMG	Cassava Mosaic Geminiviruses
EACMCV	*East African cassava mosaic Cameroon virus*
EACMMV	*East African cassava mosaic Malawi virus*
EACMV	*East African cassava mosaic virus*
EACMZV	*East African cassava mosaic Zanzibar virus*
ICMV	*Indian cassava mosaic virus*
IITA	International Institute for Tropical Agriculture
IR	Inverted repeat
LB	Luria Bertani broth
LBA	Luria Bertani agar
lhRNA	Long Hairpin RNA
MSV	*Maize streak virus*
PTGS	Post-Transcriptional Gene Silencing
PVX	*Potato virus-X*
PVY	*potato virus-Y*
RISC	RNA-induced silencing complex
RNAi	RNA interference
RT	Reverse transcription
RYMV	*Rice yellow mottle virus*
SACMV	*South African cassava mosaic virus*
shRNA	Short Hairpin RNA
siRNA	small interfering RNA
SMLCV	*Squash mild leaf curl virus*
sRNA	small RNA

ssDNA	Single-stranded DNA
ssRNA	Single-stranded RNA
TBSV	*tomato bushy stunt virus*
TEV	*tobacco etch virus*
U	Units
VIGS	Virus-Induced Gene Silencing
WTG	Whitefly-transmitted geminiviruses

CHAPTER 1

General Introduction

1.1 Cassava: The crop

Cassava *(Manihot esculenta)* originated in South America and was domesticated less than 10 000 years ago (Allem, 2002). European migrants in South America realised the potential of the perennial shrub as a food crop, and sailors subsequently exported the crop to Africa. The crop was later also introduced into Asia by traders, and it has since been an invaluable resource in large parts of the world. In fact, cassava has been dubbed the most important crop in regions at latitudes between 30^{o}N and 30^{o}S, ranging from sea level to 1800m above sea level. Internationally, Cassava is the 4th most important basic food source, after rice, wheat and maize (Scott *et al.*, 2000). Approximately 700 million people across the world rely on cassava as a staple food.

Despite the high nutritive value of cassava foliage, the crop is mainly utilized for its roots (Fig 1.1). Eighty percent of the fresh weight of cassava roots is starch (El-Sharkawy, 2004) Cassava is a resilient crop that grows well under marginal conditions where few other crops can survive.

Figure 1.1 Freshly harvested cassava roots

There is a large variety of cassava cultivars, many of which are drought tolerant, resistant to various pests, and can tolerate poor or acidic soils. As a result, cassava requires virtually no purchased inputs, and is mainly grown by resource poor small farmers. Unlike seasonal crops, cassava roots can be harvested at any time, which is an added benefit in rural, resource-poor communities. Vegetative propagation is conventionally used to propagate cassava. Woody stem cuttings are commonly used as planting material. More than 13 million hectares of cassava crops are cultivated

across the world at any given time (El-Sharkawy, 2004). Seventy percent of cassava production is currently used for human consumption. The remaining 30% is used to produce starch for industrial applications such as the food-, pharmaceutical-, chemical-, textile- and paper industries.

Researchers at CIAT (Centro International de Agricultura Tropical) and IITA (International Institute for Tropical Agriculture) have been developing improved cassava varieties with the aim of stimulating sustainable development in poor countries (Taylor *et al*., 2004). To date, many improved varieties have been produced by using conventional breeding programmes. Traditional breeding is often problematic with cassava, and this approach is unlikely to provide solutions to crop improvement on its own (Taylor *et al*., 2004). Transgenic technologies are being applied to cassava to introduce desired traits into farmer preferred cultivars or elite breeding lines.

1.2 Cassava Mosaic Disease

Even though cassava is a particularly robust plant, most cultivars are susceptible to various whitefly-transmitted geminiviruses (WTG) (Legg and Fauquet, 2004). These viruses are the causative agents of cassava mosaic disease (CMD). CMD is the most economically important viral disease of cassava (Berrie *et al.*, 1998). The first documented case of CMD was recorded in 1894 in Tanzania (Legg and Fauquet, 2004). By the end of the 1930's, CMD had spread to virtually all cassava growing environments in Africa. The occurrence of CMD has been reported in eastern parts of South Africa as well as Swaziland (Trench and Martin, 1985).

In the 1990's, a severe CMD outbreak occurred in Uganda. A large part of the country was affected, and local cassava production was virtually eliminated. The Ugandan economy was harshly affected, as crop losses resulted in damages in excess of 60 million USD per annum. The CMD epidemic peaked between 1992 and 1997, by which time farmers had abandoned the crop in large parts of the country. The resulting food shortages lead to some famine related deaths. In the same period, the epidemic had spread to the neighbouring countries of Kenya, Sudan, Tanzania and the

Democratic Republic of Congo (DRC), with similar effects on cassava cultivation. During those severe CMD outbreaks, crop losses between 20% and 95% were reported (Legg and Fauquet, 2004).

Geminiviruses

The causative agents of CMD are WTGs, a group of viruses belonging to the family *Geminiviridae* (Fondong *et al*., 2000). Geminiviruses have ssDNA genomes, typically encapsidated in twin icosahedral particles (Fig 1.2), 20-30nm in size (Harrison, 1985). Members of the family *Geminiviridae* are classified into 4 genera; *Begomovirus*, *Mastrevirus*, *Curtovirus*, and *Topocuvirus* (Fauquet, 2003). Replication of Geminiviruses occurs in the nuclei of infected plant cells (Legg and Fauquet, 2004). Firstly, they form dsDNA intermediates that are established as multiple mini-chromosomes (Pilartz *et al*., 2003). Replication then takes place through the rolling circle replication mechanism, and it has been speculated that a host recombination-dependent mechanism is also involved (Hanley-Bowdoin *et al.,* 1999; Jeske *et al.* 2001). Geminiviruses lack genes for DNA polymerases, and rely on host enzymes for replication (Hanley-Bowdoin *et al.,* 1999)

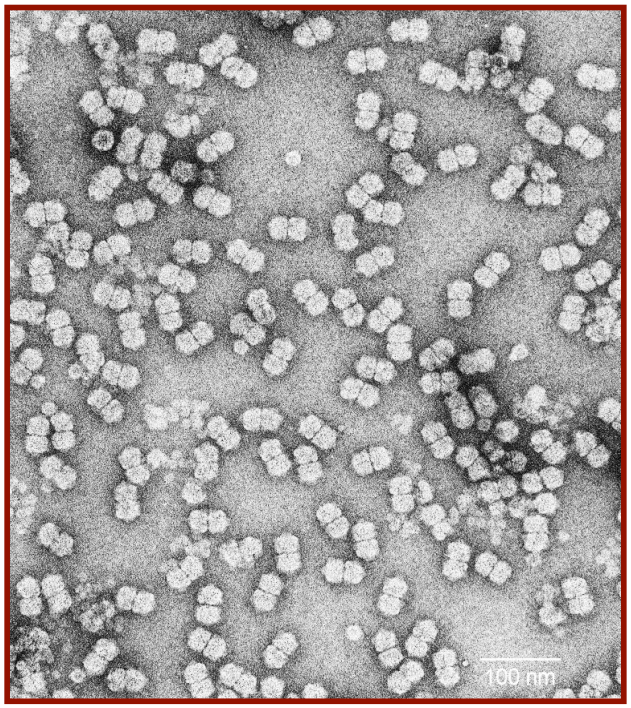

Figure 1.2 Bipartite geminate particles as seen under a transmission electron microscope

Begomoviruses

The word "Begomovirus" was derived from a *Geminivirus* called b*e*an g*o*lden m*o*saic *virus*. There are currently 8 species of cassava-infecting begomoviruses (Fauquet and Stanley, 2005)

i. ***African cassava mosaic virus* (ACMV or Cassava latent virus): ACMV currently has 13 different strains.**
ii. ***East African cassava mosaic Cameroon virus* (EACMCV): EACMCV currently has 3 known strains.**
iii. ***East African cassava mosaic Malawi virus* (EACMMV): EACMMV currently has 2 known strains.**
iv. ***East African cassava mosaic virus* (EACMV): EACMV currently has 9 known strains.**
v. ***East African cassava mosaic Zanzibar virus* (EACMZV): EACMZV currently has 3 known strains.**
vi. ***Indian cassava mosaic virus* (ICMV): ICMV currently has 7 known strains.**
vii. ***South African cassava mosaic virus* (SACMV): SACMV currently has 3 known strains, including one from Zimbabwe.**
viii. ***Squash mild leaf curl virus* (SMLCV): SMLCV currently has 4 known strains, 3 of which are known to infect cassava. These 3 strains are known as Sri-Lankan cassava mosaic virus.**

In 1998, Berrie *et al.* identified and characterized a novel cassava-infecting begomovirus which they called SACMV. Like other Begomoviruses, SACMV was found to have a bipartite ssDNA genome, consisting of a DNA-A component (2800nt), and a DNA-B component (2760nt) (Fig 1.3). The DNA-A component has 6 open reading frames (ORFs), and the DNA-B component has 2 ORFs (Berrie *et al.,* 2001). As with other begomoviruses, the 2 genome components have an intergenic region with ~95% sequence identity. Within the intergenic region lies a common region (CR) of 176bp, which contains the origin of replication (*ori*). The *ori* is a

highly conserved sequence (TAATATT/AC), situated in the loop section of a self-complementary ssDNA hairpin-loop structure, which is conserved amongst all begomoviruses (Hanley-Bowdoin *et al.,* 1999). Short reiterated motifs known as iterons can be found directly upstream of the hairpin-loop structure. Associated DNA-A and DNA-B components usually contain matching iterons. Both DNA-A and DNA-B are transcribed from a bidirectional promoter situated between nucleotides 2759 and 282.

Through phylogenetic analysis, SACMV DNA-A has been shown to have a close relationship with geminiviruses from the Old World (Berrie *et al.* 2001). The SACMV DNA-A component is reportedly closely related to EACMV type II isolates from Malawi, whereas the DNA-B component was found to be closely related to EACMV isolates from Uganda (Berrie *et al.* 2001). It has been hypothesized that recombination may play an important role in the evolution of begomoviruses. In addition, it has been reported that recombination amongst begomoviruses occurs frequently. The SACMV AC4 ORF appears to be a hotspot for recombination, and it has been difficult to determine its exact evolutionary origin. In contrast, no obvious recombination events have been detected in SACMV DNA-B.

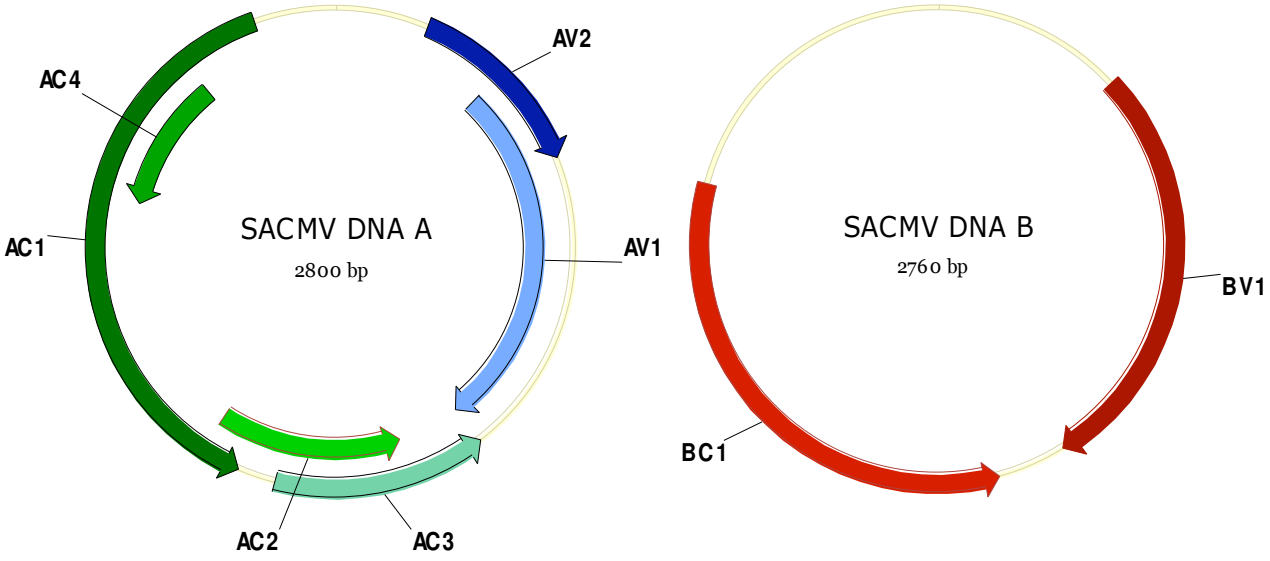

Figure 1.3 The SACMV DNA-A and DNA-B components.

DNA-A (Stanley *et al*., 1986; Hanley-Bowdoin *et al.,* 1999)

AV1: Virion sense (258 amino acids). Coat protein.

AV2: Virion sense (116aa). Proteins associated with movement.

AC1: Complementary sense (354aa). Replication-associated protein (Rep).

AC2: Complementary sense (135aa). Transcriptional activator protein (TrAP).

AC3: Complementary sense (134aa). Replication enhancement protein (REn).

AC4: Complementary sense, (98aa). Function remains unclear. Has activity as a suppressor of host RNA silencing mechanisms.

DNA-B (Stanley *et al*., 1986; Hanley-Bowdoin *et al.,* 1999)

BV1: Virion sense (258aa). Nuclear transport protein (NSP).

BC1: Complementary sense (307aa). Long distance movement protein (MP).

This genome organisation, shown above, is common amongst all begomoviruses. There are no genes coding for polymerase enzymes, and begomoviruses rely on host machinery for replication. These viruses are, however, actively involved in their own gene regulation. The AC1 gene product, Rep, initiates viral DNA replication by binding to the iterons in the IR (Fontes *et al.,* 1994). It then introduces a nick in the conserved TAATATT/AC (*ori*) sequence as indicated, allowing for rolling circle replication to begin. Reportedly, Rep also binds to the plant homologue of retinoblastoma protein (Rb), which affects the regulation of the cell cycle (Kong *et al.*, 2000). By binding to Rb, Rep is able to alter the environment of terminally differentiated cells to provide host factors that are required to support viral DNA replication. Rep is presumably a transcriptional repressor of its own promoter, thereby facilitating late gene expression and progression of the infection-cycle (Frey *et al*., 2001). The AC2 gene product, TrAP, is responsible for the transactivation of virion-sense gene expression (Sunter and Bisaro, 1992). It induces the expression of AV1, AV2, and BV1. AC2 is the only gene that has its own mono-directional promoter. TrAP has also been implicated in the suppression of plant RNA silencing mechanisms. The AC3 gene product, REn, is a replication enhancement protein that allegedly boosts viral DNA replication by several-fold, but is not essential for viral replication (Sunter *et al,* 1990). The AV2 gene product on the other hand, is supposedly required for both virus accumulation and symptom development (Padidam

et al., 1996). The AV4 gene product has been implicated in host range determination, symptom severity, RNA silencing suppression, and viral movement. However, its exact function still remains unclear (Seal *et al.,* 2006). The BV1 gene product, NSP, functions as a shuttle protein that transports viral DNA from the nucleus to the cytoplasm. NSP has been found to bind ssDNA, and move the DNA out of the nucleus. During the early infection cycle, NSP is mainly localized in the nucleus. The BC1 gene product, MP, is reportedly involved with the long distance movement of viral DNA. Thus, MP facilitates the spread of viral DNA from cell to cell (Sanderfoot and Lazarowitz, 1995). MP forms endoplasmic reticulum-derived tubules which extend through the cell wall into adjacent cells. When NSP and MP are co-expressed late in the infection cycle, NSP (with bound viral DNA) is relocated to the periphery of the cell, where MP facilitates its movement across the cell wall.

Studies have been done to elucidate the dynamics of the begomoviral bidirectional promoter (Frey *et al.,* 2001). Not surprisingly, it was observed that Rep down-regulates complementary-sense transcription, whilst TrAP concurrently up-regulates virion-sense transcription. Results reportedly indicated that complementary-sense expression was always lower than virion-sense expression, despite the AC promoter being stronger than the AV promoter. In one study, Rep apparently caused a 35-fold reduction in complementary-sense gene expression on DNA-A, and a 2-5 fold reduction on DNA-B, whilst TrAP caused an 8-15 fold increase in virion-sense gene expression on both DNA components. This is in agreement with a model of early/late gene regulation. Rep is required early in the infection cycle for replication, whilst TrAP is required late in the infection cycle to produce the coat protein and movement proteins for encapsulation and spread (Frey *et al.,* 2001).

1.3 Whitefly vectors

There are two ways by which cassava-infecting begomoviruses are transmitted in the field. In an agricultural environment, CMGs are often transmitted through the vegetative propagation of cassava with infected stem cuttings (Legg *et al,* 2004). In nature however, these viruses are transmitted by the whitefly vector *Bemasia tabaci*. Interactions between the virus and the vector are still being studied, but the virus coat

protein structure apparently determines vector specificity (Briddon *et al.,* 1990). In one study, it was found that different African cassava mosaic geminiviruses (CMG) were transmitted with similar efficiencies by African biotypes of *Bemasia tabaci*, even if they were from different geographical locations. However, when Asian biotypes of *Bemasia tabaci* were used with African CMGs, and vice versa, transmission efficiencies were found to be comparatively low (Maruthi *et al.,* 2002). This would suggest that the CMGs and their whitefly vectors co-evolve in their particular environment.

When attempting to infect cassava with CMGs, whitefly transmission experiments are often restricted by the feeding preferences of the vector (Berrie *et al.* 2001). This is further complicated by biotype incompatibilities between the vector and the test plants. Thus far, efforts to transmit begomoviruses to cassava by mechanical inoculation have also been unsuccessful. A method was subsequently developed where infections can be induced by using *Agrobacterium.* Agro-inoculation requires recombinant T-DNA plasmids that carry infectious viral clones in *Agrobacterium* (Ratcliff *et al.,* 2001). Alternatively, the viral DNA can be delivered into plant tissues by particle bombardment.

1.4 RNA interference (RNAi)

The discovery of RNAi

Post-transcriptional gene silencing, termed co-suppression at the time, was first discovered in studies with petunia flowers. Chalcone synthase (CHS) is a key enzyme in the synthesis of flavonoids, and Napoli *et al.* (1990) attempted to intensify the color of petunia flowers by over-expressing the CHS enzyme. Contrary to what was expected, transgenic plants seemed to be loss-of-function mutants with pure white flowers. They found that the developmental timing of mRNA expression from the endogenous CHS gene, as well as the CHS transgene were normal. However in transgenic plants, the endogenous mRNA levels were reduced by over 50-fold compared to wild type plants (Napoli *et al*., 1990). It was concluded that the transgene was being suppressed, and that the homologous gene was being co-suppressed by an unknown mechanism. Despite the obscure and uncharacterized pathways, co-

suppression was soon being used in plant laboratories in diverse disciplines. Mostly, it was being used for the silencing of endogenous plant genes as a functional genomics tool (Chuang and Meyerowitz, 2000).

Shortly after, the phenomenon of pathogen-derived resistance was discovered. It was observed that transgenic plants had sequence-specific virus resistance when the transgene had homology to a viral sequence. In one example, tobacco was transformed to contain both full-length copies and truncated versions of the *tobacco etch virus* (TEV) coat protein (Lindbo *et al*., 1993). After infection with TEV, transgenic plants recovered completely within 3-5 weeks. Reportedly, the recovered tissue could not be re-infected with TEV, but was still susceptible to related viruses like *potato virus Y* (PVY). This showed that the resistance was virus specific. Subsequently, PDR and co-suppression were widely used in plant studies and became a vital tool in plant molecular biology and biotechnology. However, no significant insights were gained into the mechanisms or pathways of RNAi for several years.

The role of double stranded RNA

Following the first observation of RNAi in plants, studies were done on numerous other organisms such as *Caenorhabditis elegans*, *Drosophila melanogaster* and even mammalian cells to see if a similar effect could be achieved. A pivotal breakthrough in the understanding of RNA-mediated gene silencing was made during studies by Fire *et al*. (1998) on the nematode *C. elegans*. It was previously observed that co-suppression occurred in *C. elegans* when an anti-sense RNA, complementary to an endogenous mRNA, was injected into the body cavity of a nematode (Fire *et al.*, 1991). The initial theory was that hybridization of the anti-sense RNA to the mRNA blocked the translation of that gene. This theory was disproved when efficient target gene knockdown was achieved, despite injecting a minute amount of anti-sense RNA (such that the target mRNA transcript would be in excess). A crucial observation was that dsRNA, when injected into the nematode, was a more potent inducer of gene silencing than either the sense or anti-sense strands individually (Fire, *et al.* 1998). Furthermore, only a few molecules of dsRNA per cell were sufficient for the induction of specific and potent interference. This was the first indication that the mechanism of RNAi requires a catalytic or amplification component, and is not

dependent on stochiometry.

Initially in plant studies, silencing of target sequences was mostly achieved by using anti-sense or sense constructs individually, or by overexpression of the target gene. Whilst these approaches can lead to the formation of specific dsRNA, they are not very efficient or predictable. Chuang and Meyerowitz (2000) then described, for the first time, constructs capable of direct dsRNA formation in plants. In comparison to individual sense or anti-sense transgenes, it was reported that dsRNA expressing constructs were generally more efficient and reliable inducers of gene silencing (Chuang and Meyerowitz, 2000).

The mechanism of RNAi

As mentioned before, the initial mechanism of RNAi was thought to be the hybridization of a full-length anti-sense RNA to its target mRNA. It was unclear however, whether the silencing effect was caused at a transcriptional or translational level. To investigate this, attempts were made to isolate full length anti-sense RNAs from transgenic plants exhibiting RNAi, but were unsuccessful (Hamilton and Baulcombe, 1999). Instead, when probing for low molecular weight nucleic acids, a species of small anti-sense RNAs (+/- 25nt) corresponding to the target gene was found. These sRNAs were large enough to convey sequence specificity, but small enough to pass through the plasmodesmata.

Subsequently, Hammond *et al*. (2000) were able to induce sequence specific degradation mRNAs *in vitro,* in *Drosophila* cell extracts. A multi-subunit enzyme complex was partially purified from cell extract fractions showing RNAi activity. The enzyme complex had RNA-directed nuclease activity, and it always co-fractionated with a discrete small RNA (sRNA) species consisting of approximately 25nt (Hammond *et al*., 2000). The enzyme complex was termed the RNA-induced silencing complex (RISC). It was hypothesized that the high sequence specificity of RISC was due to its association with small RNA species that serve as a guide to target mRNAs.

The isolation and the characterization of an RNase III type nuclease that specifically

cleaves dsRNAs into 21-26nt RNAs followed (Bernstein *et al.*, 2001). This enzyme is evolutionarily conserved in nematodes, flies, plants, fungi and mammals, and was subsequently called DICER. By identifying conserved motifs amongst the Dicer homologues, it was found that they all contained a PAZ domain (defined based on its conservation with the Piwi/ARGONAUTE/Zwille family)(Bernstein *et al.*, 2001).

The interactions between long dsRNA molecules, DICER, and RISC were studied further. Interestingly, the sense and the anti-sense strands of long dsRNA molecules are processed into 21-23nt sRNAs at an equal efficiency, suggesting a symmetrical processing of the dsRNA (Zamore *et al*., 2000). The cleavage of dsRNA into 21-23nt sRNAs is six times more efficient when ATP is present. This is due to an ATP-dependent RNA helicase. Furthermore, target mRNA is cleaved at 21-23bp intervals only at regions corresponding to the initial dsRNA.

RNAi is therefore a two-step process, whereby dsRNA molecules are first cleaved by DICER into 21-26nt dsRNAs, of which one strand is incorporated into the multi-subunit RISC. RISC is then guided to a target mRNA in a sequence specific manner by small antisense RNAs (later named small interfering RNAs - siRNA), followed by degradation of the transcript (Zamore *et al*., 2000; Bernstein *et al.*, 2001).

RNAi as an antiviral response in plants

It was suspected that PTGS is a natural plant mechanism in response to viral infection (Brigneti *et al.* 1998). This was confirmed in later studies where tobacco plants recover from nepoviral infection and were then immune to re-infection by the same virus (Ratcliff *et al.* 1997,1999). However, these plants were still susceptible to unrelated viruses or different strains of the same species. It was found that RNA is the target of the recovery system, as the sequence specific suppression of the nepovirus was characteristic of the recovery phenotype. It was noticed, for the first time, that this mode of recovery was very similar to transgene-mediated gene silencing.

Virus-encoded silencing suppressors were discovered shortly after the plant anti-viral silencing mechanism was reported. Mixed viral infections are quite infrequent in animal hosts, but are often encountered in higher plants. Such infections are usually

characterized by the accumulation of one of the two viruses, and a dramatic increase in symptom severity. When studying potato virus X (PVX)/potyviral synergism, it was reported that the increase in symptoms and in accumulation of a heterologous virus, such as *cucumber mosaic virus* (CMV) or *tobacco mosaic virus* (TMV), was enhanced by the PVX helper component proteinase (HC-Pro) (Pruss *et al.* 1997). It was proposed that HC-Pro contributed to the synergism by suppressing the endogenous PTGS response. In addition to HC-Pro, a viral protein from cucumber mosaic virus, 2b, was identified as a possible inhibitor of PTGS mechanisms (Brigneti *et al.* 1998). When expressing the HC-Pro and 2b proteins in plant tissues, they both resulted in the suppression of PTGS mechanisms in the host. However, it seemed like different pathways were targeted by the two proteins. HC-Pro suppressed the maintenance of PTGS in tissues where it had already been established, whereas 2b suppressed the initiation of PTGS. Subsequently, three additional suppressors of PTGS were identified; AC2, an expression transactivator protein from *African cassava mosaic virus* (ACMV), P1, a long distance movement protein from *rice yellow mottle virus* (RYMV), and 19K, a host-specific spread and symptom determinant from *tomato bushy stunt virus* (TBSV) (Voinnet *et al.*, 1999). The spatial pattern and degree of suppression varied significantly between al the RNAi suppressors. This would suggest that they have distinct modes of action against specific targets in the host silencing machinery. This was a useful feature, as it was used in future studies to elucidate the RNAi mechanisms.

The amplification and systemic spread of an RNAi signal

In several early studies of PTGS in plants, it was noted that there was an apparent spreading of gene-silencing from infected or infiltrated tissues, to distant tissues (Hamilton and Baulcombe, 1999). This was later confirmed in a study whereby transient infiltration was used to deliver silencer DNA to localized areas of plants (Voinnet *et al.*, 1998). This resulted in sequence specific silencing of the target gene throughout the plant. Antiviral silencing signals apparently spread through the plant by cell-to cell movement, thereby advancing several centimetres ahead of the viral infection front (Voinnet *et al.*, 2000). This leads to sequence specific virus resistance in uninfected tissues, thereby delaying the spread of a viral infection through a host plant. Movement of the silencing signal is reportedly uncoupled from viral movement,

and numerous studies were undertaken to determine to underlying molecular mechanisms involved.

RNAi-deficient *Arabidopsis* mutants were analysed to identify and characterize genes involved in the RNAi mechanism. One such locus, *sde*-1 (silencing defective-1), was shown to encode an RNA-dependent RNA Polymerase (RdRP)-related protein (Dalmay *et al.*, 2000). The protein, SDE-1, shares homology with the QDE-1 (quelling-deficient-1) protein that was previously characterized in quelling-deficient mutants of *N. crassa* , as well as EGO-1 from *C. elegans* (Cogoni and Macino, 1999; Dalmay *et al.*, 2000; Fagard *et al.*, 2000; Mourrain *et al.*, 2000) . An additional *Arabidopsis* protein, AGO-1, is a homolog of QDE-2 from *N. crassa* and RDE-1 from *C. elegans* (Fagard *et al.*, 2000). The similarity between AGO1, QDE-2 and RDE-1 substantiate the theory that PTGS, quelling and RNAi are mechanistically linked. Apparently, mutations at the *Argonaute1 (AGO1)* locus leads to impaired PTGS in *Arabidopsis* (Fagard *et al.*, 2000).

Interestingly, *Dalmay et al.* (1998) found that SDE-1 is absolutely required for silencing of transgenes in *Arabidopsis*, but not for virus induced gene silencing (VIGS). From this finding it was deduced that SDE-1 is an RdRP required for the production of dsRNA from transgenes. SDE-1 therefore does not affect PTGS induced by VIGS, as the VIGS vector does not rely on endogenous RdRPs for dsRNA production (Dalmay *et al.*, 2000). In related studies, it was later discovered that certain PTGS suppressor proteins prevented PTGS initiation at sites of infiltration, whereas others inhibited the systemic spread of PTGS (Voinnet *et al*, 2000). Based on these combined findings, it was proposed that an SDE-1 dependent and an SDE-1 independent branch of the PTGS pathway exists. Both pathways are dependent on the synthesis of dsRNA, and they converge at, or before the production of siRNAs (Dalmay *et al.*, 2000; Voinnet *et al*, 2000).

Subsequently, a 25nt species of siRNA has been implicated in the systemic signaling of RNAi (Hamilton *et al.*, 2002). These siRNAs appear to spread systemically through plants by cell to cell movement, and are supposedly required for the primed synthesis of dsRNA by RdRP. This then induces PTGS in distant cells where the

signal was initially absent.

The molecular characterization of RISC

RISC contains two key components; a small RNA, and an Argonaute (Ago) protein (Liu *et al*., 2004). Argonaute proteins contain PAZ and PIWI domains and are often present as multi-protein families (Cerutti *et al.*, 2000; Song *et al.*, 2004). Through various structural and biochemical analysis, it has been reported that Argonaute is the RISC component that interacts directly with small RNAs. Evidence suggests that the PAZ domain binds specifically to the single stranded 3` ends of siRNAs. Argonaute was found to contain a distinct "claw-shaped" groove with significant electrostatic potential between the PAZ and N-terminal domains (Cerutti *et al.*, 2000; Liu *et al*., 2004). The positive charges along the lining of the inner groove allow it to interact with the negatively charged phosphate backbone and the 2' hydroxyl moieties of RNA. It was also observed that the PIWI domain in Argonaute is an RNaseH domain, and is therefore responsible for the SLICER activity of RISC. The SLICER component of RISC is associated with the sequence specific cleavage of dsRNAs at discrete positions (Liu *et al*., 2004; Song *et al.*, 2004).

RNA silencing is therefore a highly complex mechanism with numerous potential applications for molecular biology. Several RNAi pathways, such as transcriptional gene silencing and endogenous gene regulation by miRNAs have not been discussed in this review, as it is not relevant to the subject matter. A recent informative review by Broderson and Voinett (2006) is recommended for additional information.

1.5 Genetic Engineering approaches

It is difficult to produce virus resistant cassava by conventional breeding methods (Zhang *et al*, 2005). This is due to the high heterozygosity and strong inbreeding depression of many elite varieties. (Taylor *et al.*, 2004). Cassava is mainly vegetatively propagated, and viral resistance traits need to be maintained over many successive vegetative cycles. Transgene-mediated approaches have been used to improve many different crop varieties in the last decade. Such approaches allow for the introduction of new resistance genes that do not naturally exist within the cassava

germpool. Seeing as RNA silencing signals appear to be systemically transmitted in plants, it is likely that suitably engineered plants could cease a viral infection, or at least delay the spread of the infection to new tissues or whitefly vectors (Chellapan *et al*., 2004).

In earlier plant studies, RNA silencing was induced with transgene constructs containing either sense, or antisense sequences from a targeted gene (Tijsterman *et al*., 2002). Currently however, hairpin RNA (hpRNA) constructs are commonly used to induce RNA silencing in plants (Waterhouse and Helliwell, 2003). In stably transformed plants, DNA transgene constructs can efficiently deliver hpRNA molecules that induce either PTGS or TGS. Thus far, hpRNA constructs have mostly been used in dicotyledonous plants, and gene delivery has been done by either particle bombardment or *Agrobacterium tumefaciens*-mediated gene transfer (Waterhouse and Helliwell, 2003). For example, wheat cultivars have been transformed to have resistance to *Barley Yellow Dwarf Virus* (BYDV-PAV) by use of hpRNA transgene constructs (Wang and Waterhouse, 2001). These hpRNA constructs derived from the BYDV-PAV polymerase gene sequence were used to transform selected wheat cultivars. The transgenic cultivars reportedly had robust resistance against BYDV-PAV. Where the transgene occurred on a single locus, the resistance phenotype was inherited by subsequent generations in a Mendelian manner (Wang and Waterhouse, 2001).

CHAPTER 2

The construction of inverted repeat (IR) constructs containing specific mismatches for the posttranscriptional degradation of viral gene products

2.1 Introduction

RNA silencing has become a widely used mechanism for the study of gene function in plants (Fusaro, *et al.*, 2006). It is also being exploited to engineer specific virus resistance against a variety of plant pathogens. In past studies, resistance to cassava-infecting begomoviruses has been achieved by engineering plants to express a viral gene in the antisense orientation (Zhang, *et al.*, 2005; Chuang and Meyerowitz, 2000). Many of the early transgene-mediated virus resistance strategies used in plants involved the use of either a sense or an antisense construct individually. As more studies were being done to elucidate the mechanisms behind antisense-suppression, it was discovered that double stranded RNA is the trigger of a similar mechanism in *C.elegans* (Fire, *et al.*, 1998). This began a series of studies to investigate the effects of dsRNA in plants. Initially, dsRNA formation was achieved in plants by using transgenes that express both a sense and an antisense fragment of a viral gene separately, each from its own promoter (Waterhouse, *et al.,* 1998). This proved to be more efficient in conferring virus resistance compared to the use of an antisense gene alone, which correlated with the studies done on *C.elegans*. Subsequently, inverted-repeat (IR) transgenes, whereby the sense and antisense gene fragments are expressed from a single promoter, have been developed (Chuang and Meyerowitz, 2000). These IR constructs are reportedly more efficient inducers of PTGS than any of the previously used constructs. Inverted repeat (IR) transgenes now form the basis of experimental RNAi in plant systems, and the process has been termed IR-PTGS. (Broderson and Voinett, 2006).

Despite the prospective applications of IR-PTGS, the technology is difficult to apply due to the genetic instability of IR constructs. DNA sequences in an IR conformation have a tendency to form a four-way helical junction, known as a cruciform structure (Duckett *et al.*, 1988). These cruciform structures are fundamentally unstable in the genomes of most prokaryotic and eukaryotic organisms, and have been shown to interfere with DNA replication (Connelly, *et al.*, 1998). Cruciforms are similar in structure to Holliday junctions (Duckett, *et al*., 1988). Several nucleases that cleave Holliday junctions and other large secondary structures, so as to prevent the replication of such sequences, have been identified (Leach, 1994; Sharples *et al.,* 1994). In addition, Holliday junctions are key intermediates for homologues recombination, and are therefore substrates of recombination enzymes (Ortiz-Lombardia, *et al.,* 1999; Liley and Norman, 1999). As a result, IR constructs are often rearranged, degraded, or simply not replicated.

To circumvent this problem, constructs have been designed to contain a sufficiently large spacer sequence between the sense and antisense arms of the IR, thereby stabilizing the DNA conformation. When these constructs are transcribed, the spacer sequence forms a large loop on the end of a dsRNA stem. It was reported, however, that these spacer sequences significantly reduce the efficiency of PTGS induction (Smith, 2000). Helliwell and Waterhouse have since designed vectors for the production of IR constructs with an enhanced stability in bacterial and plant cells. The vectors, pHANNIBAL, pKANNIBAL, and pHELLSGATE, have been designed to stabilize the IR constructs by placing an intron, from the *Pdk* gene of *Flaveria,* between the sense and antisense arms of the construct (Helliwell and Waterhouse, 2003). These intron-spliced hairpin (ihp) constructs have reportedly had an efficiency of up to 100% induction of PTGS. In addition, the vectors are based on the pART7 system, and have a built-in CaMV35S promoter and octopine synthase terminator. This feature is convenient, as it eliminates the need for additional sub-cloning into an expression vector such as pART7.

Although the pHANNIBAL system is now routinely used for the production of intron-spliced hairpin constructs, a demand exists for improved methods of constructing IR transgenes. Despite the stabilizing effect of the intron in pHANNIBAL on an IR construct, our laboratory has experienced many problems with the pHANNIBAL system. In the case of a SACMV AC1 construct that was made, the intron seemingly did not stabilize the DNA sufficiently (Taylor and Rey, unpublished data). Subsequent molecular manipulations such as cloning, sequencing, PCR amplification, restriction digestions, and transformations were troublesome, if at all possible. In addition, the large intron (~700bp) increases the overall size of the T-DNA, which is eventually inserted into the plant genome. This is undesirable, as studies have shown that large-insert T-DNAs are prone to rearrangements and deletions in both *Agrobacterium* and plant cells (Nakano *et al.*, 2005).

The present study focusses on the design and construction of mismatched IR constructs, and investigates the potential benefits of these constructs to experimental RNAi in plant systems.

2.2 Specific Aims

The aim of the current study was to develop an alternative method of producing stable IR constructs and transgenes. This will assist with the development of improved constructs that confer resistance against SACMV, and other viral pathogens. We hypothesize that the introduction of several mutations along the sense arm of an IR construct will sufficiently stabilize the DNA conformation, whilst preserving the specificity and efficiency of PTGS.

In this chapter, we contributed to the following aims:

i. Development of a progressive construct design strategy, whereby the secondary structures formed by target region DNA and RNA molecules are considered.

ii. Determination of the mutation efficiency of sodium bisulfite.

iii. Assembly of an IR construct containing a mutated sense, and wild-type antisense arm against the SACMV BC1 ORF.

iv. Cloning of the mismatched IR construct into the pART7 expression vector.

v. Cloning of the hairpin cassette construct into a plant transformation vector.

vi. Production of an additional mismatched IR construct against *Maize streak virus* (MSV), for use in future studies.

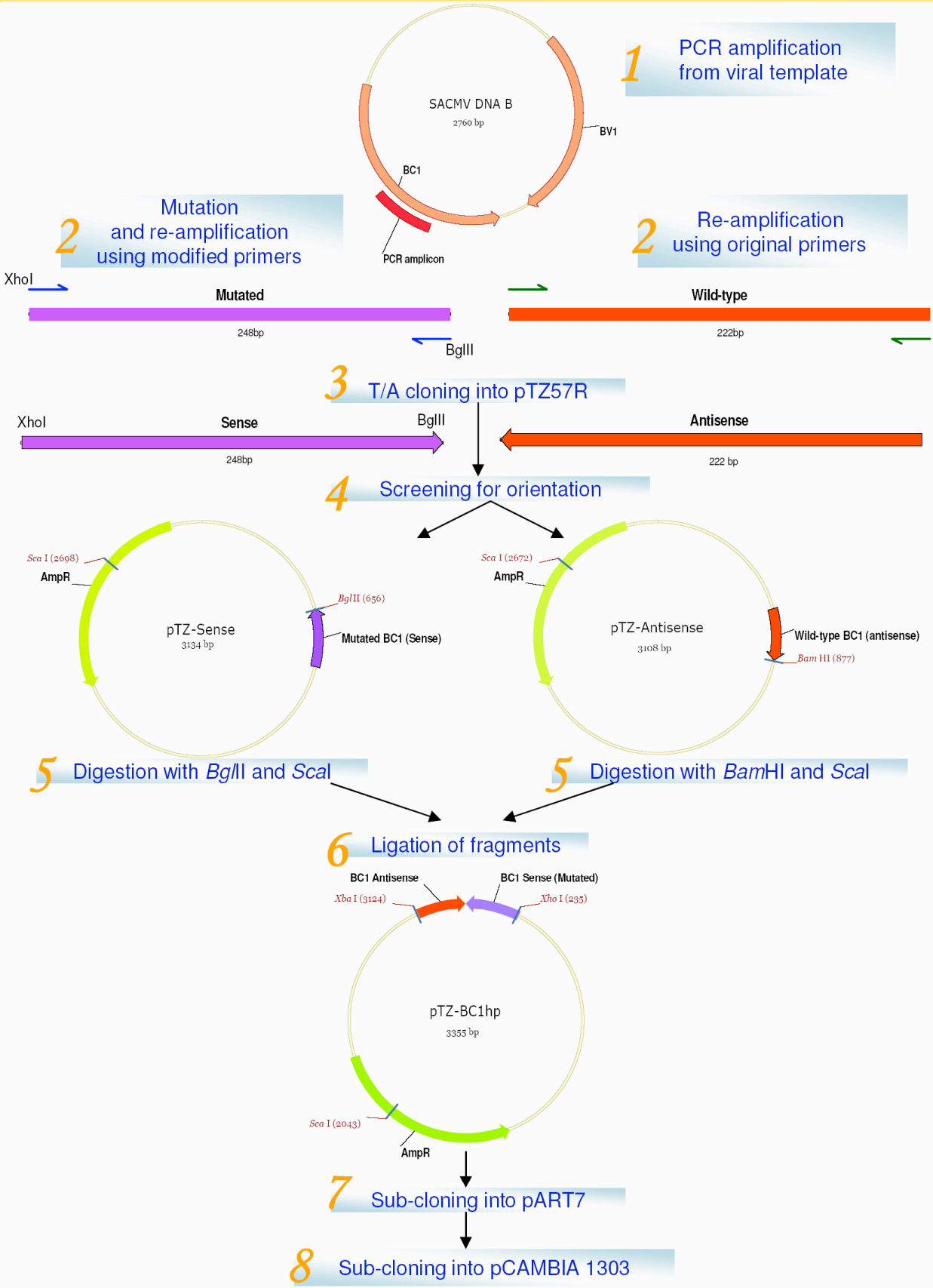

Figure 2.1 Flow diagram summarizing the methodology followed in this study

2.3 Materials and Methods

2.3.1 Isolation of geminivirus DNA

The genome of SACMV has previously been isolated, cloned and fully sequenced (Berrie, L.C. *et al.*., 2001). When these these full length clones were constructed, the DNA-A component was cut with *Sal*I at the 1865bp position, and cloned into pBluescript KS(+) (Stratagene). The DNA-B component was cut with *Eco*RI at the 2461bp position, and cloned into pBS KS(+). Plasmid DNA was isolated from the full length clones using a modified alkaline lysis extraction procedure (Sambrook *et al.*. 1989), after which the DNA was quantified on a Nanodrop 1000 spectrophotometer (Nanodrop). A purified plasmid extract containing the full length genome of *Maize streak virus* - A[Kom], was kindly provided by Dr Dionne Sheppard (School of Molecular and Cell Biology, University of Cape Town, South Africa). The full length MSV-A[Kom] clones were constructed by digesting viral DNA with *Bam*HI at the 152bp position, followed by cloning into pUC18 (Schnippenkoetter, W.H. *et al.*. 2001). The SACMV DNA-B sequence was compared to that of MSV AC1 by doing a multiple sequence alignment with the AlignX application (Invitrogen, 2006).

2.3.2 Sequence analyses and target region selection

All primers required for the polymerase chain reaction (PCR) were designed bearing in mind that the viral DNA is not in its circular form, but has been cloned as a linear molecule into a vector. The positions where the viral isolates were cut and cloned into the respective vectors had to be considered when primer binding sites were chosen, so as to prevent amplification of vector sequence. The SACMV DNA-B and MSV-A[Kom] DNA sequences were submitted to the Rensselaer Polytechnic Institute MFOLD server for secondary structure prediction at 55^{o}C and 64^{o}C (Zuker, M., 2003). The predicted secondary structure of the viral DNA was used to identify regions of the genome that have a propensity to form complex secondary structures, as these could interfere with molecular processes that are necessary when constructing an IR transgene. The sequence of the SACMV BC1 ORF was converted to RNA sequence *in silico*, and the secondary structure of the BC1 transcript was predicted using the MFOLD RNA algorithm (Zuker, M., 2003). It is necessary to choose linear RNA targets where possible, as this will facilitate target recognition and degradation by PTGS machinery (Schubert *et al.*, 2005). In addition, a multiple sequence alignment was done using the Clustal

X Multiple Sequence Alignment Program (version 1.8, 1999), whereby SACMV DNA-B was aligned with the DNA-B components of; *East African cassava mosaic virus* (EACMV), East *African cassava mosaic virus* - Uganda isolate (EACMV-Ug), *East african cassava mosaic virus* **-** Ivory Coast isolate (EACMV-Ivorycoast), and *African cassava mosaic virus* **-** Cameroon isolate (ACMV-Cameroon), so as to find regions with sequence similarity. Regions that are well conserved amongst these isolates were identified as potential targets. For SACMV DNA-B, a 222bp section of the BC1 open reading frame (ORF) was selected (1532bp-1753bp). For MSV-A[Kom], a 246bp section of the AC1 ORF was selected (1807bp-2052bp).

2.3.3 Amplification of target regions using the polymerase chain reaction

For amplification of the SACMV BC1 fragment, the primers BC1 F (unmod) (5'AAACAT TCCACGGACATACG 3`) and BC1 R (unmod) (5'TGGTAGCCCAATCTGAGACCTT3`) were used. The reaction mixture contained 0.4µM of each primer, 200µM dNTPs, 2.5mM $MgCl_2$, 2U *Taq* DNA polymerase (Eppendorf), 1.6x High Fidelity Buffer (Eppendorf), and nuclease-free water to a final volume of 50µl. Approximately 15.4ng of the SACMV DNA-B template DNA was added to the reaction mixture. The MSV AC1 fragment was amplified using the primers; MSV RepA F (Unmod) (5`AGAGCTCCCCTTTGATTGG3`), and MSV RepA R (Unmod) (5`TCCATCCATTGGAGGTCAGAAAT3`). The reaction mixture was as described for the SACMV DNA-B fragment, and 23.28ng of template DNA was added immediately before thermal cycling. Reactions were placed in an Eppendorf thermal cycler at 95^{o}C for 2 minutes to activate the *Taq* polymerase, followed by 30 cycles of denaturation at 95^{o}C for 15 seconds, annealing at 52^{o}C for 15 seconds, primer extension at 72^{o}C for 15 seconds, and a final extension step of 72^{o}C for 20 minutes for the addition of 3'-dA overhangs due to the terminal deoxynucleotidyl transferase (TdT) activity of the polymerase (Clark, J.M. *et al.*. 1988). Amplification products were purified using a High Pure PCR Product Purification Kit (Roche Applied Science), and were examined by electrophoresis on a 1.2% agarose gel containing 10ug/ml ethidium bromide. Electrophoresis was carried out in a 1x sodium boric acid (SB) buffer at 120V.

2.3.4 Mutation of PCR products

The BC1 and AC1 PCR products were quantified on a Nanodrop 1000 spectrophotometer (Nanodrop). Approximately 120ng of the BC1 fragment, and 360ng of the AC1 fragment were aliquoted into final volumes of 20µl. The EZ DNA Methylation-Gold kit (Zymo Research) was used to catalyze the deamination of cytosine residues and their conversion to uracil. The CT Conversion reagent (containing sodium bisulfite), was freshly made according to manufacturers instructions. The respective PCR products were added to 130µl CT reagent in a PCR tube, and thoroughly mixed. The mixtures were placed in a MyCycler™ Thermal Cycler (Bio-Rad), which was set to denature the DNA by heating to 98°C , then cooling to 64°C for 2.5 hours to allow deamination to occur, and finally to cool the tubes down to 4°C for storage up to 24 hours. Deamination efficiency was determined by removing samples of BC1 after being at the 64°C step for 5, 10, and 15 minutes respectively. Following deamination, the DNA was purified through a series of washes with a desulphonation buffer and an ethanol-containing wash buffer. The purified DNA was finally eluted from a silica-based spin-column. On recommendation from the manufacturer, 4µl of the eluted DNA was used for downstream PCR amplifications.

2.3.5 Strand specific amplification of sodium bisulfite-treated PCR products

Sodium bisulfite treated SACMV BC1 fragments were amplified using a set of primers derived from those used in **2.3.3** ; BC1 F (mod – *Xho*I+*Spe*I) (5`GATCCTCGAGACTAGT AAATATTCTACGGACATACG 3`) and BC1 R (mod - BglII) (5`GATCAGATCTTAGT AGCCCAATCTAAGACCTTGT3`). These primers were designed to preferentially amplify the positive strand of the sodium bisulfite-treated DNA template. In addition, they contain restriction endonuclease sites that are added on to the 3` and 5` ends of PCR products. Amplification of the sodium bisulfite-treated DNA was also done using the original primer set, BC1 F (unmod) and BC1 R (unmod). Sodium bisulfite-treated MSV AC1 fragments were similarly amplified using the original primers, MSV RepA F (Unmod) and MSV RepA R (Unmod), as well as a modified primer set; MSV RepA F (Mod + *Spe*I) (5`GATCACTAGTAGAGTTCTCCTTGATTGG3`), and MSV RepA R (Mod + *Bgl*II +*Bcl*I) (5`CTAGAGATCTTGATCATCCATCCATTAGAGATCAGAAAT3`).The reaction mixtures contained 0.4µM of each primer, 200µM dNTPs, 2.5mM $MgCl_2$, 1.6x High Fidelity Buffer (Eppendorf), 2U *Taq* DNA polymerase (Eppendorf), 4µl of the modified PCR

products from **2.3.4**, and nuclease-free water to a final reaction volume of 50µl. Reactions were cycled in an Eppendorf thermal cycler at 95^{o}C for 2 minutes to activate the *Taq* DNA polymerase, followed by 30 cycles of denaturation at 95^{o}C for 15 seconds, annealing at 52^{o}C for 15 seconds, primer extension at 72^{o}C for 15 seconds, and a final extension step of 72^{o}C for 20 minutes for the addition of 3'-dA overhangs. Amplification products were purified using a High Pure PCR Product Purification Kit (Roche Applied Science), and were examined by electrophoresis on a 1.2% agarose gel containing 10ug/ml ethidium bromide. Electrophoresis was carried out in a 1x sodium boric acid (SB) buffer at 120V.

2.3.6 Cloning of PCR products

Purified PCR products from **section 2.3.5** were quantified on a Nanodrop 1000 spectrophotometer (Nanodrop). PCR products from both sodium bisulfite-treated and untreated templates, respectively, were cloned into the pTZ57R vector (Fermentas) using the InsT/A Clone PCR product cloning kit (Fermentas). The pTZ57R vector was pre-cleaved with *Eco*32I and treated with terminal deoxynucleotidyl transferase to generate 3`-ddT overhangs at both ends. As recommended by the manufacturer, 39.96ng (0.54pmol ends) of the SACMV BC1 PCR product (sodium bisulfite treated and untreated, respectively) was added to 165ng linear pTZ57R (0.54pmol ends). Similarly, 44.28ng (+/- 0.54pmol ends) of the MSV AC1 PCR product (sodium bisulfite treated and untreated, respectively) was added to 165ng linear pTZ57R (0.54pmol ends). The ligation mixtures contained 10% v/v PEG4000, ligation buffer, 5U T4 DNA ligase (Fermentas), and nuclease free water to a final volume of 30 µl. In addition, a ligation mixture containing only linear pTZ57R was done as a negative control. The ligation mixes were incubated at 22^{o}C for a minimum of 1 hour, after which they were used to transform competent *E.coli* DH5α cells. The competent cells were initially stored at -70^{o}C, and were thawed on ice. Following this, 15µl of the ligation mix was added to 50µl of competent cells and incubated on ice for 20 minutes. Cells were then heat shocked at 42^{o}C for 90 seconds, and placed on ice for 2 minutes. The presumptive transformed cells were spread plated onto LB agar plates containing 100 µg/ml Ampicillin, and a mixture of X-Gal and IPTG for blue/white screening. Plates were incubated at 37^{o}C overnight, and blue/white screening was used to select clones with inserts. Several white colonies were randomly selected, inoculated into 3ml LB broth containing 100 µg/ml Ampicillin, and incubated at 37^{o}C overnight.

2.3.7 Screening of clones for inserts and orientation

Plasmid DNA was extracted from the presumptive clones using an alkaline lysis-based High Pure Plasmid Miniprep kit (Roche Applied Science). A selection of restriction endonucleases were used to digest the respective plasmid extractions, thereby identifying clones that contain inserts in the desired orientation. Clones containing the mutated SACMV BC1 insert were screened by double digestion with *Eco*RI and *Xho*I (Fermentas), whilst clones containing the original SACMV BC1 insert were screened by digestion with *Hinc*II (Fermentas). Clones containing the mutated MSV AC1 insert were screened by double digestion with *Eco*RI and *Bgl*II (Fermentas), whilst clones containing the original MSV AC1 insert were screened by digestion with *Eco*RI and *Xho*I (Fermentas). Restriction fragments were examined by electrophoresis on a 1% agarose gel, containing 10µg/ml ethidium bromide. Electrophoresis was carried out in a 1x sodium boric acid (SB) buffer at 120V.

2.3.8 Sequence determination and analysis

Clones presumed to contain inserts in the desired orientations were selected, and sent for automated sequencing by Inqaba Biotechnical Industries (Pretoria, South Africa). The universal M13/pUC reverse primer (5'd[CAGGAAACAGCTATGAC]3'), corresponding to the N-terminus of β-galactosidase, was used to sequence the multiple cloning site of pTZ57R and any inserts contained within. Raw sequencing data was edited using the Chromas software (version 1.45) (Griffith University, Australia). Subsequent sequence analysis was done using the Vector NTI Advance suite of software (version 10.3) (Invtrogen, 2006). A multiple sequence alignment was done to compare the sequences of mutated BC1 clones to the full length SACMV BC1 sequence. The mutated MSV AC1 clones were similarly aligned to the full length MSV AC1 sequence, as described above. From the multiple alignments, the number of cytosine to thymine mutations could be determined for mutated clones. In addition, the presumed orientation of mutated inserts could be confirmed.

2.3.9 Construction of mismatched IR constructs

Based on screening by restriction digestion and the analysis of sequencing data, clones containing mutant or wild-type inserts in the desired orientations were selected. Plasmid DNA was extracted from these clones using an alkaline lysis-based High Pure Plasmid Miniprep kit (Roche Applied Science). Two restriction endonucleases, *Sca*I and *Bgl*II (Fermentas), were used to digest the DNA from clone B4, which contains a mutated SACMV BC1 fragment in the sense orientation. Restriction fragments were examined by electrophoresis on a 1% agarose gel, and a band corresponding to 2kb was excised. DNA was extracted from the gel slice using a MinElute Gel Extraction Kit (Qiagen), and quantified on a Nanodrop 1000 spectrophotometer (Nanodrop). The DNA from clone E22, which contains a wild-type SACMV BC1 fragment in the antisense orientation, was digested with *Sca*I and *Bam*HI (Fermentas). Restriction fragments were examined by electrophoresis on a 1% agarose gel, and a band corresponding to 1.3kb was excised and purified as described above. DNA from clone F3, containing a mutated MSV AC1 fragment in the sense orientation, was digested as per clone B4. DNA from clone G3, containing a wild-type MSV AC1 fragment in the antisense orientation, was digested as per clone E22. Restriction fragments from clones F3 and G3 were examined by electrophoresis on a 1% agarose gel, and bands corresponding to approximately 2.1kb and 1.3kb respectively, were excised, purified, and quantified as previously described. In all instances, agarose gels contained 10µg/ml ethidium bromide, and electrophoresis was carried out in a 1x SB buffer at 120V.

For the BC1 hairpin construct, an IR conformation was achieved by ligating the purified clone B4 fragment to the purified clone E22 fragment, as these have compatible cohesive ends. Similarly, the MSV AC1 hairpin construct was made by ligating the clone F3 fragment to the clone G3 fragment. Aforementioned ligation reactions were done in a 1:1 ratio. For the efficient ligation of the B4 and E22 fragments, approximately 150ng of each purified fragment was required, whereas the efficient ligation of the F3 and G3 fragments required only 50ng of each. Ligation mixtures were made up in 1x ligation buffer (Fermentas), and contained 5% PEG4000, 5U T4 DNA ligase (Fermentas), and nuclease-free water to a total volume of 30µl. The ligation mixes were incubated at 22^{o}C for a minimum of 1 hour, after which they were used to transform competent *E.coli* DH5α cells. The competent cells were initially stored at -70^{o}C, and were thawed on ice. Following this, 15µl of the ligation mix was added to 50µl of competent cells and incubated on ice for 20 minutes. Cells were then heat shocked at 42^{o}C for 90 seconds, and placed on ice for 2 minutes. The presumptive

transformed cells were spread plated onto LB agar plates containing 100 µg/ml Ampicillin and were incubated at 37°C overnight. Several clones were randomly selected the following day, inoculated into 3ml LB broth containing 100 µg/ml Ampicillin, and incubated at 37°C overnight.

2.3.10 Screening of clones for IR sequences

Plasmid DNA was extracted from the presumptive clones using an alkaline lysis-based High Pure Plasmid Miniprep kit (Roche Applied Science). Restriction endonucleases were used to cut the pTZ57R vector on either side of the multiple cloning site, thereby releasing the entire insert. The SACMV BC1 IR clones were screened by double digestion with *Xho*I and *Xba*I (Fermentas). The MSV AC1 IR clones were screened by double digestion with *Sal*I and *Xba*I (Fermentas). Restriction fragments were examined by electrophoresis on a 1% agarose gel, containing 10ug/µl ethidium bromide. Electrophoresis was carried out in a 1x SB buffer at 120V. Clones with inserts corresponding to the expected sizes of the IR constructs (~500bp) were selected for sequence analysis.

2.3.11 Sequence determination of putative IR constructs

Putative IR clones were sent for automated sequencing by Inqaba Biotechnical Industries (Pretoria, South Africa). All clones were sequenced from both orientations by using the universal M13/pUC forward primer (5'[GTAAAACGACGGCCAG]3'), and the M13/pUC reverse primer (5'[CAGGAAACAGCTATGAC]3'). Raw sequencing data was edited using the Chromas software (version 1.45) (Conor McCarthy School of Health Science, Griffith University, Australia). The Vector NTI Advance suite of software (version 10.3) (Invtrogen, 2006) was used to analyze and annotate the sequences. RNA sequence was generated *in silico* from the DNA sequencing data, and submitted to the Rensselaer Polytechnic Institute RNA MFOLD server for secondary structure prediction at 25°C (Zuker, M., 2003).

2.3.12 Sub-cloning of IR constructs into an expression cassette

Based on restriction digestion and sequence analyses, clones containing the SACMV BC1, and the MSV AC1 IR constructs were selected for sub cloning into pART7. The BC1hp7 and MSVhp7 clones were digested as described in **section 2.3.10**, so as to release the hairpin

constructs from the multiple cloning site of pTZ57R. Restriction fragments were examined by electrophoresis on a 1% agarose gel. Bands corresponding to approximately 500bp were excised from the gel. DNA was extracted from the gel slice using a MinElute Gel Extraction Kit (Qiagen), and quantified on a Nanodrop 1000 spectrophotometer (Nanodrop). The pART7 vector was linearized by digestion with *Xba*I and *Xho*I (Fermentas). Subsequently, to remove the 5` terminal phosphates from the vector, linearized pART7 was treated with 2U calf intestinal alkaline phosphatase (CIAP) (Boehringer Mannheim), and incubated for 1 hour at 37^{o}C. The linear, dephosphorylated, pART7 DNA was examined on a 1% agarose gel. Single bands corresponding to 5kb were excised from the gel, and DNA was extracted and quantified as described previously.

Both the AC1 and BC1 IR fragments had compatible cohesive ends to the linearized pART7 fragments. Ligation reactions were set up by adding a 1:10 ratio (in pmol ends) of vector to insert, which required approximately 100ng of either the BC1 or AC1 fragments, and 100ng of linear pART7. Control ligations contained 100ng linearized, dephosphorylated pART7 only. Ligation mixtures were made up in 1x ligation buffer (Fermentas), and contained 5% PEG4000, 5U T4 DNA ligase (Fermentas), and nuclease-free water to a total volume of 30µl. The ligation mixes were incubated at 22^{o}C for a minimum of 1 hour, after which they were used to transform competent *E.coli* DH5α cells as described previously. The presumptive transformed cells were spread plated onto LB agar plates containing 100 µg/ml Ampicillin and were incubated at 37^{o}C overnight. Several clones were randomly selected the following day, inoculated into 3ml LB broth containing 100 µg/ml Ampicillin, and incubated at 37^{o}C overnight.

2.3.13 Screening of pART7 hairpin cassette clones

Plasmid DNA was extracted from the presumptive clones using an alkaline lysis-based High Pure Plasmid Miniprep kit (Roche Applied Science). Restriction digestion was used to screen putative recombinant plasmids for the presence of either BC1 or AC1 IR constructs. A double digestion of the plasmids was performed using *Sac*I and *Xba*I (Fermentas). As a negative control, pART7 plasmid DNA was digested with the same set of enzymes. Restriction fragments were examined by electrophoresis on a 0.8% agarose gel containing 10µg/ml ethidium bromide. Electrophoresis was carried out in a 1x sodium boric acid (SB) buffer at 120V. Clones containing either the SACMV BC1 or MSV AC1 hairpin cassette were

identified, and selected for further manipulations.

2.3.14 PCR amplification of hairpin cassette constructs

Due to a lack of useful restriction endonuclease sites located on either end of the pART7 promoter and terminator, it was necessary to clone the completed hairpin cassettes back into pTZ57R to facilitate subsequent cloning steps into a plant transformation vector. To achieve this, PCR amplification of both the AC1 and BC1 hairpin cassettes was done using the pART 7(cassette)F (5`[TTAACGTTTACAATTTCCCATTCGC]3`) and pART7(cassette)R (5`[GGAATTGTGAGCGGATAAC]3`) primers. The reaction mixture contained 0.4µM of each primer, 500µM dNTPs, 2.5mM $MgCl_2$, 2U Triplemaster Polymerase mix (Eppendorf), 1X Tuning buffer (Eppendorf), and nuclease free water to a final volume of 50µl. The amplification efficiency was tested by adding either 10ng or 20ng of template DNA to the reaction mixture. In addition, a positive control amplification was done using 10ng of pART7. Reactions were cycled in an Eppendorf thermal cycler at 93^{o}C for 3 minutes to activate the polymerase mix, followed by 35 cycles of denaturation at 93^{o}C for 30 seconds, annealing at 55^{o}C for 30 seconds, primer extension at 68^{o}C for 3 minutes, and a final extension step of 68^{o}C for 15 minutes for the addition of 3'-dA overhangs to PCR products. Amplification products were examined by electrophoresis on a 0.8% agarose gel containing 10µg/ml ethidium bromide. Electrophoresis was carried out in a 1x sodium boric acid (SB) buffer at 120V.

2.3.15 Cloning of hairpin cassette amplicons into pTZ57R

The PCR products from **section 2.3.14** were cloned into the pTZ57R vector using the InsT/A Clone PCR product cloning kit (Fermentas). Ligation mixtures contained 165ng (0.54pmol ends) linear pTZ57R, 4µl of unpurified PCR products from **section 2.3.14**, 5U T4 DNA ligase (Fermentas), 1X ligation buffer, and nuclease free water to a final volume of 30µl. In addition, a negative control containing only linear pTZ57R in the ligation mixture was done. The ligation mixtures were incubated at 22^{o}C for a minimum of 1 hour, after which they were used to transform competent *E.coli* DH5α cells as previously described. The presumptive transformed cells were spread plated onto LB agar plates containing 100 µg/ml Ampicillin, and a mixture of X-Gal and IPTG for blue/white screening. Plates were incubated at 37^{o}C overnight, and blue/white screening was used to select colonies with inserts. Several white

colonies were randomly selected, inoculated into 3ml LB broth containing 100 µg/ml Ampicillin, and incubated at 37°C overnight.

2.3.16 Screening of pTZ57R hairpin cassette clones

Plasmid DNA was extracted from the presumptive clones using an alkaline lysis-based High Pure Plasmid Miniprep kit (Roche Applied Science). Restriction digestion was used to screen putative recombinant plasmids for the presence of either BC1 or AC1 hairpin cassette constructs respectively. To determine the approximate size of inserts, double digestions were done using *EcoR*I and *Pst*I (Fermentas). To confirm the orientation of the insert, pBC1hp7E(i) was digested with *Sac*I and *Bsp*HI (Fermentas). At this point, the MSV AC1 IR constructs in pTZ57R were stored for future studies, and were not used further within the context of this project. The SACMV BC1 hairpin cassette construct, contained within clone BC1hp7E(i), was used for all subsequent manipulations.

2.3.17 Sub-cloning of a SACMV hairpin cassette into pCAMBIA1303

Plasmid DNA was extracted from *E.coli* DH5α cells, containing the pCAMBIA1303 vector, by use of an alkaline lysis-based High Pure Plasmid Miniprep kit (Roche Applied Science). A triple digestion of pBC1hp7E(i) was done by first incubating the DNA with *Eco*RI and *Hind*III in 1x buffer R (Fermentas). The reaction volume was then doubled to 70µl, and constituted with 1x buffer O before *Bsp*HI (Fermentas) was added. A double digestion of pCAMBIA1303 was done using *Eco*RI and *Hind*III (Fermentas). Subsequently, pCAMBIA1303 was dephosphorylated by incubation with CIAP (Boehringer Mannheim) for 1 hour at 37°C. Both the pBC1hp7E(i) and pCAMBIA1303 restriction fragments were examined by electrophoresis on a 0.8% agarose gel. Single bands corresponding to ~3kb of pBC1hp7E(i), and ~12.4kb of pCAMBIA1303, were excised from the gel. DNA was extracted and purified from the gel slices using a MinElute Gel Extraction Kit (Qiagen), and quantified on a Nanodrop 1000 spectrophotometer (Nanodrop).

The SACMV BC1 hairpin cassette fragments had cohesive ends that are compatible with the linearized pCAMBIA1303 fragments, and were ligated together. A 1:1 ratio of vector to insert was used (4.89pmol ends from each), which required 539ng of the BC1hp7E(i)-, and 130ng of the pCAMBIA1303 fragments respectively. Ligation mixtures contained 5U T4

DNA ligase (Fermentas), 10x PEG4000 (V/V), 1x ligation buffer, and nuclease free water to a final volume of 40µl. A ligation mixture containing only linearized, dephosphorylated pCAMBIA1303 was set up as a negative control. The ligation mixtures were incubated at 22^{o}C for a minimum of 1 hour, after which they were used to transform competent *E.coli* DH5α cells. The competent cells were initially stored at -70^{o}C, and were thawed on ice. Following this, 15µl of the ligation mix was added to 50µl of competent cells and incubated on ice for 20 minutes. Cells were then heat shocked at 42^{o}C for 90 seconds, and placed on ice for 2 minutes. To allow for the expression of kanamycin resistance genes, 500µl fresh Luria broth (LB) was added to the cells, and they were incubated at 37^{0}C for 12 minutes. Of this, 100µl was spread plated onto LB agar plates containing 100 µg/ml Kanamycin, as well as X-Gal and IPTG for blue/white screening. Plates were incubated at 37^{o}C overnight, and blue/white screening was used to select colonies with inserts. White colonies were selected, inoculated into 3ml LB broth containing 100 µg/ml kanamycin, and incubated at 37^{o}C overnight.

2.3.18 Screening of pCAMBIA1303 hairpin cassette clones.

Plasmid DNA was extracted from a presumptive clone using an alkaline lysis-based High Pure Plasmid Miniprep kit (Roche Applied Science). The clone, BC1hpCAM, was screened for the presence of the BC1 hairpin cassette by digestion with *EcoR*I and *Hind*III (Fermentas). As a negative control, pCAMBIA1303 was digested with the same set of enzymes. To confirm the sequence and orientation of the complete insert, several single digestions with different enzymes were done. Double digestions were not necessary, as only enzymes with at least 2 recognition sites within the region of interest were selected. pBC1hpCAM was digested with *Pst*I, *Sac*I, *Sma*I, *Xba*I, and *Xho*I (Fermentas) respectively. Restriction fragments were examined by electrophoresis on a 0.8% agarose gel containing 10ug/ml ethidium bromide.

2.4 Results

2.4.1 Sequence analysis and target selection

The DNA sequences of MSV and SACMV DNA-B were entered into the MFOLD DNA algorithm for secondary structure prediction. Secondary structures appeared to be present at 55^{o}C, with minor hairpin structures remaining intact along the length of the DNA. PCR primers were designed to hybridize to linear sections of the DNA. The predicted secondary structure of the SACMV BC1 RNA was composed almost entirely of hairpin structures and complex folds, with a few distinguishable linear regions or large loops.

When the sequences of the DNA-B components from SACMV, EACMV, EACMV-Ivorycoast, and ACMV-Cameroon were aligned, they were found to have approximately 38% sequence identity. However, when the SACMV DNA B component was aligned with that of EACMV and EACMV-Ug, they shared 90% and 91% sequence identity respectively (Table 2.1). Several small clusters of sequence that is conserved amongst all the aligned viruses were found, despite the SACMV DNA-B component having only 75% and 57% sequence identity with the EACMV-Ivorycoast and ACMV-Cameroon sequences respectively (Table 2.1 and Fig 2.2.A).

The SACMV BC1 coding regions that contained conserved sequence was then mapped onto the predicted DNA and RNA secondary structure charts. The SACMV target region was selected by finding an area that contains a high number of conserved nucleotides located on relatively linear stretches of DNA and RNA (Fig 2.2.B and Fig 2.3). The MSV target region was chosen by finding the largest stretch of linear DNA within the AC1 coding sequence (Fig 2.4.A). Oligonucleotide primers were designed to amplify a 222bp fragment of SACMV BC1 (from 1532bp to 1753bp) (Fig 2.5.A). A target region of 246bp within the AC1 ORF was chosen for MSV (from 1807bp to 2052bp) (Fig 2.5.B).

A multiple sequence alignment of SACMV BC1 and MSV AC1 was done, and they were found to contain approximately 42.4% sequence identity. Interestingly, MSV AC1 only shares 37.2% sequence identity with SACMV AC1, which also codes for a replication-associated protein.

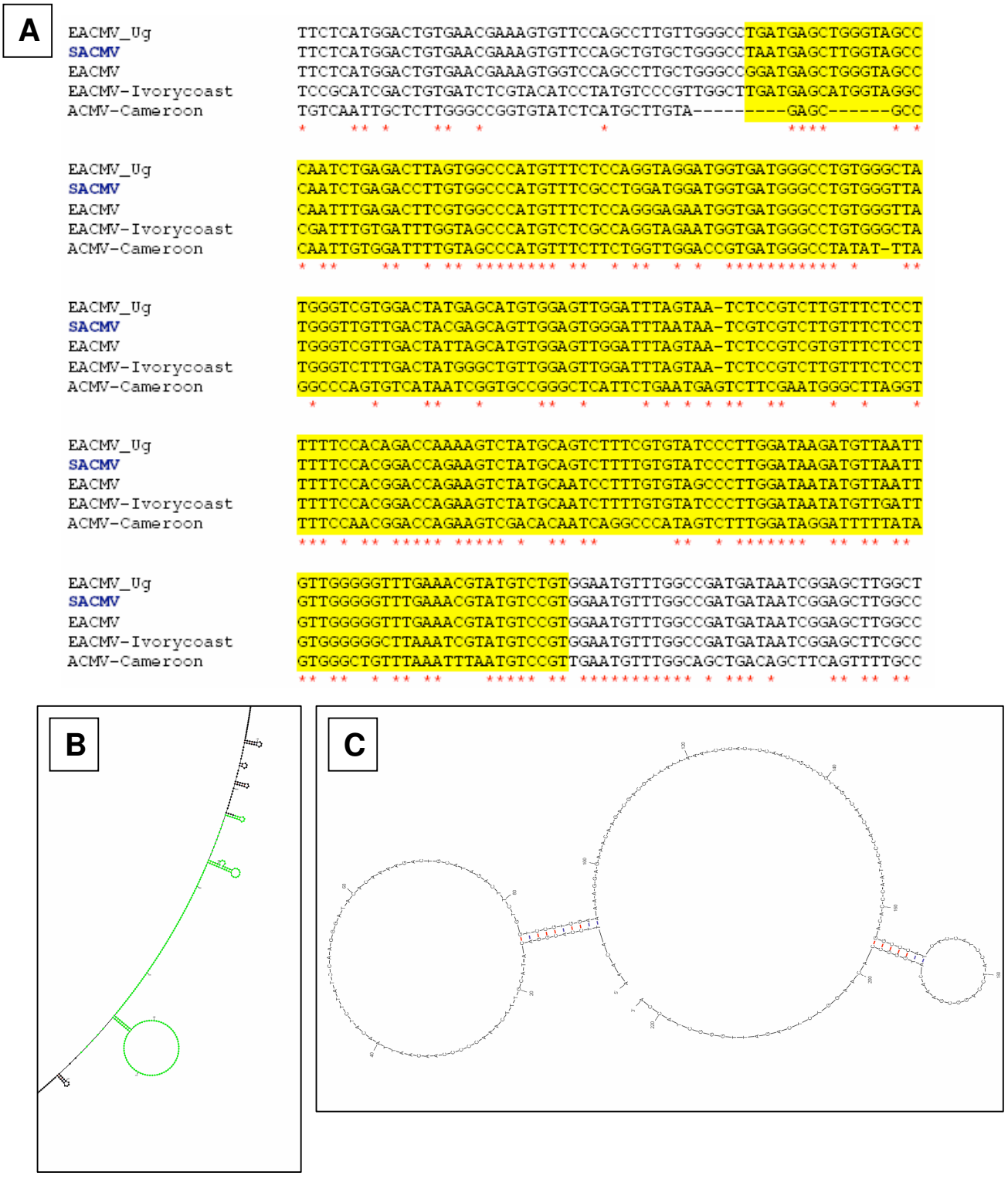

Figure 2.2 The SACMV BC1 target site selection, based on: (A) Multiple sequence alignments between SACMV, EACMV, EACMV-Ivorycoast, and ACMV-Cameroon, where the target region is highlighted in yellow; secondary structure prediction of the SACMV **(B)** viral DNA at 55°C (The chosen target region is highlighted in green.), and **(C)** PCR fragment of the target region at 64°C (single stranded).

Table 2.1 Similarity table comparing the percentage sequence identity between 5 different cassava-infecting begomoviruses

	ACMV-Cameroon	EACMV-Ivorycoast	EACMV-Ug	EACMV	SACMV
ACMV-Cameroon		56	57	58	57
EACMV-Ivorycoast			76	76	75
EACMV_Ug				91	90
EACMV					91
SACMV					

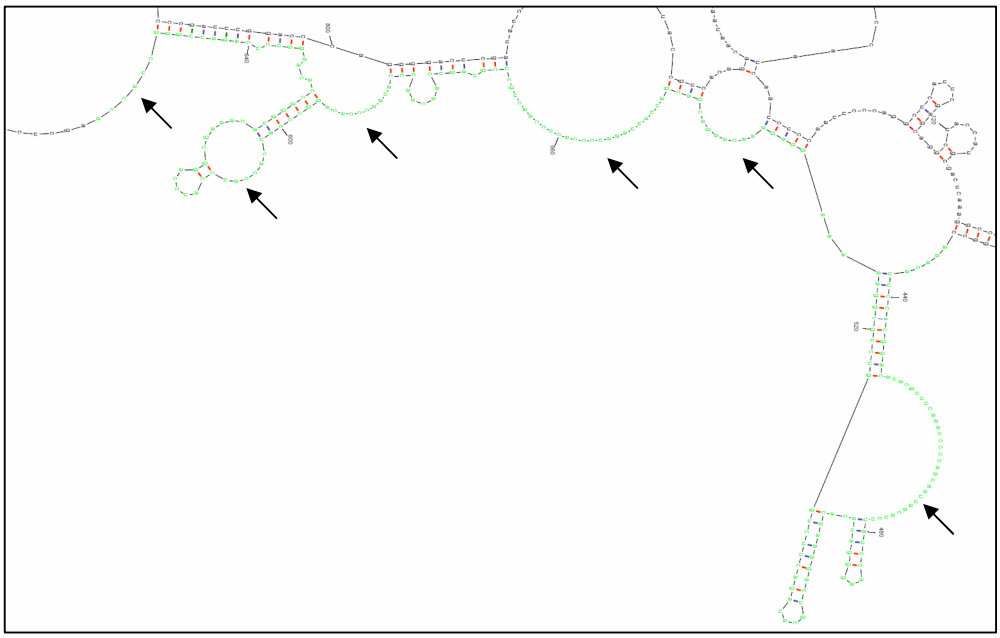

Figure 2.3 A portion of the predicted secondary structure of SACMV BC1 RNA at 37°C, with the targeted region highlighted in green. The target region was chosen due to stretches of linear sequences (as indicated by arrows) that are easily accessible for degradation by RNAi machinery

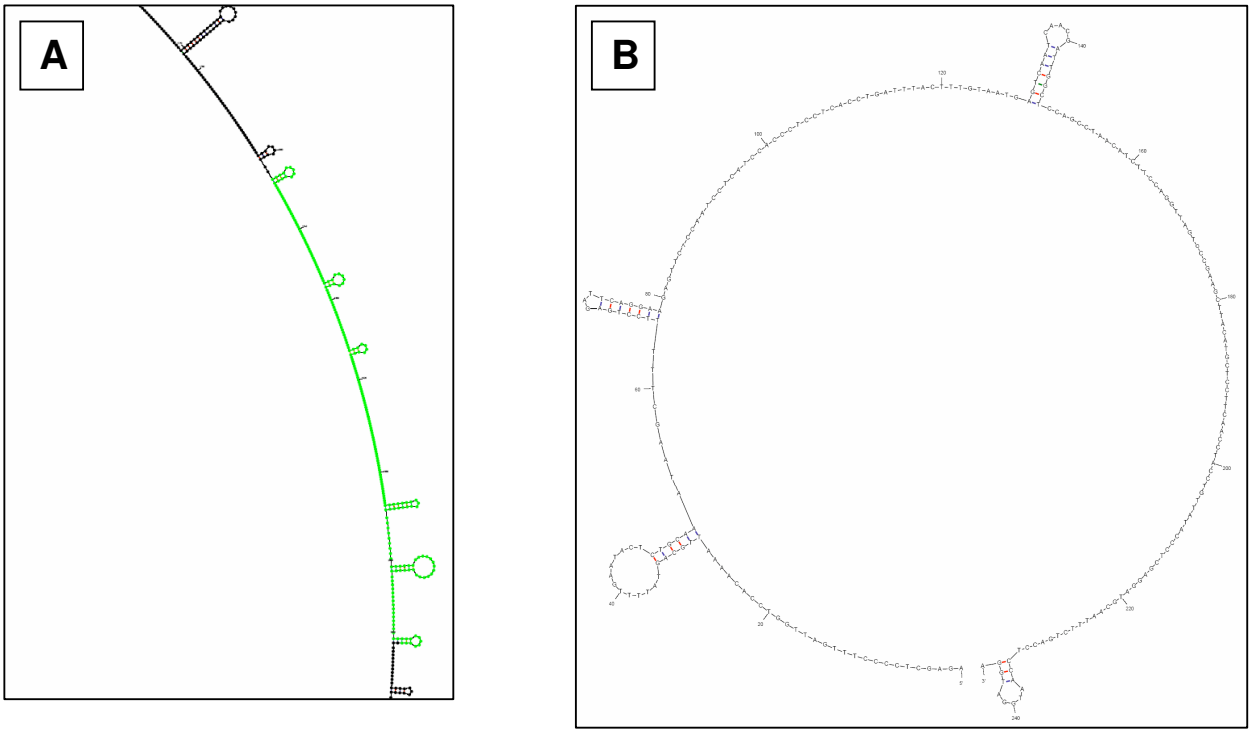

Figure 2.4 The MSV AC1 target site selection, based on secondary structure prediction of **(A)** the MSV viral DNA at 55°C (with the targeted region highlighted in green), and **(B)** the PCR fragment of the target region at 64°C (single stranded).

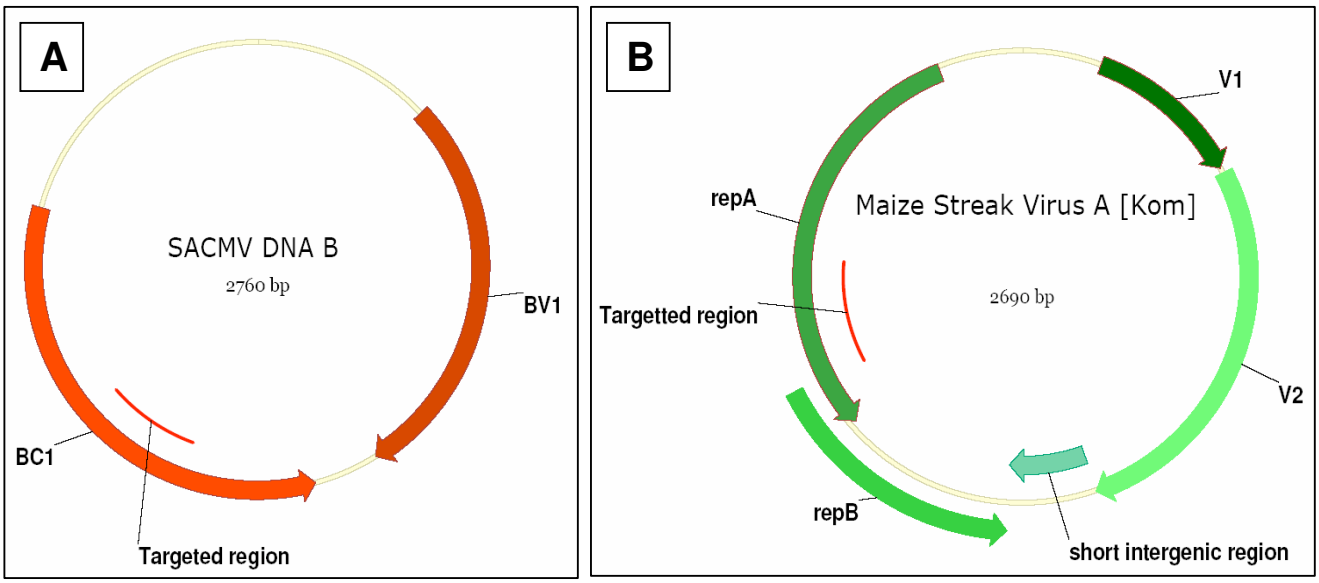

Figure 2.5 Diagrams showing the regions of the (A) SACMV BC1, and (B) MSV AC1 open reading frames that were chosen as targets for PTGS.

2.4.2 PCR amplification and mutagenesis of target fragments

Both the SACMV BC1 and MSV AC1 target fragments were successfully amplified from the full length viral clones at an annealing temperature of 52^{o}C (Fig 2.6). Aliquots of the PCR products were then mutated by incubation with sodium bisulfite, a known mutagen. To test the efficiency of cytosine deamination, the AC1 PCR product was incubated with sodium bisulfite for time points of 5, 10, 15 and 150 minutes. The MSV AC1 PCR product was incubated with sodium bisulfite for 150 minutes only, which is the incubation period recommended by the manufacturer. Both the mutated and original wild-type fragments were successfully re-amplified using the original sets of primers, as well as a second set of modified primers (Fig 2.7). The modified primers were designed to selectively amplify the sequence on the positive strand of the mutated template. The amplification efficiency achieved when original primers were used on mutated templates was comparable to that of when the modified primers were used. Similarly, the modified primer set appeared to be equally efficient to the original primers when used on the original wild type templates.

2.4.3 Cloning of mutated and wild type target fragments

The cloning of mutated and wild type target fragments from SACMV BC1 and MSV AC1 was successful, as the control plate contained only blue colonies, whereas the experimental plates contained mainly white colonies. An *Eco*RI and *Xho*I double digestion was used to screen clones for mutated BC1 inserts in the sense orientation (Fig 2.8.A). Clones yielding restriction fragments of approximately 2746bp and 2860 bp were selected, whereas those producing 40bp and 3094bp fragments were discarded. Clones containing the wild-type BC1 fragments were screened for inserts in the anti-sense orientation by digestion with *Hinc*II (Fig. 2.8.B). Clones yielding fragments of 96bp and 3012bp were selected, whereas those yielding 164bp and 2944bp fragments were discarded. Clones containing mutant MSV AC1 inserts were screened for inserts in the sense orientation by double digestion with *Eco*RI and *Bgl*II (Fig 2.8.C). Clones yielding 2986bp and 2860bp fragments were discarded, whereas those displaying 40bp and 3118bp fragments were retained. Clones containing wild-type AC1 inserts were screened for inserts in the antisense orientation by double digestion with *Eco*RI and *Xho*I (Fig 2.8.D). When fragments of 246bp and 2886bp were produced, the clones were retained. Those yielding fragments of 65bp and 3067bp were discarded.

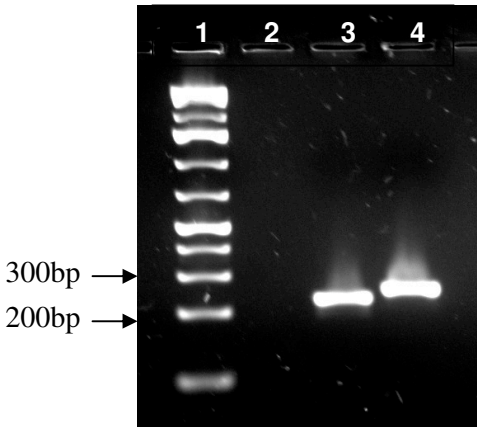

Figure 2.6 1.2% Agarose gel electrophoresis of wild-type BC1 and AC1 PCR products from full length viral clones. A ~220bp amplicon was produced for BC1 (lane 3), and a ~240bp amplicon for AC1 (lane 4). An O'Generuler 1kb Ladder Plus (Fermentas) was used (lane 1).

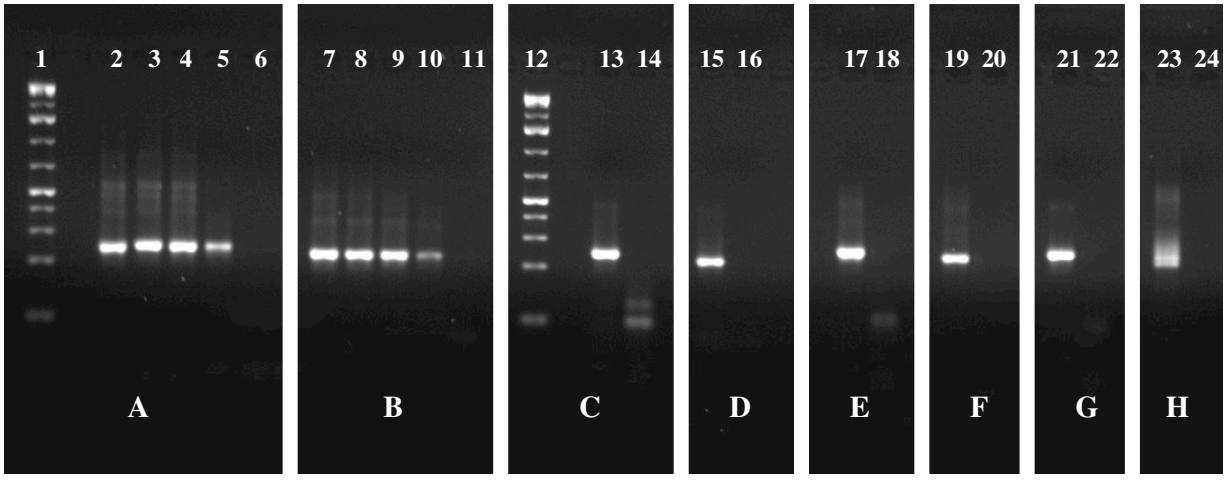

Fig 2.7: 1.2% Agarose gel electrophoresis showing the amplification efficiency of modified or original primers on mutated template DNA. **Modified primers** were used on **mutated** BC1**(A)** and AC1**(E)** templates, and also on *wild type* BC1 **(C)**, and AC1**(G)** templates. Similarly, the *original primers* were used on **mutated** BC1**(B)** and AC1**(F)** templates, and also on *wild type* BC1 **(D)**, and AC1**(H)** templates. The BC1 fragment was mutated for either 5, 10, 15 or 150 minutes (Lanes 2, 3, 4, and 5, respectively, and Lanes 7, 8, 9, 10, respectively). The AC1 fragments were mutated for 150 minutes only. The sizes of amplicons were estimated in relation to an O'Generuler 1kb Ladder Plus (Fermentas). Negative controls were done for each set of reactions (Lanes 6, 11, 14, 16, 18, 20, 22, and 24).

The A1, B4, C3, D1, and F3 clones were presumed to contain either mutated BC1 or AC1 inserts in the sense orientation, and were sent for automated sequencing. Clones containing wild type BC1 or AC1 inserts were re-screened to confirm that they do indeed contain inserts in the anti-sense orientation, and clones E22 (BC1) and G3 (AC1) were selected (Fig 2.9).

2.4.4 Sequence analysis of mutated clones

Sequencer output files were manually screened and edited where necessary to ensure the quality and consistency of the sequences, and to remove areas where a large amount of uninterpretable background noise is present. The sequences were individually aligned against either SACMV DNA-B or MSV where appropriate. In addition to confirming the orientation of the insert, it was possible to determine the number of C to T mutations, as well as the strand selected during strand-specific PCR.

Clones A1, B4, C3, and D1 contained BC1 inserts that had been mutated with sodium bisulfite for 5, 10, 15, and 150 minutes respectively. Clone F3 contained an AC1 insert that had been treated with sodium bisulfite for 150 minutes. Clones A1, B4, C3, and F3 were found to have been mutated with and efficiency of 55-80% (Fig 2.10.A). Clone A1, however, contained an insert in the anti-sense orientation, which is unfavorable. Clone D1, which had been treated with sodium bisulfite for 2.5 hours, was mutated with an efficiency of only 10%. Interestingly, the sequence of the D1 clone contains G to A mutations, rather than C to T mutations (Fig 2.10.B). Seeing as the insert in clone D1 was in the sense orientation, the G to A mutations can only be attributed to adverse amplification of the negative strand of mutated BC1. There were no considerable differences in the number of mutations between the 5, 10, and 15 minute sodium bisulfite-treated BC1 inserts. The MSV AC1 inserts, having been sodium bisulfite-treated for 2.5 hours, contained a substantially increased number of mutations when compared to the BC1 inserts. A multiple sequence alignment of the all the mutated BC1 clones was done. Mutations did not necessarily occur at the same cytosine residues on each clone. In fact, no distinct pattern of mutated sites as opposed to non-mutated sites could be distinguished.

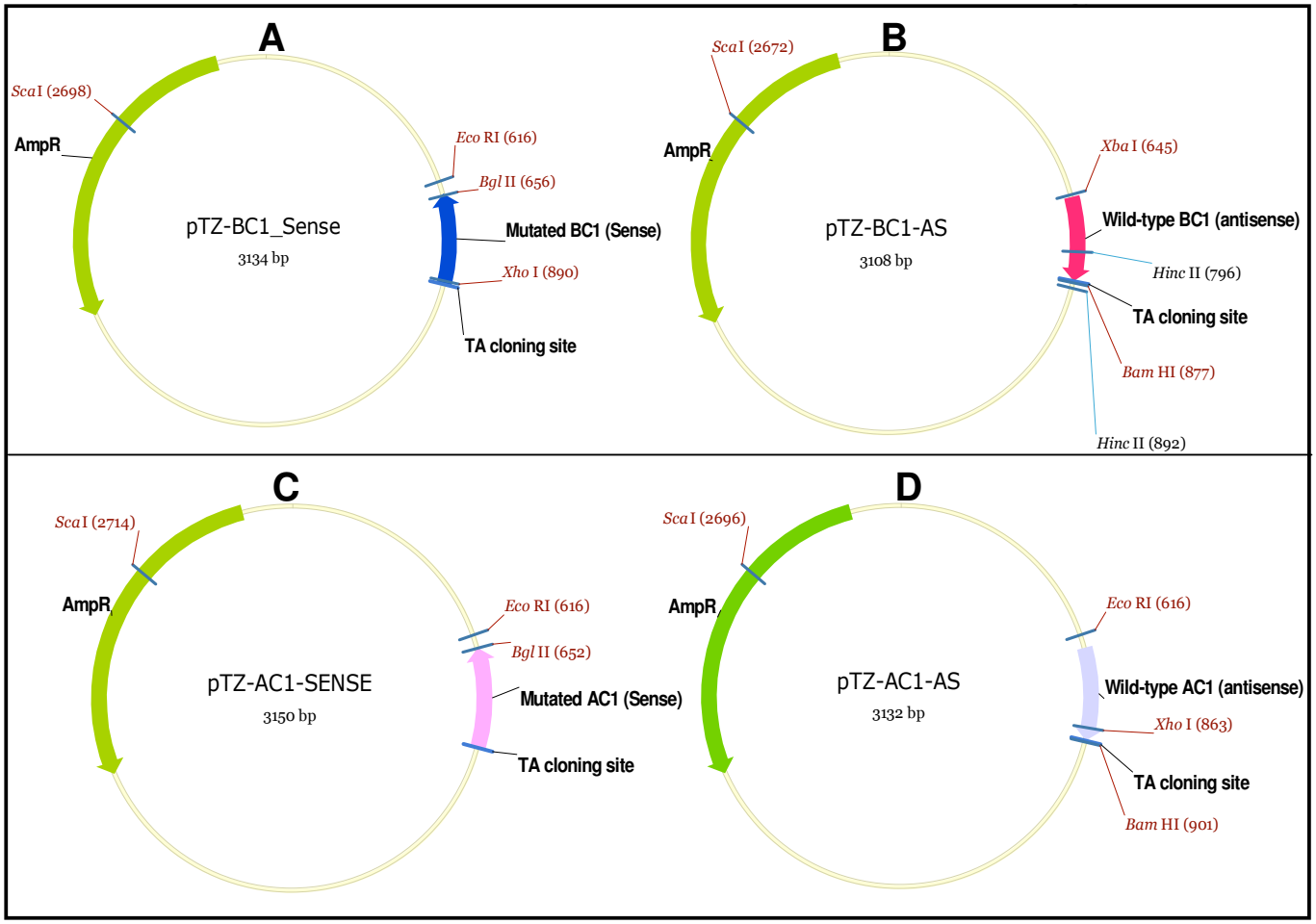

Figure 2.8 Diagram showing the favored orientations of mutated **(A, C)**, and wild-type **(B, D)** fragments of the SACMV BC1 ORF **(A, B)**, and the MSV AC1 ORF **(C, D),** after being cloned into the pTZ57R vector (Fermentas). Clones were screened for fragments inserted in the sense **(A,C)**, or antisense **(B,D)** orientations by digestion with restriction endonucleases.

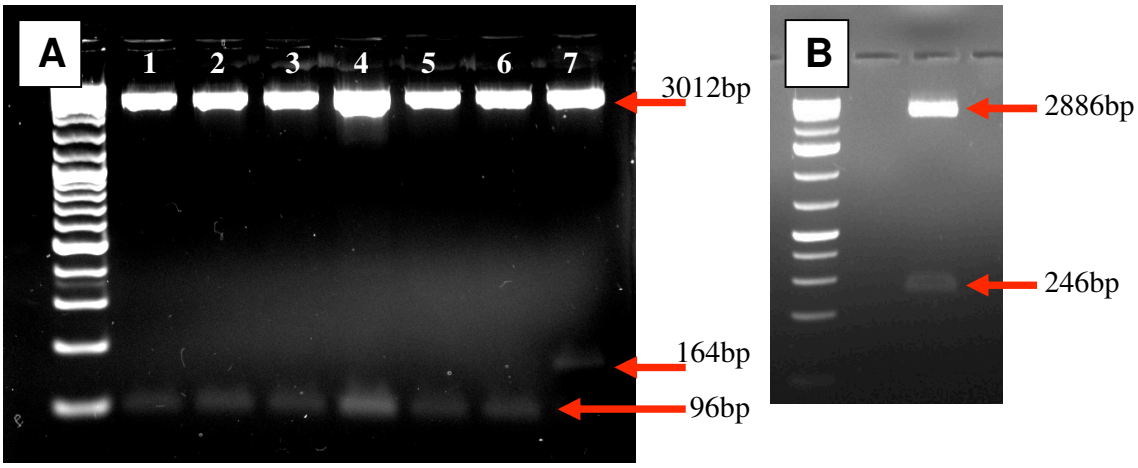

Figure 2.9 1% Agarose gel electrophoresis, showing **(A)** clones E22-E28 (Lanes 1-7), containing a wild-type SACMV BC1 insert, and **(B),** clone G3, containing a wild-type MSV AC1 insert. Clones were screened by restriction digestion. Clones E22-E27, and clone G3 yielded fragments confirming that they are in the antisense orientation. The sizes of restriction fragments were estimated in relation to an O'Generuler 1kb Ladder Plus (Fermentas)

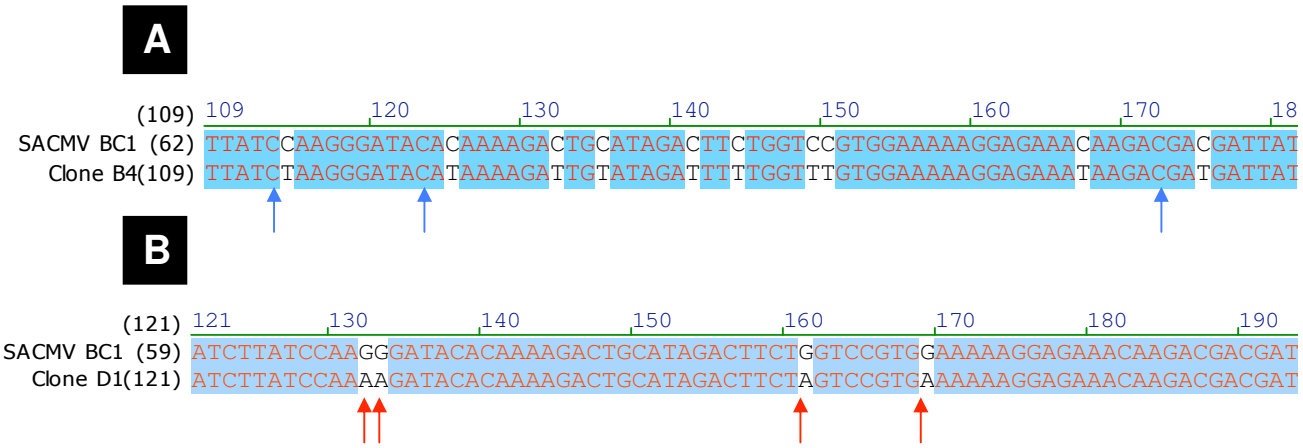

Figure 2.10 A portion of the multiple sequence alignments comparing the wild-type SACMV BC1 sequence to that of clone B4 **(A),** and clone D1 **(B).** Clone B4 had 39 cytosine to thymine mutations, although not all cytosine residues were mutated (as indicated by blue arrows). Clone D1 had only 7 mutations whereby guanine residues had been replaced by adenines (as indicated by red arrows).

Table 2.2 The efficiency of deamination, catalysed by sodium bisulfite, at various incubation times

Clone name	Description	% Cytosine to Thymine changes*	Guanine to Adenine changes	Correct Orientation
A1	BC1 treated 5 min	60	0	N
B4	BC1 treated 10 min	56	0	Y
C3	BC1 treated 15 min	55	0	Y
D1	BC1 treated 2.5h	0	10	Y
F3	AC1 treated 2.5h	82	0	Y

2.4.5 Construction of mismatched IR clones

Clone B4, which has 39 C-T mutations, was selected along with clone E22 for the construction of the SACMV BC1 mismatched IR construct. The double digestions of clones B4 and E22 with *Sca*I ,and either *Bgl*II or *Bam*HI respectively, yielded fragments of expected sizes (Fig 2.11.A). The 2kb fragment from B4 was successfully ligated to the 1.3kb fragment from E22, as numerous colonies were present. The clones grew on agar plates containing 100ug/ml ampicillin, which suggested that the ampicillin resistance gene in pTZ57R was once again intact after being cut and separated at the *Sca*I site.

Clone F3, which has 58 C-T mutations, was selected along with clone G3 for the construction of the MSV AC1 mismatched IR construct. Fragments of expected sizes were produced when double digestions of clones F3 and G3 with *Sca*I ,and either *Bgl*II or *Bam*HI respectively, were done (Fig 2.11.B). The 2.1kb fragment from F3 was successfully ligated to the 1.3kb fragment from G3, as numerous colonies were present. The clones grew on agar plates containing 100ug/ml ampicillin, which suggested that the ampicillin resistance gene in pTZ57R was once again intact after being cut and separated at the *Sca*I site.

Clones containing putative IR constructs were then screened by restriction digestion. The putative head-to-head dimers were cut from the multiple cloning site of pTZ57R (Fig 2.12 and Fig 2.13). All the BC1 clones yielded fragments of approximately 466bp, which is the size of the SACMV BC1 IR construct. Similarly, all the MSV AC1 clones yielded fragments of approximately 538bp, which is the expected size of the construct (Fig 2.13). The clones BC1hp7 and MSVhp3 were selected, and sent for automated sequencing.

Sequencer output files were manually screened and edited where necessary to ensure the quality and consistency of the sequences. The sequences from clones BC1hp7 and MSVhp3 were analyzed and annotated using the Vector NTI Advance software suite, and both were found to contain the IR constructs as was expected. The DNA sequences were converted to RNA sequence and submitted to the RNA MFOLD server. Despite having 17.5% mismatched basepairs along the sense arm, a stable hairpin structure containing a long dsRNA stem is still formed from the SACMV BC1 IR construct (Fig 2.14.A). The MSV AC1 IR construct folded into a long hairpin structure, even though it appeared as if the loop region had been destabilized slightly by the mutations (Fig 2.14.B).

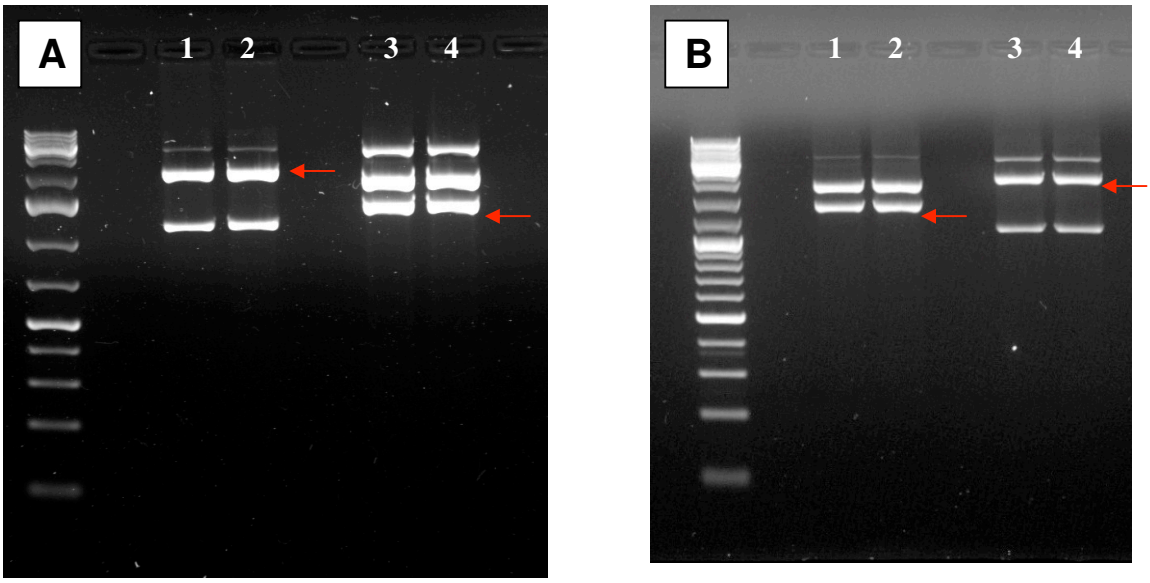

Figure 2.11 1% Agarose gel electrophoresis, showing the digestion of **(A)** clones B4 and E22 (Lanes 1-2 and 3-4, respectively), and **(B)** clones G3 and F3 (Lanes 1-2, and 3-4, respectively). Clones B4 and F3 were digested with both *Sca*I and *Bgl*II, whereas clones E22 and G3 were digested with both *ScaI* and *Bam*HI. Red arrows indicate the bands of expected sizes that were excised and purified. The sizes of restriction fragments were estimated in relation to an O'Generuler 1kb Ladder Plus (Fermentas)

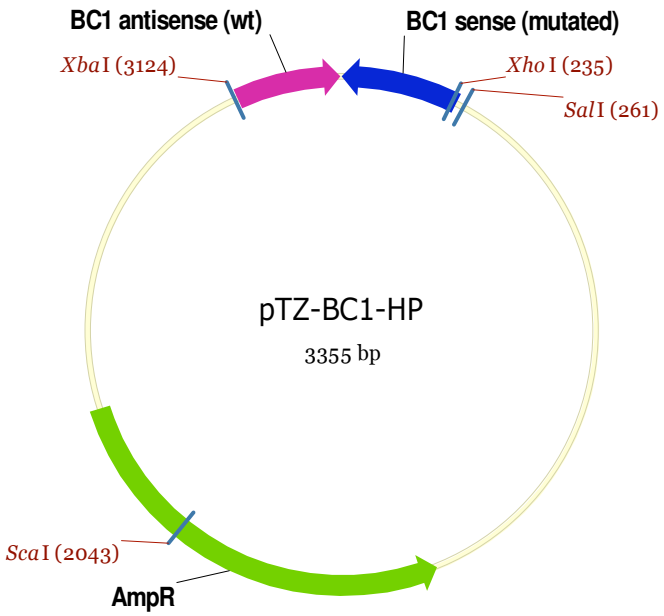

Figure 2.12 Diagram showing the inverted repeat conformation created in pTZ57R through the ligation of a sense fragment (e.g. clone B4) to an antisense fragment (e.g. clone E22).

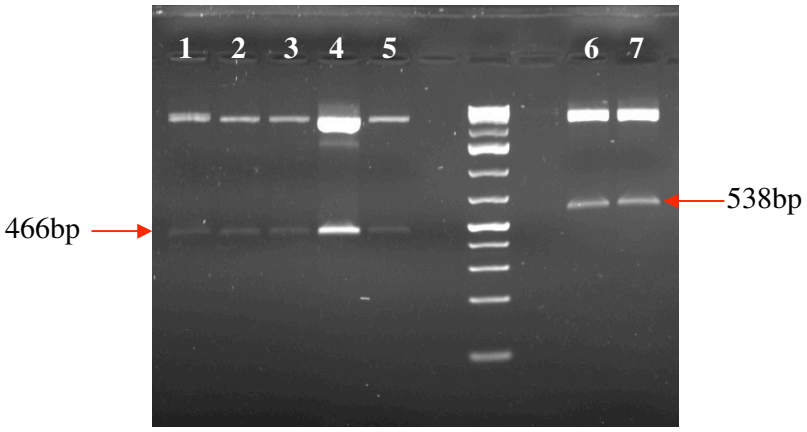

Figure 2.13 Putative BC1 IR clones (Lanes 1-5) were screened by digestion with *Xba*I and *Xho*I, thereby producing restriction fragments of ~466bp. Putative AC1 IR clones (Lanes 6-7) were screened by digestion with *Xba*I and *Sal*I, thereby producing fragments of 538bp. The restriction fragments were examined by electrophoresis on a 1% agarose gel. Appropriate fragments were excised, purified, and cloned into pART7. Clones BC1hp7 (Lane 4), and MSVhp3(Lanes 6+7) were selected. The sizes of restriction fragments were estimated in relation to an O'Generuler 1kb Ladder Plus (Fermentas).

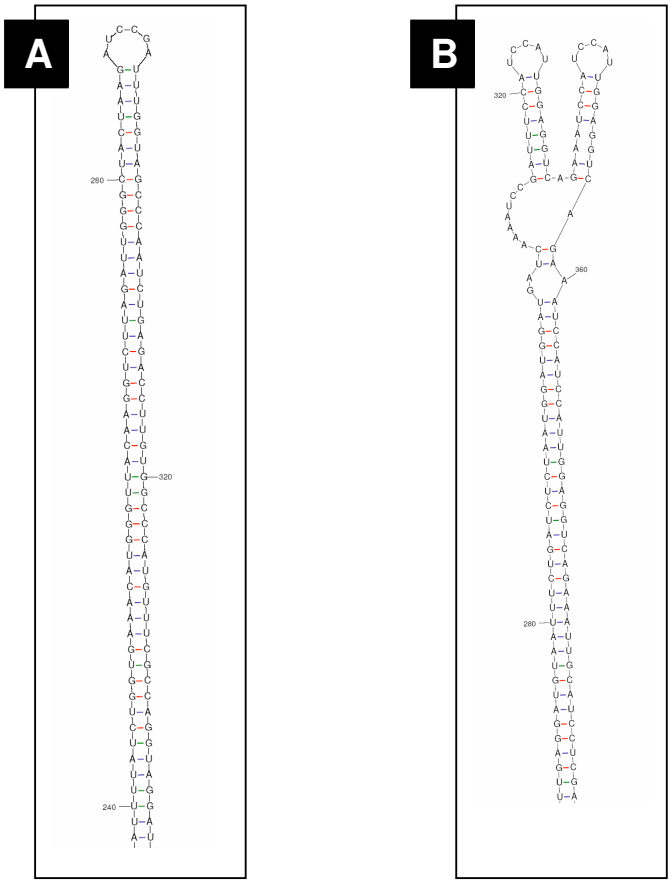

Figure 2.14 RNA secondary structure predictions of **(A)** a BC1 IR construct, and **(B),** an AC1 IR construct. Guanine-Uracil (GU) basepairs exist at positions that have been mutated on the sense strand, and can be seen along the stem of each hairpin.

2.4.6 Sub-cloning of IR constructs into pART7

Seeing as pTZ57R is not an expression vector, it was necessary to sub-clone the IR constructs into a vector containing a plant promoter and terminator. The pART7 vector used in this study contains a multiple cloning site, flanked by a CaMV 35S promoter on the one side and and an octopine synthase gene containing a plant terminator sequence on the other. The 466bp and 538bp fragments produced by cutting the SACMV BC1 and MSV AC1 IR constructs, respectively, out of the pTZ57R multiple cloning site, were excised from an agarose gel and purified (Fig 2.13). The pART7 vector was linearized and dephosphorylated for ligation to the IR constructs.

Ligations appeared to be successful, as numerous colonies were present on the experimental plates, whereas none were visible on the negative control plate. Random clones were then screened for the presence of the IR constructs by double digestion with *Sac*I and *Xba*I. The presence of a 1.9kb fragment was characteristic of clones containing the IR construct (Fig 15, Fig. 16). The restriction fragments produced by the MSV AC1 construct were marginally larger than those produced for the SACMV BC1 construct, which corresponds to what was expected. The BC1hp7E and MSVhp3E clones were selected for further manipulations.

2.4.7 PCR amplification and cloning of hairpin cassettes into pTZ57R

By using a long template amplification system with the pART7(cassette) primers, both the BC1 and AC1 hairpin cassettes were fully amplified to produce ~2.9kb amplicons (Fig 2.16, Fig 2.17). The amplification efficiency in reactions containing 10ng of template DNA was comparable to those containing 20ng. The hairpin cassettes were successfully cloned back into pTZ57R, as numerous white colonies were present on experimental plates, whereas the control plate contained blue colonies only.

The clones were screened for inserts by doing double digestions with *Eco*RI and *Pst*I. This digestion was problematic as restriction fragment sizes of 2825bp, 2791bp, and 292bp were produced, and the former two bands are indistinguishable on a standard agarose gel. Nonetheless, clones were selected based on the presence of the 292bp fragment, and BC1 hairpin cassette clones were further screened for orientation by digestion with *Sac*I and *Bsp*HI. The MSV AC1 hairpin cassette clones were stored for use in future studies, and were

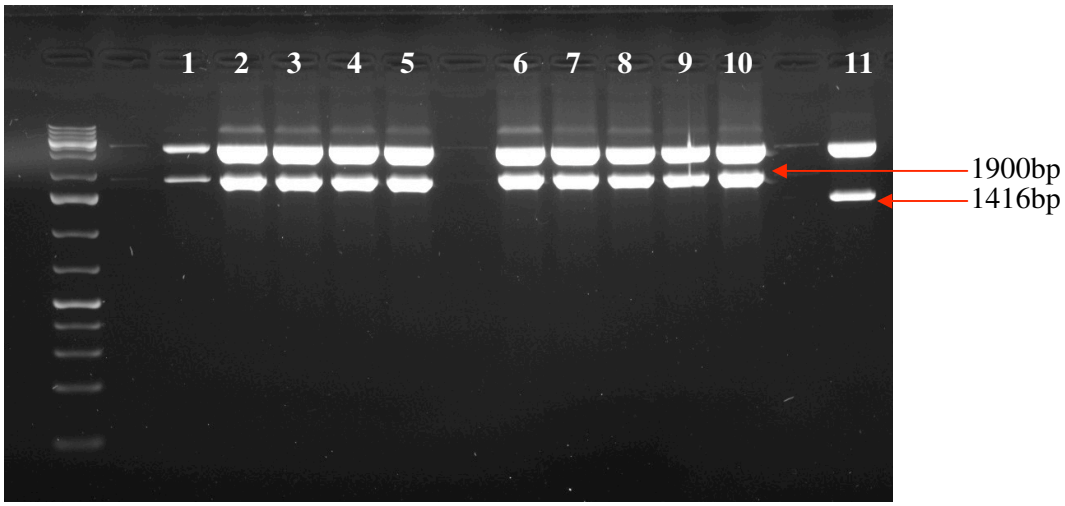

Figure 2.15 Putative clones containing either the BC1 (Lanes 1-5), or the AC1 (Lanes 6-10) IR cassette in pART7 were screened by double digestion with *Sac*I and *Xba*I. The pART7 vector was digested with the same enzymes as a negative control (Lane 11). The restriction fragments were examined by electrophoresis on a 1% agarose gel. All clones produced fragments of expected sizes. Clone BC1hp7E (Lane 5) and MSVhp3E (Lane 10) were selected for further manipulations. The sizes of restriction fragments were estimated in relation to an O'Generuler 1kb Ladder Plus (Fermentas).

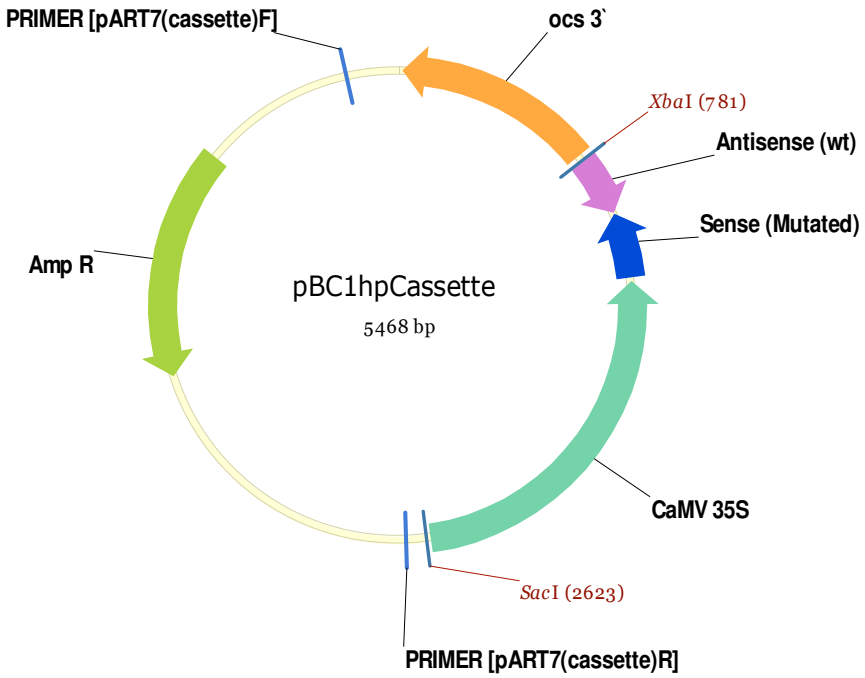

Figure 2.16 Diagram representing the conformation of either the BC1 or AC1 hairpin cassette construct in pART7. The IR construct is situated between a CaMV 35S promoter, and an ocs terminator. The binding sites of the pART7(cassette) primers are situated on either end of the expression cassette.

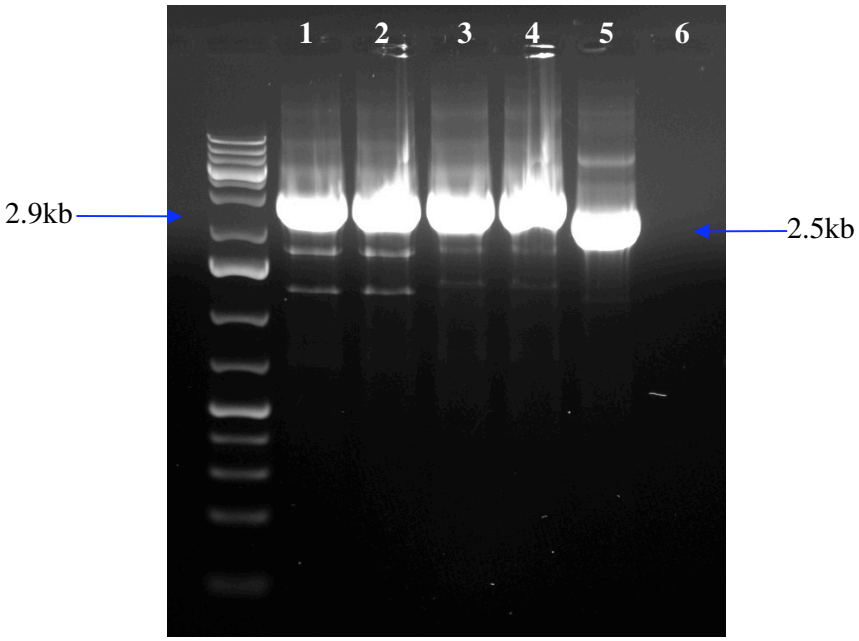

Figure 2.17 0.6 % Agarose gel electrophoresis of PCR amplicons yielded from pBC1hp7E (Lanes 1 and 2), or pMSVhp3E (Lanes 3 and 4) templates. Template concentrations of 10ng (Lanes 1 and 3) or 20ng (Lanes 2 and 4) was used. The pART7 vector was amplified as a positive control (Lane 5). In addition, a negative control was done using H_20 (Lane 6). All fragments corresponded with expected amplicon sizes. The sizes of PCR amplicons were estimated in relation to an O'Generuler 1kb Ladder Plus (Fermentas).

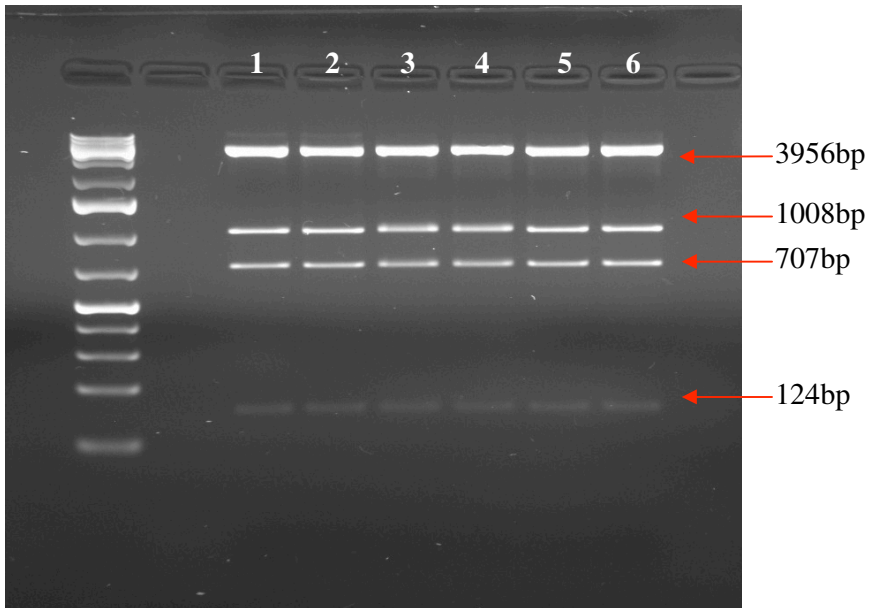

Figure 2.18 The orientation of the BC1 hairpin cassette in pTZ57R was confirmed by performing a double digestion using the *Sac*I and *Bsp*HI enzymes on pBC1hp7E(i) (Lanes 1-6). The restriction fragments were examined by electrophoresis on a 1% agarose gel. The bands produced, as indicated by red arrows, indicated the orientation of insertion. The sizes of restriction fragments were estimated in relation to an O'Generuler 1kb Ladder Plus (Fermentas).

not processed any further within this project. The BC1hp7E(i) clone was chosen for further manipulations.

The double digestions of pBC1hp7E(i) successfully determined its orientation, as 4 distinct fragments of approximately 3956bp, 1008bp, 707bp, and 124bp were produced (Fig 2.18).

2.4.8 Sub-cloning of the BC1 hairpin cassette into pCAMBIA1303

Several cloning strategies were attempted in an effort to sub-clone the BC1 hairpin cassette into pCAMBIA1303. The size of the cassette is almost equal to the size of the pTZ57R vector, which makes it impossible to separate the fragments adequately on a standard agarose gel. Progress was made by using the *Bsp*HI enzyme to digest the vector sequence, whilst using *Eco*RI and *Hind*III to release the cassette from the pTZ57R multiple cloning site (Fig 2.19). A ~3kb restriction fragment was purified from the agarose gel (Fig 2.20). The pCAMBIA1303 vector was suitably linearized and dephosphorylated for ligation to the cassette fragment. The ligations and transformations were successful, as one clone was present the following day. The negative control plate contained no colonies. In an effort to optimize the cloning of hairpin cassettes into pCAMBIA vectors, the efficiency was significantly enhanced by incubated the transformed *E.coli* cells in Luria broth immediately before spread plating onto antibiotic media.

The clone BC1hpCAM was screened for the presence of the BC1 hairpin cassette by double digestion with *Eco*RI and *Hind*III (Fig 2.21, Fig 2.22B). A band corresponding to approximately 3kb was produced, which correlates with the size of the cassette (Fig 2.22B). In addition, pBC1hpCAM was subjected to a series of single digestions with *Pst*I, *Sac*I, *Sma*I, *Xba*I, and *Xho*I to serve as a confirmation of the sequence and orientation of the hairpin cassette (Fig 2.22A). With the exception of the *Sma*I digest, all the digestions produced fragments of expected sizes. *Sma*I has a recommended incubation temperature of 30^{o}C, and its failure to cleave the DNA twice, as was expected, is possibly due to suboptimal incubation conditions.

pBC1hpCAM was subsequently used for the transformation of *Nicotiana bethamiana,* as will be discussed in chapters to follow.

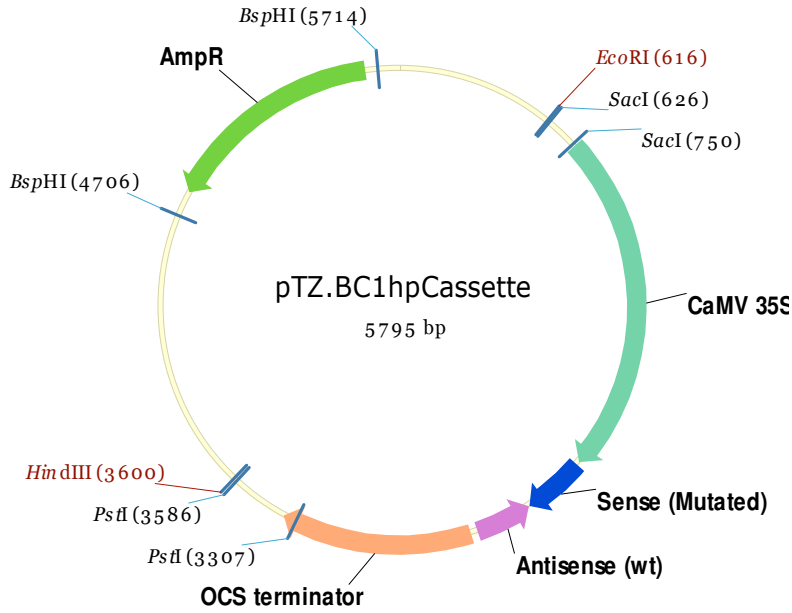

Figure 2.19 Diagram illustrating the conformation of the BC1 hairpin cassette in pTZ57R

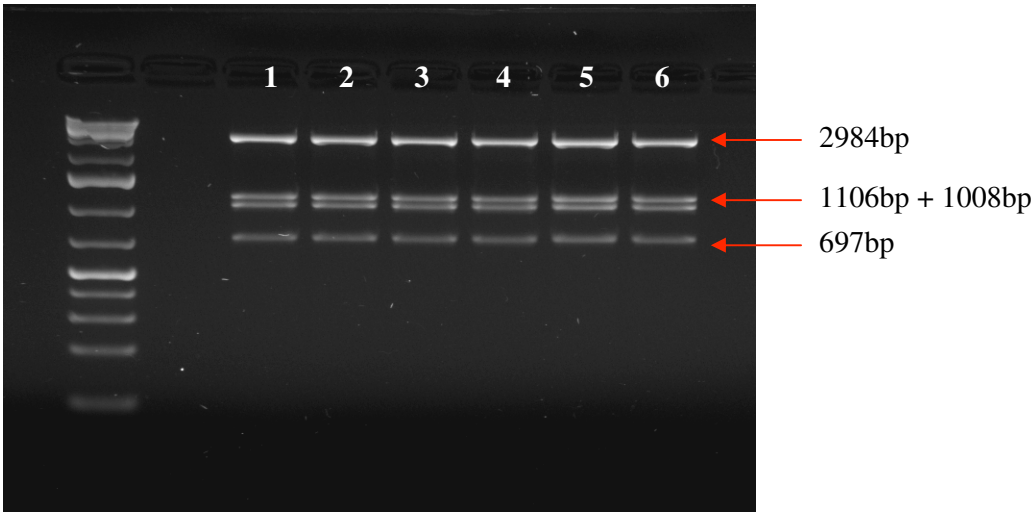

Figure 2.20 Sub-cloning of the BC1 hairpin cassette into pCAMBIA1303 was achieved by performing a triple digestion of pBC1hp7E(i), using *Eco*RI, *Hind*III, and *Bsp*HI (Lanes 1-6). The restriction fragments were examined by electrophoresis on a 1% agarose gel. Four fragments of expected sizes were produced, as indicated by red arrows. The 3kb fragment contains the hairpin cassette construct, and was subsequently extracted from the gel for cloning into pCAMBIA1303. The sizes of restriction fragments were estimated in relation to an O'Generuler 1kb Ladder Plus (Fermentas).

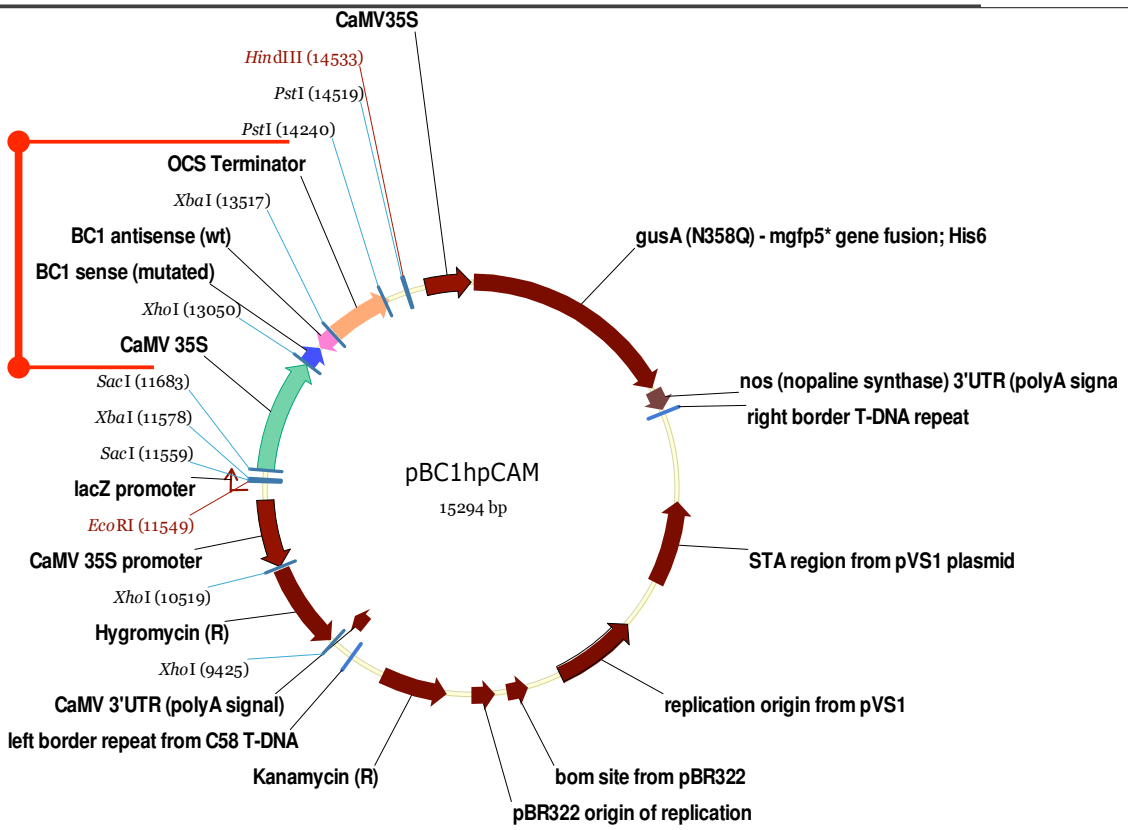

Figure 2.21 Diagram illustrating the conformation of the BC1 hairpin cassette in pCAMBIA1303

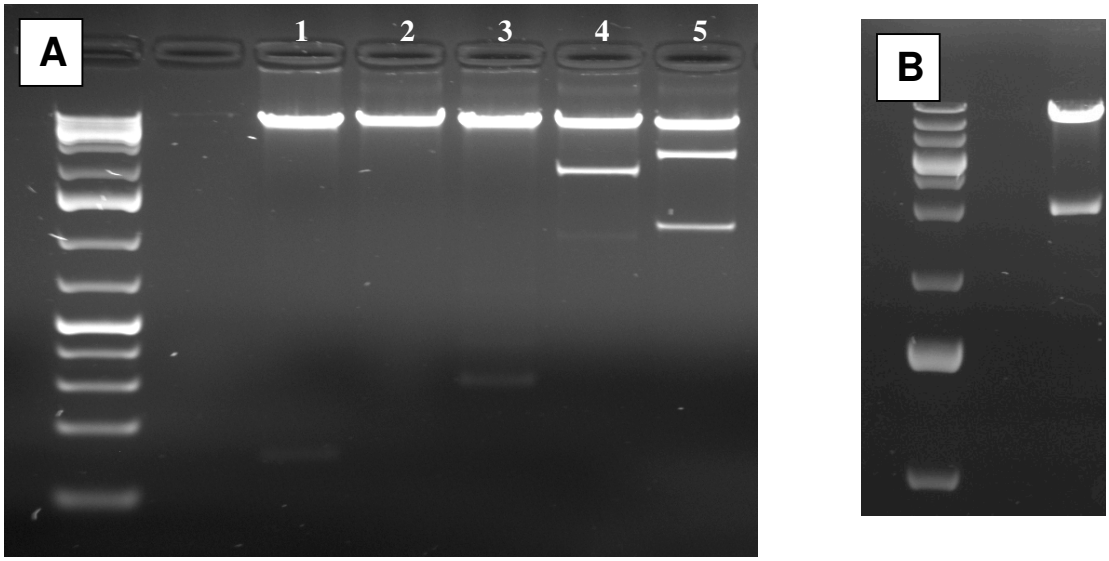

Figure 2.22 The putative BC1 hairpin cassette in pCAMBIA1303 was screened to confirm the presence of the insert by restriction digestion. pBC1hpCAM was digested with **(A)** *Sac*I (Lane 1), *Sma*I (Lane 2), *Pst*I (Lane 3), *Xba*I (Lane 4), *Xho*I (Lane 5), and **(B)** *Eco*RI and *Hind*III. With the exception of *Sma*I, all digestions produced fragments of expected sizes. The restriction fragments were examined by electrophoresis on a 1% agarose gel. The sizes of restriction fragments were estimated in relation to an O'Generuler 1kb Ladder Plus (Fermentas).

2.5 Discussion

The aim of this study was to develop novel inverted repeat (IR) constructs for the induction of PTGS in plants. Sodium bisulfite mutation was used to construct mismatched hairpin cassettes against the SACMV BC1, and MSV AC1 open reading frames.

Engineering constructs for multiple virus resistance

RNA silencing forms part of an innate defense mechanism in plants, whereby dsRNA accumulation leads to the degradation of cognate mRNA (Voinnett *et al.*, 1999). This phenomenon has been exploited to produce transgenic plants with resistance to one, or several viral pathogens (Bucher *et al.*, 2006, Zhang *et al.*, 2005). Due to the nature, and epidemiology of cassava mosaic geminiviruses, we aimed to design IR constructs that could induce PTGS of several species or quasispecies. Recombination amongst cassava mosaic geminiviruses (CMG) has been widely observed (Padidam *et al.*, 1999). A high degree of sequence variation is reportedly common amongst EACMV-like viruses, such as SACMV. In contrast, viruses derived from ACMV generally maintain a high degree of sequence similarity (Pita *et al.*, 2001). In previous studies by Zhang and colleagues, resistance to several ACMV quasispecies was achieved by targeting conserved regions of their genomes. (Zhang *et al.*, 2005). Multi-virus resistance can be useful in areas where mixed infections occur frequently. Some of the most severe recorded CMD outbreaks were seemingly due to mixed infections of ACMV and EACMV. As a result, we decided to find regions of sequence in the SACMV BC1 ORF that are homologues to; an ACMV variant, EACMV, and two EACMV quasispecies.

After the secondary structures of the BC1 nucleic acids were considered, a suitable target region was found. Within this region, there was a high degree of consensus, and blocks of up to 11bp share complete sequence identity amongst the 5 variants. Due to the ~90% sequence identity between SACMV, EACMV, and the Ugandan variant of EACMV, it can be expected that the construct will be effective against any of those viruses and similar quasispecies in the area. Similarly, the target region on SACMV has an 80% sequence identity to the Ivory Coast variant of EACMV. Due to large blocks having sequence identity of up to ~50bp, it is highly probable that at least one or more transgene-derived ~20nt siRNAs will find a

complementary binding site on the viral mRNA. Due to the siRNA primed RdRP6 amplification of RNAi signals, a single siRNA with an affinity to the target transcript is sufficient to efficiently induce PTGS (Dalmay, *et al.*, 2000).

Target selection for maximum siRNA efficacy

Most recent examples of genetic engineering for virus resistance involves the construction of long IR/hairpin constructs in systems such as pHANNIBAL or similar. In most cases, either a full-length or partially truncated copy of the target gene was used for the construction of the hairpin cassettes (Hartmut *et al.*, 2004; Huang, G., *et al.*, 2006; Fusaro *et al.*, 2006; Sunikumar *et al*. 2006). The resultant hairpin would then consist of several hundreds of base pairs (up to ~1kb), thereby leading to the production of a large population of transgene-derived siRNAs. Whilst this may seem like an effective strategy, it increases the possibility of off-target effects. Even though off-target silencing has more commonly been observed in animal systems, it should not be ruled out in plants, and an unnecessarily large population of siRNAs increases the probability of non-target silencing (Mansoor, *et al.*, 2006). As little as 20bp sequence identity between any endogenous plant coding sequence and the target sequence could lead to the posttranscriptional silencing of the endogenous gene. In addition, sequence identity between endogenous promoters or other regulatory regions and the target sequence may result in *de novo* methylation and transcriptional gene silencing of the endogenous gene (Wassenegger, 2000; Jones *et al.*, 2001). We therefore proposed an improved method of construct design, whereby smaller populations of highly effective siRNAs are produced, thereby increasing the efficacy of silencing whilst reducing the probability of non-target silencing.

Long dsRNA cannot be used in animal systems, and the efficacy of shRNA and siRNAs need to be optimized to achieve maximum silencing of target genes. We believe that it is similarly possible to design optimal long hairpin RNAs (lhRNA) in plants. Thermodynamic characteristics intrinsic to a particular siRNA are crucial for its selection by RISC, and the subsequent activity of that siRNA against its target gene (Khvorova, *et al.*, 2003). However, siRNA activity is reportedly affected more severely by complex secondary structures in the target region. There is a direct correlation between the extent of gene silencing and the local free energy in the mRNA target region (Schubert, *et al.* 2005). Therefore, the selection of a suitable target region is crucial for efficient gene silencing.

In this study, we scrutinized the secondary structure of the SACMV BC1 transcript, and identified a region containing several large loops and linear stretches of RNA (Fig 2.2.B). Theoretically, this target region would be more accessible to RISC, and would subsequently be degraded more efficiently. Geminivirus transcripts are known to have strong fold-back structures (Chellappan, *et al*., 2004; Vanitharani, *et al*. 2005), which increases the importance of having specifically engineered constructs. Our hairpin constructs were designed to produce a population of approximately 10-12 siRNAs with a high affinity to the target transcript. The efficiency of these constructs must be confirmed in a model plant system. This will be discussed in greater detail in chapter 3.

Mutation by sodium bisulfite for the construction of mismatched IR cassettes

In this study, we aimed to produce IR constructs with specific mutations on the sense arm only. We hypothesized that these mismatched IRs would be more stable than perfectly matched IRs. The stability of mismatched IRs will be discussed in a subsequent section.

The mismatched constructs in this study were created by introducing cytosine to thymine mutations on the sense arm, prior to assembly of the IR. These mutations were caused by deamination of cytosine by the mutagen sodium bisulfite. This chemical mutagen is ideal, as it specifically deaminates cytosine without affecting adenine, guanine or thymine (Mukai *et al*., 1970). When cytosine is treated with sodium bisulfite, only uracil and transamination products are yielded (Shapiro and Weisgras, 1970). To date, sodium bisulfite has commonly been used to screen genomic DNA for methylation or secondary structures, and we report the first application of this technology in the context of genetic engineering and RNAi.

Our results indicate that short periods of exposure to bisulfite is sufficient to catalyse an acceptable number of mutations. Although manufacturers recommendations state that the DNA should be exposed to sodium bisulfite for 2.5 hours, we found that there was no substantial difference in the the number of mutations occurring after 5 minutes of exposure. As mentioned earlier, bisulfite is commonly used to screen genomic DNA for methylation at a specific locus, which would require a prolonged period of exposure to ensure that the target region is mutated if not methylated. When short, concentrated PCR fragments, as used in this study, are mutated, an exposure time of 5-10 minutes seems to be sufficient to produce a large enough population of mutated template fragments for subsequent PCR amplification reactions. It was peculiar that the BC1 fragment mutated for 2.5 hours had such a low rate of

mutation, when compared to the identical templates incubated for a much shorter period. Seeing as the BC1 PCR fragments used were identical for the 5, 10, 15 and 150 minute reactions, a satisfactory explanation of this observation is not possible in terms of the structure of the DNA. In addition, the MSV PCR fragments were efficiently mutated after an exposure time of 2.5 hours, which rules out any effects of the prolonged exposure time. Seeing as the rate of catalyses is highly dependent on the pH for this reaction, it is possible that there may have been some pH variation amongst the samples, although this cannot be substantiated any further. Reportedly, at pH values above 7.0, the rate of catalyses is significantly reduced (Shapiro and Weisgras, 1970).

Interestingly, a substantial difference in the mutation efficiency of sodium bisulfite was observed between the SACMV BC1 and MSV AC1 fragments. A likely reason for this is the secondary structure elements that are present in the BC1 ssDNA at 64^{o}C (Fig 2.2.C). In comparison with the secondary structures present in the AC1 ssDNA at that temperature (Fig 2.4.B), the BC1 structure has a lower ΔG value as a result of its 2 stable hairpin-loop structures. It has previously been established that bisulfite reacts strongly with ssDNA and unpaired bases (Gough, *et al*., 1986). Indeed, many of the non-mutated C residues in our samples were situated either within a dsDNA stem structure, or in the close vicinity thereof at 64^{o}C. We can therefore conclude that the selection of a target DNA region will directly affect the degree of mutation by sodium bisulfite. This is due to the relative stabilities of integral secondary structures present at 64^{o}C.

The efficiency of strand-specific PCR amplifictaion of mutated template DNA

In this study, we aimed to produce IR constructs whereby the DNA secondary structure would be sufficiently destabilized without in turn destabilizing the RNA secondary structure. In so doing, the formation of cruciforms could be minimized without affecting the folding of the subsequent RNA hairpins for the induction of PTGS.

Seeing as bisulfite catalyzed deamination only affects cytosine residues, two species of PCR products may exist after the mutation of the template. The positive and the negative strands of the mutated template DNA molecules will yield PCR products with different sequences. Products amplified from the positive strand will contain cytosine to thymine mutations when read in the sense orientation. Conversely, PCR products from the negative strand will contain guanine to adenine mutations when read in the sense orientation. Primers were therefore

designed to allow for strand-specific PCR amplification of the positive strand of the mutated template DNA, as we were interested in engineering C-T mutations rather than G/A mutations on the sense strand of our constructs. The antisense strand of the IR constructs cannot be mutated, as this would compromise the binding of subsequently formed siRNAs to target sequences, thereby compromising the induction of PTGS. We were interested in C-T mutations in the DNA, as this would lead to GU mismatches in the RNA hairpin, which will be discussed in more detail further on.

Primers for strand specific amplification were designed so that the terminal nucleotide at the 3` end of the forward primer would be mismatched if bound to a mutated template strand, whereas the 3` end of the reverse primer would be unaffected by mutations on the template strand. In this way, the positive strand will be amplified from the mutated template more efficiently than the negative strand. The 3` end of the forward primer is effectively not mismatched with the amplification product of the mutated sense strand, and will hence amplify these products more efficiently than the original negative strand. In this way, a single amplification product is produced with C-T mutations when read in the sense orientation.

Strand specific PCR failed on the D1 clone due to the low efficiency of mutation in that case, as discussed earlier. Seeing as the template DNA was not mutated at the binding site of the forward primer, amplification of the positive and negative strands proceeded as would be expected on wild-type DNA. The fragment in clone D1 was found to have G-A mutations, and therefore originated from the negative strand of the mutated template.

The assembly, sub-cloning and subsequent stability of IR constructs

In recent times, IR transgenes have become the basis of experimental RNAi in plant systems (Broderson and Voinett, 2006). Unfortunately, there are limits to the technology, as inverted repeat constructs exceeding 150bp have been found to cause genetic instability in prokaryotes and many lower eukaryotes (Gebow, *et al.* 2000). In *E.coli,* inverted repeats may cause cell death, and are often deleted or rearranged rapidly. It has been reported in numerous studies that IR constucts recovered from *E.coli* have a partial or complete deletion of either the sense or antisense arm (Brunier, *et al*., 1988). The genetic instability caused by IRs are due to the formation of four-way helical junction known as a cruciform (Ducket *et al*., 1988). Cruciform structures are highly unstable, and can only form in negatively supercoiled DNA such as plasmids (Shlyakhtenko, *et al*., 1998). IR transgenes are therefore difficult to manipulate

during cloning and plant transformation procedures, where the process depends on the replication and maintenance of the plasmid containing the construct. In addition, cruciform structures may form in eukaryotic cells due to sufficient amounts of negative supercoiling that occurs. This may lead to genetic instability of the IR transgene in plant cells.

In this study, we successfully assembled IR constructs using a simple T/A cloning vector-based strategy. We were subsequently able to sub-clone the IR construct into an expression vector, and later into a binary plant transformation vector. In addition, the amplification of the entire hairpin cassette was achieved without the use of DMSO or other agents that relax secondary structure. Similarly, automated sequencing was done using standard primers and conditions. In all cases, our constructs were replicated and maintained in standard *E.coli* DH5α, and there was no need to use IR-tolerant cells such as Sure Cells (Stratagene). In many studies with inverted repeat constructs, the aforementioned molecular manipulations were not possible. In one such study, Balliet and colleagues attempted the functional characterization of one of three herpes simplex virus-1 origin of replications, OriL (Balliet, *et al*., 2005). The sequence of OriL consists of a perfect 144bp inverted repeat. As a result, the OriL sequence could not be readily mutated by site-directed mutagenesis, it could not be sequenced by standard automated DNA sequencing procedures, and the IR could not be stably propagated in *E.coli*. Interestingly, OriS, one of the other HSV-1 origin of replications, was more stable and could be fully characterized and manipulated using the molecular approaches attempted on OriL. Despite the extensive sequence homology between OriL and OriS, it was was found that the latter is a 45bp imperfect IR, which accounts for its increased stability. This correlates with our results, where one mismatched arm of the IR seemingly had a significant stabilizing effect on the construct.

The effect of GT mismatches on the thermodynamics of various DNA molecules has previously been determined, and the data was consistent with the "nearest-neighbour" parameters for Watson-Crick base pairs (Allawi and SantaLucia, 1997). In this controlled study, the effect of a single GT mismatch was found to be context dependent. For example, a single GT mismatch may reduce helix stability when the mismatch is located between two AT base pairs. In addition, it was reported that GT mismatches caused slight structural perturbations that were highly localized. If a single GT base pair can reduce the stability of a helix, we believe that numerous GT mismatches along the stem of an intrinsically unstable cruciform structure will significantly affect the thermodynamic favorability for the formation of that structure. Our data is consistent with this theory, as our IR constructs behaved like

linear molecules during molecular manipulations that would not be possible if cruciform structures were present. In addition, our constructs were efficiently propagated by a strain of *E.coli* that does not support the replication of cruciform structures (Sharples, *et al.*, 1994; Connelly, *et al*., 1998).

Predicted stability of mismatched RNA hairpins

It was of utmost importance that mismatched IR constructs made in this study decreased the stability of DNA secondary structures without compromising the formation dsRNA, which is required to induce PTGS. RNA-RNA binding interactions are the sum of two energy contributions. Essentially, the energy gained from intermolecular hybridization needs to exceed the energy required to free the respective binding regions from any intramolecular interactions that they may be involved in (Muckstein, *et al*., 2006). In the current study, the mismatches created in the RNA hairpins effectively reduce the amount of free energy gained by the hybridization of the two arms. As a result, it is possible that sections of the individual arms may find more favorable intramolecular interactions, and will therefore fold in on itself rather than hybridize to the opposite arm.

Automated sequencing was done to confirm the presence of IRs in the constructs produced for this study. The sequences were submitted to the MFOLD application to predict RNA secondary structure. Both the SACMV BC1 and MSV AC1 IRs folded into long hairpin RNA molecules. The AC1 hairpin was evidently more unstable than the BC1 hairpin. Whilst the BC1 RNA folded into an almost-perfect hairpin with a 6bp loop, small sections of the AC1 RNA appeared to fold back on itself (Fig 2.14.A,B). Towards the loop section of the hairpin, the folding of short sections of the sense and anti sense arms folded back onto their respective strands. This causes the formation of two smaller stem-loop structures, along with an unpaired 'bubble' region. We can therefore conclude that the number of mutations near the loop region of the AC1 hairpin has significantly destabilized the loop. As a result, intramolecular interactions are more favorable.

GU base pairs are unusually stable in comparison with other non-Watson and Crick base pairings, and are processed as canonical base pairings by folding algorithms (Schroeder, *et al*., 1996). In fact, short hairpin loops closed by GU base pairs are approximately 0.7kcal/mol more stable than loops closed by GC/CG base pairs (Giese, *et al*., 1998). It has also been shown that the orientation of the purine and pyrimidine bases in a base pair have a marked

influence on the stability of a hairpin, especially at the closing base pair (Vecenie and Serra, 2004). For example, short hairpins closed by UG base pairs, are 1.3 kcal/mol less stable than those closed by GU base pairs. Due to the unusual stability of GU mismatches, especially when they are the closing base pair, they have been found to increase the relative stabilities of other non-Watson and Crick base pairings adjacent to them (Vecenie, *et al*., 2006). Consequently, it may be unfavorable to have too many GU mismatches, and the mutation efficiency achieved on the BC1 construct produced an ideal number of mismatches on the sense arm. As a result, the secondary structure of the BC1 DNA was sufficiently destabilized, whilst the stability of the RNA hairpin was relatively unaffected. Whilst the MSV AC1 construct had stable DNA, the RNA hairpin structure seems to be compromised around the loop region, due to the number of GU mismatches localized there.

CHAPTER 3

Agrobacterium-mediated transformation of *Nicotiana benthamiana*

3.1. Introduction

Cassava transformation

Cassava is one of the major staple food crops in the developing world, and it is already being cultivated on more than 16 million hectares of land worldwide (Taylor, *et al*., 2004). It is a primary source of food for 700 million people internationally, and is the 2nd most important source of calories in Africa (Fauquet, 2004). The majority of cassava is cultivated as a sustenance crop by resource-poor farmers and communities in developing countries. Despite this, cassava has major potential for industrial starch production to be used in the paper, textile, and biofuel industries, amongst others. For this reason, the genetic improvement of cassava has become a priority in many countries. Despite this, cassava is a difficult and poorly studied plant. In an effort to enhance global food security and afford economic opportunities to developing nations, the Global Cassava Partnership for Genetic Improvement (GCP-GI) was founded in October 2002 (Fauquet, 2004). This partnership aims to streamline cassava research and prioritize the delivery of genetically improved cassava cultivars.

There are currently four main systems of cassava transformation that have successfully been used to yield stable transgenic plants. Friable embryogenic callus has been transformed by either particle bombardment or *Agrobacterium*-mediated gene-transfer, and plants were subsequently regenerated through somatic embryogenesis (Gonzalez de-Schopke, *et al*.,1998; Taylor, *et al*., 2001). Similarly, cotyledon fragments have been transformed by either particle bombardment or *Agrobacterium*-mediated gene-transfer, and shoot regeneration was used to produce full plants (Li, *et al*., 1996; Zhang, *et al*., 2000). The remaining two systems involve *Agrobacterium*-mediated gene transfer to embryogenic structures or immature leaf explants, which are later regenerated through somatic embryongenesis (Arias-Garzon and Sayre, 2003; Siritunga and Sayre, 2003).

Agrobacterium-mediated transformation reportedly results in single-copy insertion in approximately 50% of reported cases, whereas particle bombardment leads to multi-copy insertions in 90% of reported cases (Taylor, *et al*., 2001). Multiple insertions of a transgene have been linked to transgene silencing and genetic rearrangements (Meza, *et al*., 2002). As a

result, *Agrobacterium*-mediated gene transfer has become a transformation agent of choice for the production of transgenic cassava.

Agrobacterium-mediated gene transfer

In the 1970's, a soilborne pathogen known as *Agrobacterium tumefaciens* was found to be the causing agent of crown-gall tumors in plants, and further investigation revealed that this was due to plasmid encoded virulence genes (Van Larebeke, *et al*., 1974). It was subsequently observed that small sections of these tumor inducing (Ti) plasmids were permanently transferred to the plant genome, which gave rise to further studies of *Agrobacterium's* potential use as a vector for DNA transfer (Chilton, *et al*. 1977). *Agrobacterium* has since become widely used and studied due to its unique ability for trans-kingdom gene transfer, and the transformation of plants, fungi, various prokaryotes, and even human cells have been reported (Kunik *et al*., 2001). The genetic transformation of plant cells has been particularly useful in agricultural biotechnology.

The molecular mechanisms behind *Agrobacterium*-mediated gene transfer remain somewhat vague, despite intensive research spanning several decades. Many major economically important crops such as corn, soybeans, cotton, canola, potatoes and tomatoes have been genetically transformed by *Agrobacterium*-mediated gene transfer (Gelvin, 2003). Not all crops are equally susceptible to infection by *Agrobacterium*. Early work indicated that the Ti plasmid is involved in host range determination (Thomashaw, *et al*., 1980). The ability of particular plants to be transformed by *Agrobacterium* can be predicted based on whether or not they form crown gall tumors upon infection with a particular strain. Several virulence factors on the Ti plasmid, such as *virC*, *virF* and *virH* have reportedly been implicated in the host range determination of *Agrobacterium* (Yanofsky and Nester, 1986; Jarchow, *et al*., 1991; Regensburg-Tuink and Hooykaas, 1993). It has been found that a particular Ti plasmid may interact differently with a particular bacterial genome, thereby affecting the host rage of that strain (Hood, *et al*., 1987).

Agrobacterium tumefaciens-mediated gene transfer is based on the ability of *Agrobacterium* to transfer a section of its large tumor-inducing (Ti) plasmid into the genome of a plant. Generally, the transferred section of DNA does not exceed ~10% of the overall size of the plasmid, and these sections of DNA are known as T-DNA (Ballas and Citovsky, 1997). It has been found that T-DNA is always flanked by 25bp border sequences that are highly

homologous and arranged in a direct repeat orientation (Peralta and Ream, 1985; Rubin, 1986). These sequences are reportedly polarized, and can be defined as being either a right or a left border (Jen and Chilton, 1986). Some products of the *Agrobacterium* virulence genes, such as VirD1 and VirD2 endonucleases, have been shown to bind to the border sequences where-after VirD2 can reportedly cause single stranded nicks in the bottom strand (Stachel, *et al*., 1986). The VirD2 protein apparently binds to the 5' end of single stranded nicks, and this ssDNA T-strand, as it is termed, is then transferred to the plant (Tinland, *et al*., 1994). The binding of VirD2 specifically to the right border ensures that a sense copy of the T-DNA is inserted into the plant genome.

Other products of the virulence genes, such as the VirA and VirG proteins, are reportedly involved in signaling pathways, and the transcriptional activation of additional virulence genes. VirA is a sensory protein that is apparently activated in the presence of certain phenolic compounds released by wounded plants (Jin, *et al*., 1990). VirA then phosphorylates VirG, which is involved with transcriptional activation or enhancement of additional virulence genes.

The VirD4, VirF, and several VirB proteins are involved in the secretion of the T-DNA/VirD2 complex by forming channel membranes, ATPases, or pilus structures (Jones, *et al*., 1996; Vergunst, *et al*., 2000). The VirE2 and VirD2 proteins are known to be the essential components of *Agrobacterium* mediated gene transfer. VirE2 is thought to form a complex with the single stranded T-DNA, along with VirD2 which is bound to the 5` end, and this complex is then transferred to plant cells (Howard, *et al*., 1989). The exact molecular mechanism remains controversial, and several conflicting models have been proposed, mostly dealing with the transportation of T-DNA into the nucleus and integration of the T-DNA into the plant genome.

It has been suggested that the transformation efficiency of crop species like cassava, which are particularly recalcitrant to transformation, could be improved by manipulating the plant and not the bacterium. Several plant genes involved in *Agrobacterium*-mediated transformation have been identified. Interestingly, these genes are reportedly up-regulated in plant species that are readily transformable. This suggests that it may be possible to improve plant genetic engineering by enhancing the expression of particular plant genes involved in *Agrobacterium* mediated transformation.

Despite all the advances made in the optimization of *Agrobacterium*-mediated transformation of cassava, currently available methods remain labor intensive, inefficient, and requires upwards of 8 months for completion. For technologies such as RNAi, where numerous transgene constructs need to be screened and tested for efficacy, these methods are simply too laborious, expensive, and inefficient.

In similar studies utilizing PTGS in transformation-recalcitrant species of plants, tobacco has been used as a model system to test the efficacy of stably integrated RNAi constructs *in vivo,* before further transformations were attempted (Nakatsuka, *et al*., 2007). It is the aim of the current study to optimize a transformation and regeneration protocol for *Nicotiana benthamiana*, which will serve as a rapid model system to test inverted-repeat, and other gene silencing constructs *in vivo*. In addition, real time RT-PCR assays for gene-knockdown were designed and optimized. This work will contribute to future studies towards the development of virus-resistant transgenic cassava.

3.2 Specific Aims

The aim of the current study was to develop and optimize a rapid method for the *in vivo* screening of stably integrated gene silencing constructs in *Nicotiana benthamiana*. This will allow for the selection of efficient gene silencing constructs, thereby reducing the amount of labor-intensive transformations and screening required to produce virus-resistant transgenic cassava.

In this chapter, we contributed to the following aims:

i. Transformation of *Agrobacterium tumefaciens* strain AglI with a mismatched IR construct (pBC1hpCAM).

ii. Optimization of *Agrobacterium*-mediated gene transfer to *N.benthamiana* leaf disks.

iii. Comparison of the transformation efficiency between *N.benthamiana* leaf disks and auxiliary buds.

iv. Optimization of procedures to regenerate fully grown, rooted *N.benthamiana* plants from transformed leaf disks.

v. Design and optimization of a real time absolute quantitative RT-PCR assay to assess SACMV gene knockdown.

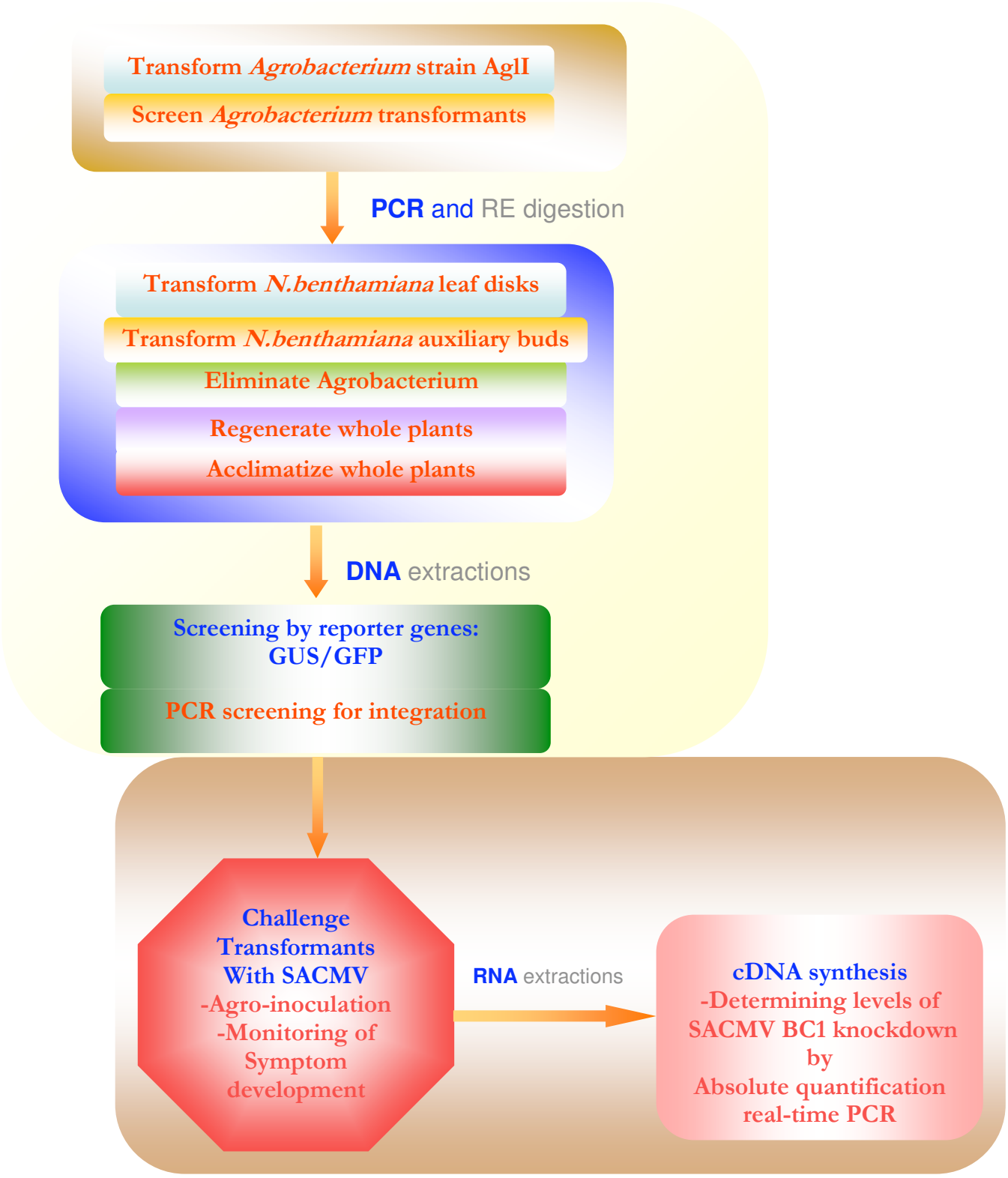

Figure 3.1 Flow diagram giving an overview of the main methodology followed in this study.

3.3 Materials and methods

3.3.1 Transformation of *Agrobacterium tumefaciens*

Agrobacterium tumefaciens strain AglI was transformed with pBC1hpCAM using a modified version of the freeze-thaw method by Holsters, *et al.*, (1978). An overnight culture of *A.tumefaciens* strain AglI was sub-inoculated into Luria Bertani broth (LB) containing 100µg/ml carbenicillin. The cells were incubated at 28°C until an OD_{600} of 0.66 was reached. The culture was chilled on ice, and centrifuged at 5000 rpm for 10 minutes at 4°C. The pellet was resuspended in 20mM ice cold calcium chloride. Approximately 1µg of purified pBC1hpCAM was added to the cells, after which they were flash-frozen in liquid nitrogen. Following this, cells were thawed on a 37°C heating block for 5 minutes, and then incubated with gentle shaking in 1ml LB broth for 3 hours at 28°C. Cultures were finally spun down and resuspended in 0.1ml LB, before being spread plated onto Luria Bertani agar (LBA) plates containing 100µg/ml carbenicillin and 100µg/ml kanamycin. Plates were incubated at 28°C for 3 days in the dark. Colonies were then randomly picked off these plates and inoculated into fresh LB broth containing 100µg/ml carbenicillin and 100µg/ml kanamycin.

3.3.2 Screening of putative *Agrobacterium* transformants

Plasmid DNA was extracted from the presumptive clones using an alkaline lysis-based High Pure Plasmid Miniprep kit (Roche Applied Science). Purified plasmid DNA was quantified on a Nanodrop 1000 spectrophotometer (Nanodrop). Restriction digestion and PCR amplification was done to screen the *Agrobacterium* transformants for pBC1hpCAM. Double digestions using *Eco*RI and *Hind*III (Fermentas) were done to screen for the presence of a 2.8kb fragment. In addition, a digestion with *Xho*I (Fermentas) was done to confirm the presence of the hairpin cassette.

PCR amplification was done using the pART 7(cassette) primers, as these would only amplify the plasmid DNA if the cassette from pART7 is present. The reaction mixture contained 0.4µM of each primer, 500µM dNTPs, 2.5mM $MgCl_2$, 2.5U High Fidelity Polymerase Blend (Roche Applied Science), 1X FastStart High Fidelity reaction buffer (Roche Applied Science), 5% DMSO (v/v), and nuclease free water to a final volume of 50µl. Approximately 20ng of template DNA was added to the reaction mixture. In addition,

amplifications were done using 10ng of pART7 as a positive control, and 10ng of pCAMBIA1303 as a negative control. Reactions were cycled in a MyCycler™ Thermal Cycler (Bio-Rad) at 95°C for 2 minutes to activate the polymerase mix, followed by 35 cycles of denaturation at 95°C for 30 seconds, annealing at 55°C for 30 seconds, primer extension at 72°C for 3 minutes, and a final extension step of 72°C for 10 minutes. Amplification products and restriction fragments were examined by electrophoresis on a 0.8% agarose gel containing 10µg/ml ethidium bromide. Electrophoresis was carried out in a 1x TAE (Tris-Acetate EDTA) buffer at 80V.

3.3.3 Transformation of *Nicotiana Benthamiana* leaf disks and auxiliary buds

A modified version of an optimized tobacco transformation protocol by Narváez-Vásquez, *et al*. (1992), was followed. Leaf disks (0.5 cm x 0.5 cm) were cut from the young leaves of one month old *N.Benthamiana* plants, grown from seed on Murashige and Skoog media (MS2), pH 5.8, supplemented with 2% sucrose and solidified with 0.8% purified agar (Murashige and Skoog, 1962). The leaf disks were then incubated overnight at 25°C, adaxial side down, on solid MS2 media. Similarly, auxiliary buds were cut from one month old tobacco plants, and sub-cultured on MS2 media overnight.

A small aliquot of frozen *Agrobacterium,* containing pBC1hpCAM, was grown up at 28°C overnight in 30ml LB broth containing 100µg/ml kanamycin and 100µg/ml carbenicillin. The following day, 1ml of the overnight culture was sub-inoculated into 30ml fresh LB broth containing 100µg/ml kanamycin and 100µg/ml carbenicillin. The culture was incubated at 28°C , with gentle shaking, until an OD_{600} of ~1.0 was reached. Cells were then pelleted by centrifugation at 5000 rpm for 15 minutes, after which they were resuspended in 10ml freshly prepared and autoclaved liquid MS2 media. At this stage, 40µl of a 50mM acetosyringone stock solution was added to the resuspended cells.

The *Agrobacterium* solutions were poured into sterile 100ml Schott bottles in a laminar flow hood. Approximately 25-40 leaf disks/auxiliary buds per bottle were then aseptically transferred into the *Agrobacterium* solutions. Agroinfiltration was done in a vacuum chamber at 85kPa for 10 minutes. Following this, the bottles were sealed and incubated on a shaking platform at room temperature for 30 minutes with gentle swirling. Leaf disks and auxiliary buds were then aseptically removed and placed adaxial side down onto solid MS2 media. Co-

cultivation of *Agrobacterium* and the tobacco explants then proceeded at 28°C for three days in the dark.

A total of seventy leaf disks were transformed. Of these, forty leaf disks were transformed using *Agrobacterium* strain AglI containing pBC1hpCAM. A further twenty were transformed using *Agrobacterium* strain AglI containing pCAMBIA1303 as a positive control. As a negative control, ten leaf disks were treated with *Agrobacterium* strain AglI only. A total of twenty auxiliary buds were transformed. Half of these were transformed using *Agrobacterium* strain AglI containing pBC1hpCAM, whilst the other half were transformed with *Agrobacterium* strain AglI containing pCAMBIA1303 as a positive control.

3.3.4 Removal of *Agrobacterium* after co-cultivation

After three days of co-cultivation, leaf disks and auxiliary buds were rinsed three times with freshly prepared and autoclaved liquid MS2 media containing 500mg/l cefotaxime. The explants were then incubated at room temperature for two hours in fresh liquid MS2 media containing 500mg/l cefotaxime.

Leaf disks were then transferred, adaxial side down, onto solid MS2 media containing 500mg/l cefotaxime, 1.0mg/l BAP and 0.1mg/l NAA. Auxiliary buds were transferred to solid MS2 media containing 500mg/l cefotaxime only. These were incubated in a growth chamber at 25°C under a 16 hour photoperiod for one week.

3.3.5 Antibiotic selection of transformants

For the antibiotic selection of transformants, leaf disks were aseptically transferred to solid MS2 media containing 30mg/l hygromycin, 1.0mg/l BAP and 0.1mg/l NAA. Auxiliary buds were aseptically transferred to solid MS2 media containing 30mg/l hygromycin and 250mg/l cefotaxime only. Explants were incubated in a growth chamber at 25°C under a 16 hour photoperiod for three weeks.

3.3.6 Rooting and shooting of putative transformants

After the three week incubation period, any shoots appearing on leaf disks were allowed to elongate slightly before being excised and transferred to fresh media. Shoots were either transferred to; (A) rooting media (MS2 containing 1.0mg/l NAA, 0.1mg/l BAP, and 250mg/l cefotaxime), (B) elongation media (MS2 containing 1.0mg/l BAP, 0.1mg/l NAA, 1.0mg/l GA_3 and 250mg/l cefotaxime), or (C) plain MS2 media. Plants were incubated in a growth chamber at 25°C under a 16 hour photoperiod until sufficient rooting had occurred.

3.3.7 Screening for putative transformants by the histochemical detection of GUS (beta-glucoronidase)

The GUS assay was performed according to a modified protocol by Sambrook and Russel (2001). A staining buffer (0.1mM sodium phosphate, pH 7.0; 10mM EDTA, pH 8.0; 0.1% Triton X-100; 1mM $K_3Fe(CN)_6$) was prepared and 1ml 0.1M X-Gluc in dimethylformamide (Fermentas) was added to this. Explants were submerged in the staining solution for 24 hours at 37°C. Blanching was then done by washing the tissues with several changes of 50% ethanol until the tissues were completely white. Tissues were then examined on an Olympus XZ60 dissecting microscope (Japan), and photographed using a Nikon DXM1200 digital camera (Japan).

3.3.8 Screening for putative transformants by the visualization of green fluorescence protein (GFP)

Visual detection of GFP fluorescence in whole plants was performed using a 100 W handheld long-wave ultraviolet lamp (Blacklight, GE products). Confocal microscopy was performed under a Leica DMR module coupled to a Leica TCS-NT system. A 100 mW Argon ion laser was used to produce excitation light at 488 nm (emission filter, 522 nm).

3.3.9 Acclimatization of putative transformants

Acclimatization procedures were carried out based on a modified protocol of Pierce and Rey (by personal communication, 2005). Putative transformed lines were removed from tissue

culture, and residual MS2 media was rinsed from the roots. To retain the required nutrients and humidity, the putative transformants were planted in peat pellets (Jiffy Products International), and placed in seed trays covered with plastic wrap. Plants were incubated in a growth chamber at 25°C under a 16 hour photoperiod. Three or more small slits were made in the plastic covers weekly, thereby systematically acclimatizing the plants. After three weeks, the plastic covers were removed and plants were watered daily or as required. Twenty one putative transformants were acclimatized as described.

3.3.10 Extraction of total nucleic acids (TNA)

TNA was extracted from explants using the cetyl trimethyl ammonium bromide (CTAB) extraction method of Doyle and Doyle (1987). For each plant, a 50mg sample of tissue was snap frozen in liquid nitrogen and ground into a fine powder. The fine powder was immediately suspended in 500µl extraction buffer (2% CTAB, 20mM EDTA, 1.4M NaCl 100mM Tris, pH 8.0) at 65^{o}C, and 1µl β-mercaptoethanol was added. The tubes were incubated at 65^{o}C for 60 minutes. TNA was extracted from the aqueous layer by adding 500µl chloroform:isoamyl alcohol (24:1), inverting, and centrifuging at 14000 rpm at 4^{o}C for 10 minutes. This step was repeated to ensure maximum purity of the final extract. Nucleic acids were precipitated with an equal volume of isopropanol, and centrifuged at 14000 rpm at 4^{o}C for 10 minutes. The pellet was washed with 500µl ice-cold 70% ethanol and centrifuged as before. Finally, the pellet was vacuum dried and resuspended in 50µl TE buffer (10mM Tris, pH 8.0, 1mM EDTA) containing 20 µg/ml RNase A (Fermentas). The genomic DNA extracts were quantified on a Nanodrop 1000 spectrophotometer (Nanodrop).

3.3.11 Screening for putative transformants by PCR amplification of *hptII*

To screen putative transformants for the transgene, PCR amplification of a 200bp fragment of the *hptII* gene on pCAMBIA1303 was done. The primer set hptII F (5'[CTATTTCTTTGCCCTCGG]3`) and hptII R (5'[TTCGATGATGCAGCTTGG]3`) were used. The reaction mixture contained 0.4µM of each primer, 200µM dNTPs, 2.5mM $MgCl_2$, 2U Econo*Taq* DNA polymerase (Lucigen), 1x EconoTaq Buffer (Lucigen), and nuclease-free water to a final volume of 50µl. Approximately 500ng of the genomic DNA template was added to the reaction mixture. Reactions were cycled in a MyCycler^{TM} Thermal Cycler (Bio-Rad) at 95^{o}C for 2 minutes to activate the *Taq* DNA polymerase, followed by 30 cycles of

denaturation at 95°C for 15 seconds, annealing at 57.5°C for 15 seconds, primer extension at 72°C for 15 seconds, and a final extension step of 72°C for 5 minutes. As a negative control, genomic DNA extracted from a wild-type tobacco plant. As a positive control, pCAMBIA1303 was used. Amplification products were examined by electrophoresis on a 1.2% agarose gel containing 10µg/ml ethidium bromide. Electrophoresis was carried out in a 1x TAE (Tris-Acetate EDTA) buffer at 80V.

3.3.12 Agroinfection of putative transformants

Full length SACMV DNA-A and DNA-B head to tail infectious dimers were previously constructed and cloned into the pBIN19 binary vector, and are mobilized in *A.tumefaciens* strain C58C1 (Berrie, *et al*. 2001). Two overnight *Agrobacterium* cultures (one containing the DNA-A dimer and the other containing the DNA-B dimer) were inoculated into 10ml LB broth containing 100µg/ml carbenicillin and 50µg/ml rifampicin. The cultures were incubated at 28°C until an OD_{600} of approximately 0.4 was reached. The cells were then centrifuged at 8000 rpm in 1ml aliqouts, and the pellet was washed with sterile distilled water. After a second centrifugation, cells were resuspended in 200µl LB broth and an equal ratio of the two *Agrobacterium* cultures were mixed. Plants were inoculated with the *Agrobacterium* mixture by injecting a total of 30µl into 3 different positions along the stem.

After one week of acclimatization, twenty one putative transformants and six wild type *N.benthamiana* plants were infected as described. In addition, six wild type *N.benthamiana* plants were infected with *Agrobacterium* strain C58C1 (lacking pBIN19 with the infectious dimers). After inoculation with the infectious dimers, plastic covers were replaced and acclimatization proceeded as described. As a negative control, six healthy wild type *N.benthamiana* plants were grown in peat pellets (Jiffy Products International) from seed, and were maintained separately in a growth chamber at 25°C under a 16 hour photoperiod.

3.3.13 RNA extractions from putative transformants

Total RNA was extracted from SACMV infected *N.Benthamiana* plants at 23 days post-infection (dpi) (putative transgenic plants) and 28dpi (wild type plants). RNA extraction procedures were adapted from the Sigma Tri-Reagent technical bulletin (Sigma). For each plant, a 100mg sample of young leaf tissue was snap frozen in liquid nitrogen and ground

into a fine powder. The fine powder was suspended in 1ml Tri-Reagent (Sigma), and incubated at room temperature for 5 minutes. RNA was separated from DNA and protein by the addition of 200µl chloroform, followed by vigorous shaking, incubation at room temperature for 15 minutes, and centrifugation at 13.4 rpm for 10 minutes at 4°C. RNA was precipitated from the aqueous phase by addition of 500µl isopropanol, and incubation for 10 minutes at room temperature. After being centrifuged for 10 minutes at 4°C, the pellet was washed with 75% ethanol to remove residual chloroform, and centrifuged again. The pellets were briefly air dried, resuspended in 100µl RNAse-free water, and quantified on a Nanodrop 1000 spectrophotometer (Nanodrop). The purity of the extracts were assessed based on the A_{260}/ A_{280} and A_{260}/ A_{230} ratios. After quantification, 1.5µl Ribolock RNAse inhibitor (Fermentas) was added to each sample.

3.3.14 cDNA synthesis from healthy and SACMV-infected *N.Benthamiana*

To denature intrinsic secondary structures, RNA samples were incubated at 70°C for 10 minutes and were plunged into ice immediately prior to cDNA synthesis. Approximately 1µg of RNA was then added to the cDNA synthesis reaction mixtures on ice. The mixtures contained 1x iScript reaction mix with a blend of oligo (dT) and random hexamer primers (BioRAD), 1U iScript Reverse Transcriptase (BioRAD), and nuclease free water to a final volume of 20µl. Tubes were placed in a MyCycler™ Thermal Cycler (Bio-Rad), and incubated for 5 minutes at 25°C to activate the reverse transcriptase and allow for primer annealing, 30 minutes at 42°C for primer extension, and 5 minutes at 85°C to stop the reaction by denaturing the reverse transcriptase. On manufacturers recommendations, a maximum of one-tenth of the cDNA reaction volume, typically 2µl, was added to downstream PCR reactions.

3.3.15 Quantitative real time PCR (Absolute quantification)

Absolute quantification of the BC1 transcript in SACMV-infected *N.Benthamiana* (transformed and wild-type) was done using the cartridge-purified BC1 upstream F(5'[TACGATAACCGACCCAGTTGCGTT]3') and BC1 upstream R(5'[TGCGACTCAA AGGCCGATGTATGA]3') primers to amplify a 100bp region of BC1, situated upstream of the BC1 target region. PCR reactions were set up as recommended in the documentation of the LightCycler® FastStart DNA Master SYBR Green I kit (Roche Applied Science).

Reaction mixtures contained 4mM $MgCl_2$, 0.5µM of each primer, 1µl of 10x LightCycler FastStart DNA Master SYBR Green I, and 2µl sample DNA. Reactions were aliquoted into LightCycler capillary tubes prior to the addition of template DNA. After template DNA was added, the capillaries were sealed and centrifuged for 15 seconds at 3000 rpm. Cycling conditions consisted of an activation mode of 95°C for 5 min, followed by 33 cycles of 95°C for 5 sec, 55°C for 10 sec, and 72°C for 10 sec, with a single acquisition (fluorescence detection at 520nm at the end of the elongation phase for each cycle). A melting curve was performed on the PCR products by heating to 95°C, cooling to 65°C for 30 sec, and slowly heating to 95°C at a rate of 0.1°C/s with continuous measurement of fluorescence at 520nm. The DNA was cooled to 40°C for 10 sec.

The full-length SACMV DNA-B in pBLUESCRIPT was used to amplify the BC1 fragments from known template concentrations of; 10ng/µl, 1.0ng/µl, 100pg/µl, 10pg/µl, and 1.0pg/µl, in duplicate. The average crossing points of these standards were used to plot a standard curve on axis of fluorescence against log template concentration. Subsequently, the number of BC1 transcript molecules present per sample could be calculated by using the following equation:

$$\text{Molecules of transcript} = [(X\text{g DNA}) / (8.58\text{x}10^{5}\text{g.mole}^{-1})] \text{ x } (6.022\text{x}10^{23}\text{molecules.mole}^{-1})$$

Where X is the amount of BC1 cDNA present in grams, as calculated off the standard curve by the Lightcycler data analyses software, LCDA (version 5.32, Roche Applied Science). The constant value of $6.022\text{x}10^{23}\text{molecules.mole}^{-1}$represents Avogadro's number, also known as the Loschmidt constant. The molar mass of the single stranded SACMV DNA-B particles, $8.58\text{x}10^{5}\text{g.mole}^{-1}$, was calculated as follows:

$$\text{Anhydrous Molecular Weight} = (A_n \text{ x } 313.21) + (T_n \text{ x } 304.2) + (C_n \text{ x } 289.18) + (G_n \text{ x } 329.21)$$

Where A_n ,T_n ,C_n , and G_n are the numbers of respective nucleotides present in the SACMV DNA-B viral molecule.

To confirm the melting curve analyses, PCR products were examined by electrophoresis on a 0.8% agarose gel containing 10µg/µl ethidium bromide. Electrophoresis was carried out in a 1x TAE (Tris-Acetate EDTA) buffer at 80V.

Putatively transgenic rooted samples were infected with SACMV during the acclimatization procedure. After twenty-three days, the number of BC1 transcript molecules present in infected plants was determined and compared that of wild-type infected plants at 23 dpi.

An additional study was done on SACMV-infected wild type tobacco at 21 dpi, to determine the number of BC1 transcript molecules present in the symptomatic leaf tissues as opposed to asymptomatic leaf tissues.

3.3.16 The effect of ethylene on the morphology of regenerating plants

Plants showing symptoms of vitrification were sub-cultured on MS2 media with an ethylene scrubber, potassium permanganate. The ethylene scrubber was prepared based on a modified method by Park, *et al*. (2004). A saturated solution of potassium permanganate was prepared by adding 7.43g of crystals to 100ml water at 25°C with gentle swirling. Approximately 100g perlite was added to the potassium permanganate solution to form a soaked perlite slurry. Disposable plastic test-tube caps were filled with the perlite-potassium permanganate slurry, and were sterilized by autoclaving. The sterile potassium permanganate cups were placed on top of solidified MS2 media in glass tissue culture vessels. Nodal cuttings of vitrified plants were sub cultured in these vessels and incubated in a growth chamber at 25°C under a 16 hour photoperiod.

3.4 Results

3.4.1 Screening of putative *Agrobacterium* transformants

After a 3 day incubation period, many putative transformed *Agrobacterium* colonies were present on the LBA plates with antibiotics. Plasmids were isolated from random colonies and screened for pBC1hpCAM by restriction digestion and PCR amplification. Based on an initial screening with *Eco*RI and *Hind*III, four randomly picked colonies all contained a putative pBC1hpCAM plasmid, as restriction fragments of ~12kb (vector backbone) and ~2.8kb (BC1 hairpin cassette) were produced. Further screening was then done by PCR amplification of the cassette, as well as an additional digestion of the putative pBC1hpCAM with *Xho*I. Initial attempts to amplify the hairpin cassette from putative *Agrobacterium* transformants were unsuccessful. All attempts failed when the reaction conditions that were optimized for amplification of the pBC1hpCAM template isolated from *E.coli* was used. After further optimization, it was found that the addition of 5% DMSO (v/v) was sufficient to optimize PCR conditions, and an amplicon of ~2.9kb, as expected, was produced (Fig 2.3). In addition, restriction digestion with *Xho*I produced fragments of 11.7kb, 2.5kb, and 1.1kb, which confirmed that the transformed *Agrobacterium* contained pBC1hpCAM, and that the hairpin cassette was intact (Fig 2.3). Amplification of the positive control, pART7, produced an amplicon of approximately 2.5kb as expected. The negative control, pCAMBIA1303, did not amplify.

3.4.2 Transformation of *N.Benthamiana* leaf disks and auxiliary buds

When overnight cultures of *Agrobacterium* containing the respective plasmids for transformation were sub-inoculated, it was noted that those containing pBC1hpCAM required a prolonged incubation step at 28°C to reach an OD_{600} of ~1.0. The incubation period was increased by approximately 55% when compared to an *Agrobacterium* culture containing pCAMBIA 1303. Leaf disks were then co-cultivated with the respective *Agrobacterium* cultures for three days after agroinfiltration, at which time slight bacterial growth was visible around the edges of the leaf disks and auxiliary buds. These were washed and plated on MS2 media containing cefotaxime for 1 week, after which no bacterial growth was present on or around the explants.

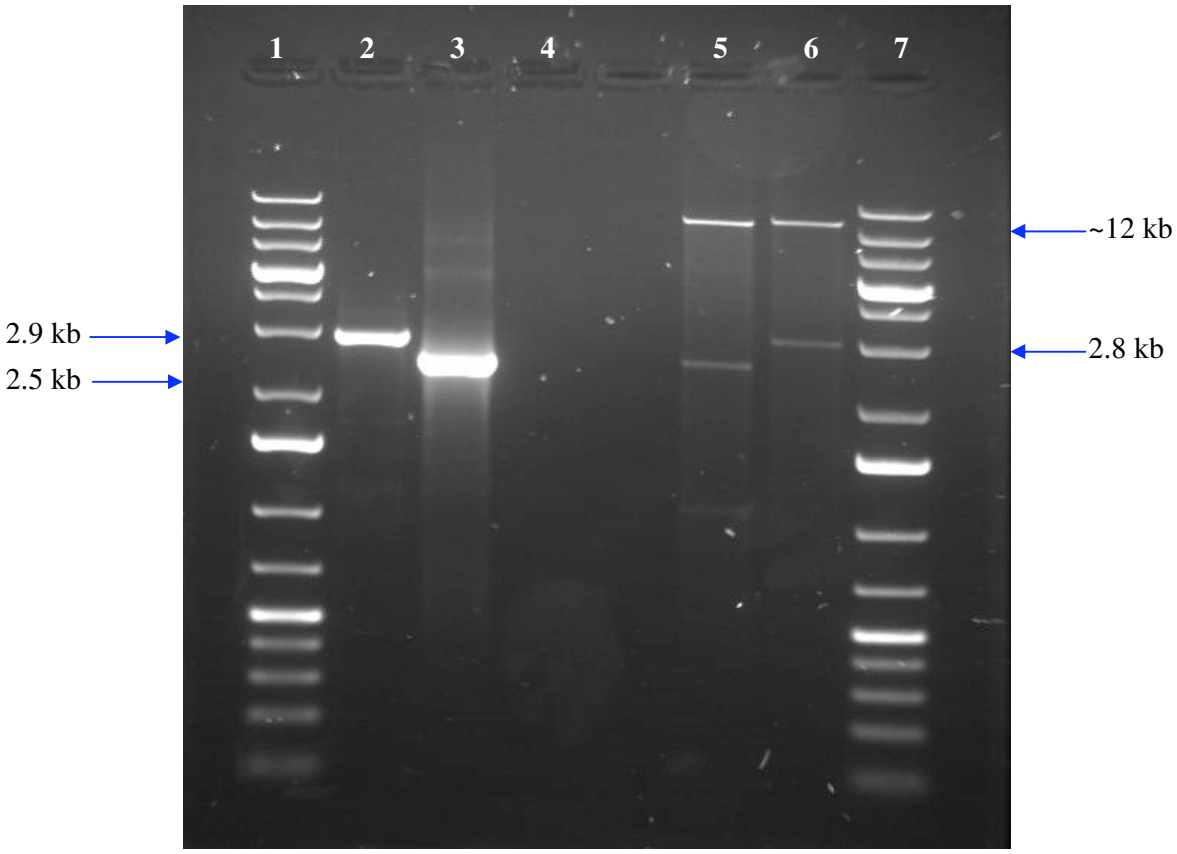

Figure 3.2 0.8% Agarose gel showing PCR amplification of the BC1 hairpin cassette (2.9 kb) from a putative *Agrobacterium* strain AglI transformant (Lane 2). A positive control, pART7, was amplified to produce an amplicon of expected size (Lane 3). The negative control, pCAMBIA1303, did not amplify (Lane 4). Also shown are the restriction fragments generated by digesting plasmids isolated from the putative transformant with *Xho*I (Lane 5) and *Eco*RI (Lane 6). Fragments of expected sizes were produced in all cases, thereby proving that transformations were successful, and that the *Agrobacterium* strain AglI culture that was screened contained pBC1hp7CAM. The sizes of amplicons were estimated in relation to an O'Generuler 1kb Ladder Plus (Fermentas) (Lanes 1 and 7).

3.4.3 Antibiotic selection and regeneration of putative leaf disk transformants

After one week's incubation on MS2 with cefotaxime, the leaf disks had started to expand, swell, and curl inwards from the cut edges (Fig 3.3.A,B). This continued once the leaf disks were transferred to selection media containing hygromycin and hormones for shoot induction. After approximately one week on selection media, the leaf disks had curled up almost completely, and tissues had taken on a thick, brittle texture. Approximately 14-20 days later, small nodes appeared sporadically around the cut edges of the leaf disks (Fig 3.3.B). After 7 days, many of these nodes had started growing small shoots, which were allowed to elongate until a leaf and stem structure was clearly visible (Fig 3.3.C,D). At this point, shoots were excised and transferred to either plain MS2 media, MS2 media with an excess of NAA for root induction, or MS2 media with giberillic acid for the elongation of shoots (Fig 3.3.F,G,H) Once shoots were excised, the leaf disks were placed back on the shooting media, where additional shoots continued to emerge for approximately six weeks, at which time the remaining leaf disk tissue became necrotic. No leaf disk, including the positive and negative controls, were observed to die as a result of selection on hygromycin. In fact, untransformed, negative control leaf disks appeared healthy, and began producing nodes and shoots in advance of their putative transgenic counterparts (Fig 3.3.E). Every leaf disk produced a minimum of 6 shoots, with an average of 10-12 shoots being produced per leaf disk over an eight week period. A set of approximately 120 shoots were transferred to plain MS2 media, rooting media, or elongation media, respectively.

Shoots placed on rooting media were observed to dedifferentiate from the base of the shoot upwards, and after approximately 2 months, the shoots were completely reduced to masses of callus tissue. Shoots placed in elongation media were observed to elongate rapidly, although the stems were abnormally thin and long. The majority of these shoots became increasingly thread-like towards the apex, an dried out as a result. Despite this, many fresh shoots emerged from the base of the stem and did not grow with such rapidity. These shoots were thicker and more robust than the initial shoots, but did not resemble wild type tobacco (Fig 3.4.D). The tissue had a glassy appearance and a brittle texture (Fig 3.4.F, G). Leaves developed, but were irregular in shape, size and texture (Fig 3.4.F, G). None of the shoots on the elongation media rooted. Similarly, shoots placed on plain MS2 media with no hormones or antibiotics developed into abnormal plants with irregular features, despite initially appearing more robust when compared to plants placed on rooting or elongation media (Fig 3.4.E).

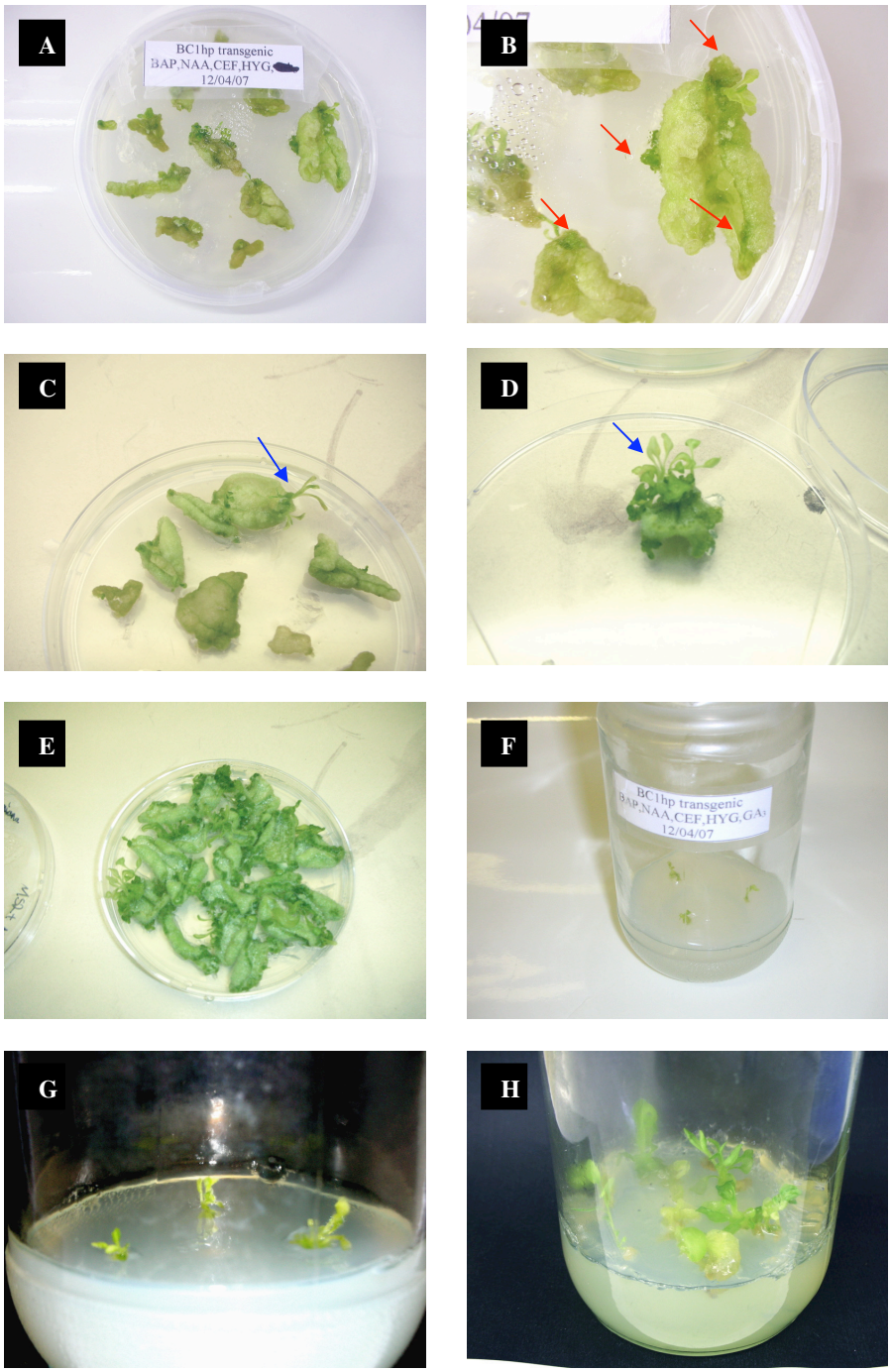

Figure 3.3 Photographs showing; (**A** and **B**) the swelling and curling of leaf disks and the appearance of nodes around the cut edges, as indicated by red arrows, (**C** and **D**) the growth of shoots from nodes on the leaf disks, as indicated by blue arrows, (**E**) untransformed leaf disks growing vigorously and shooting on selection media containing hygromycin, (**F** and **G**) shoots excised from leaf disks and placed in fresh media, and (**H**), shoots after 1 week on plain MS2 media.

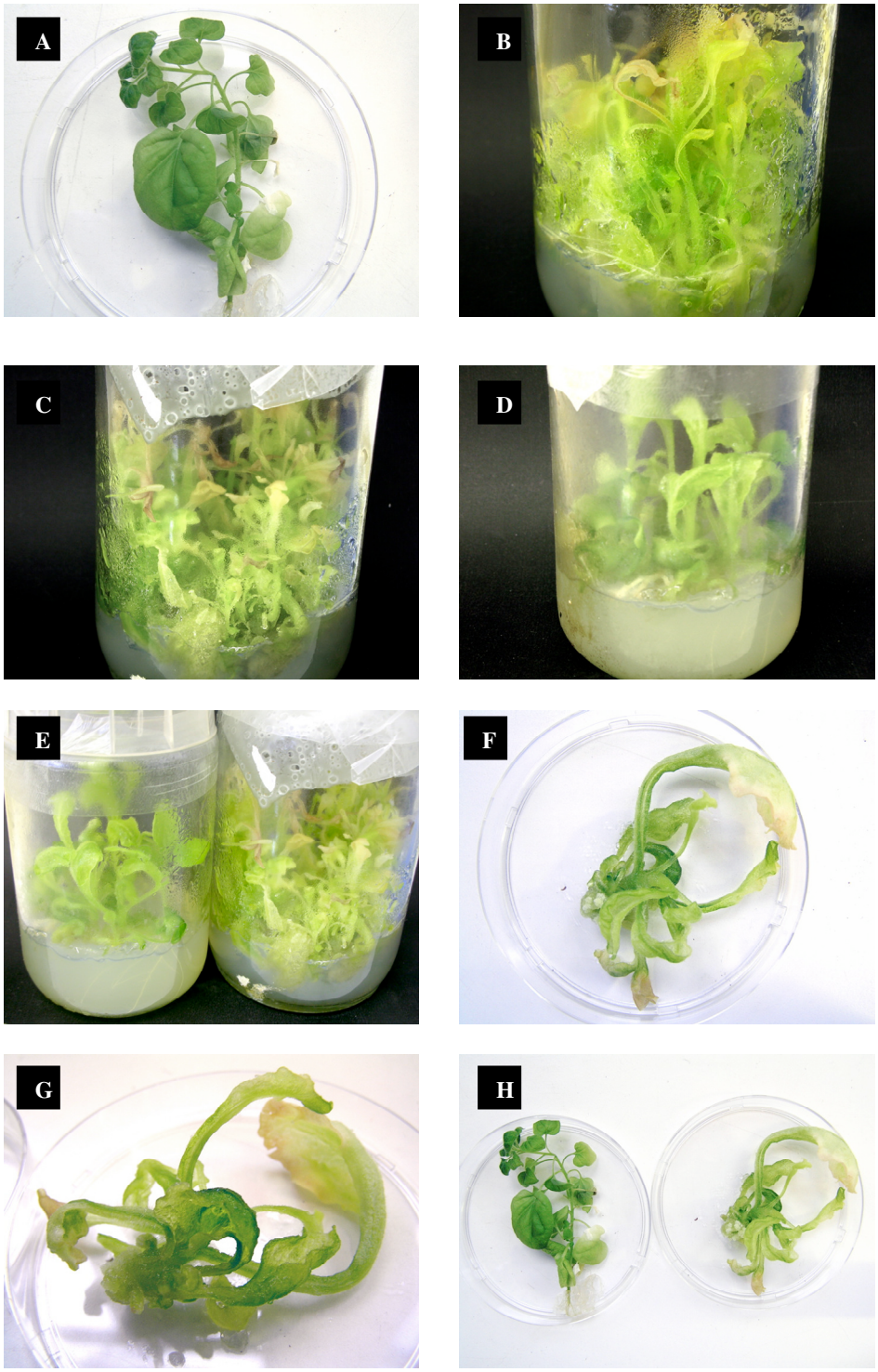

Figure 3.4 Photographs showing; (**A**) Wild-type, healthy tobacco taken from tissue culture, (**B**) putatively transformed tobacco shoots placed on elongation media, (**C**) negative controls/untransformed tobacco placed on elongation media, and (**D**) putatively transformed tobacco shoots placed on plain MS2 media. The majority of putatively transformed plants were abnormal, and had glassy, brittle tissues with deformed leaves (**F** and **G**). The putative transformants placed on different media were compared to one another (**E**), and to wild type healthy tobacco (**H**).

Despite this, approximately 7% of shoots on plain MS2 media grew into plants that were phenotypically normal, and resembled wild-type tobacco. Many of these phenotypically normal plants rooted. However, the majority of plants on plain MS2 had a thick, glassy appearance that was consistent with that of the shoots placed on elongation media, and similarly, these shoots did not root either (Fig 3.4.D, H). The overall rooting efficiency on plain MS2 media was approximately 17.5%. In all instances, the development of control plants was similar to that of the experimental plants, and correspondingly, tissues appeared glassy and brittle whilst rooting was absent in the majority of plants (Fig 3.4.C).

In several instances, the abnormal plants were observed to root through a small lump of callus tissue situated at the base of the shoot, although these roots were not morphologically consistent with those of wild-type tobacco. Random rooted and unrooted samples, being either phenotypically normal or abnormal, were selected for further screening.

3.4.4 Antibiotic selection and regeneration of putative auxiliary bud transformants

After being co-cultivated with *Agrobacterium*, and subsequently being incubated on MS2 media with cefotaxime, the auxilliary buds were transferred to MS2 media containing hygromycin for antibiotic selection. After three weeks, none of the auxiliary buds had died on the selection media. The auxiliary buds developed into small plants with several shoots, and their overall appearance and growth rate was consistent with that of wild-type tobacco. However, none of the auxiliary buds had rooted after three weeks, and several random plants were selected for further screening by use of the GUS assay.

3.4.5 Screening for putative transformants by the histochemical detection of GUS (beta-glucoronidase)

Two weeks after *Agrobacterium*-mediated transformation, random leaf disks and auxiliary buds were incubated in staining buffer to detect the T-DNA-encoded beta-glucoronidase enzyme. Several blue spots could be seen across the surface of the leaf disks (Fig 3.5.E-H). In contrast, most of the auxiliary buds were completely white (Fig 3.5.A-D). In some cases, blue spots were visible on the callus tissue at the base the auxiliary buds (Fig 3.5.C). This callus originated from small pieces of stem tissue that was attached to the auxiliary bud at the time

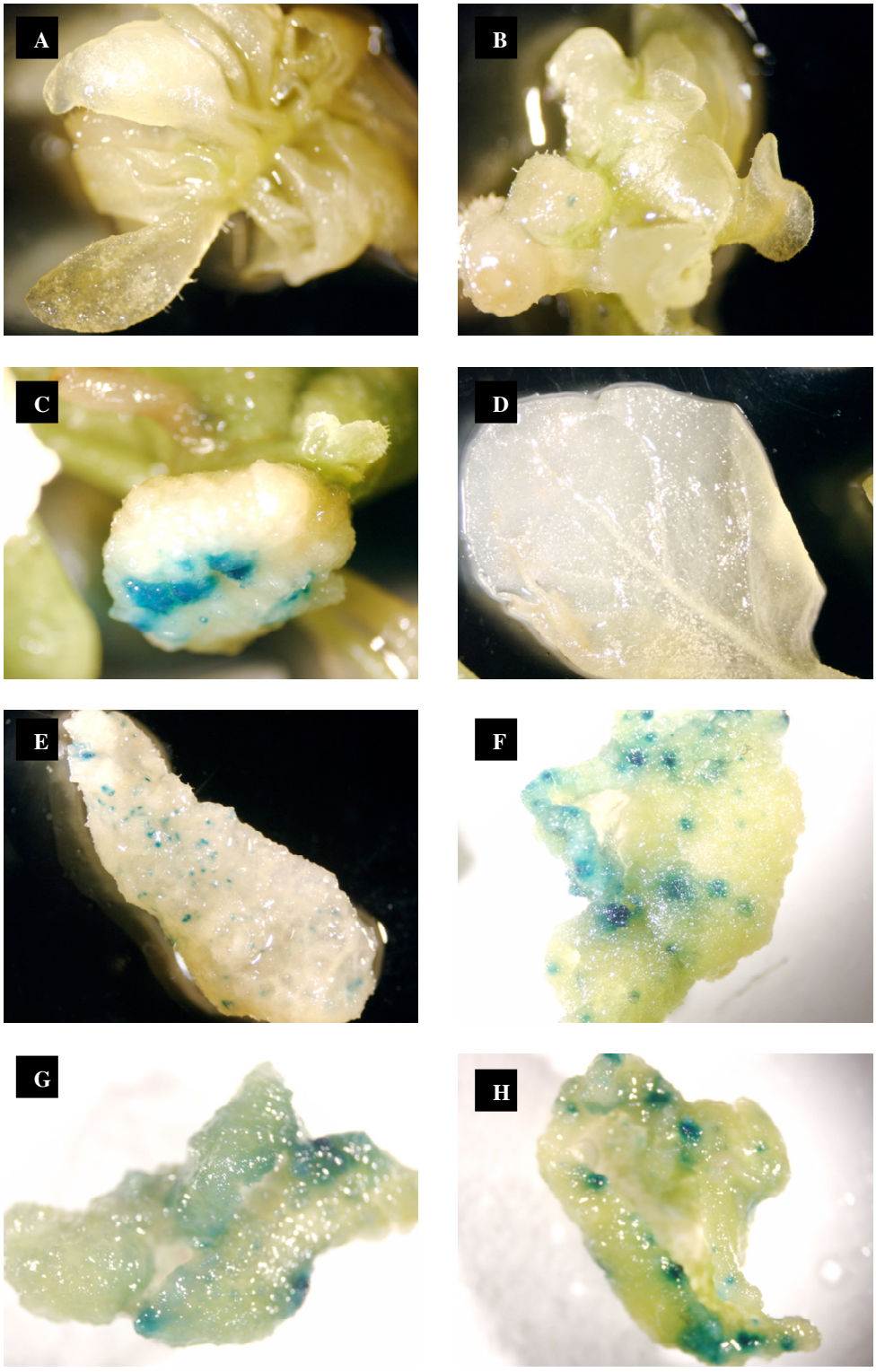

Figure 3.5 Photographs showing the histochemical detection of GUS in *N. benthamiana* auxiliary buds (**A**-**D**) and leaf disks (**E**-**H**). It was noted that GUS was only present in callus tissue at the base of auxiliary buds (**C**), whereas leaf disks contained GUS in localized areas all over the surface of the leaf disk.

of excision from the parental plant. As was expected, positive control leaf disks displayed blue spots, whereas negative controls were completely white. Both positive and negative control auxiliary buds were completely white.

Random shoots were excised as they emerged from nodes on leaf disks, and were stained to detect GUS. Whilst some shoots appeared to be negative or chimeric, the majority were completely blue (Fig 3.6). Positive controls stained completely blue or had blue spots in the case of chimeras, and negative controls stained white, as expected.

After being incubated on plain MS2 media for several weeks, random rooted and unrooted samples were selected, and stained for the detection of GUS. Seemingly, there was no correlation between the detection of GUS and the rooting status of the plant. Based on the GUS assay results, there were fully transformed and chimeric plants in both the rooted and unrooted sample sets (Table 3.1) (Fig 3.7). Positive controls stained completely blue or had blue spots in the case of chimeras, and negative controls stained white, as expected.

3.4.6 Screening for putative transformants by the visualization of green fluorescence protein (GFP)

Thin sections of putatively transformed leaf disks were studied under a confocal microscope. Large aggregates of GFP were visible in tissues from leaf disks transformed using pBC1hpCAM, which was consistent with fluorescence detected in leaf disks transformed using pCAMBIA1303 as a positive control (Fig 3.8.A-D). No green fluorescence was detected in negative control leaf disks, and a photograph of the red autofluorescence as detected though the red channel is shown instead (Fig 3.8.E).

The long-wavelength UV hand lamp could not be used to detect GFP in putatively transformed whole plants due to the glassy, brittle nature of tissues. Both experimental samples and controls displayed a white/blue fluorescence, and the usual red autofluorescence was very faint in comparison to fully grown, wild-type plants.

Attempts to detect green fluorescence from the putatively transformed auxiliary buds were unsuccessful under the long-wavelength UV hand lamp, and only red autofluorescence could be detected. At this point, it was concluded that the auxiliary bud transformations had failed,

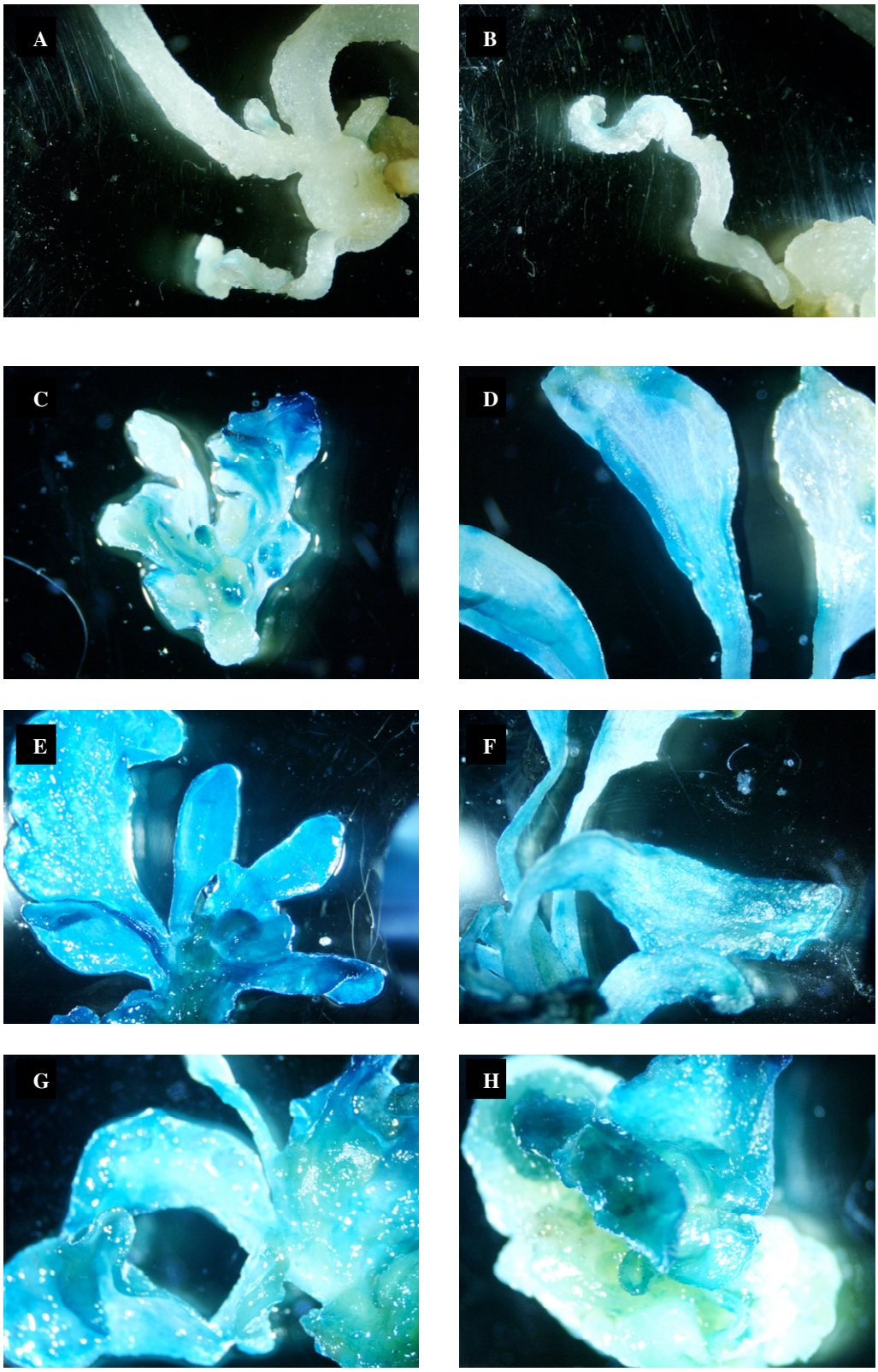

Figure 3.6 Photographs showing the histochemical detection of GUS in young shoots emerging from transformed *N. benthamiana* leaf disks. Chimeras were detected in some cases (**A-C**), but the majority of shoots were completely transformed (**D**-**H**).

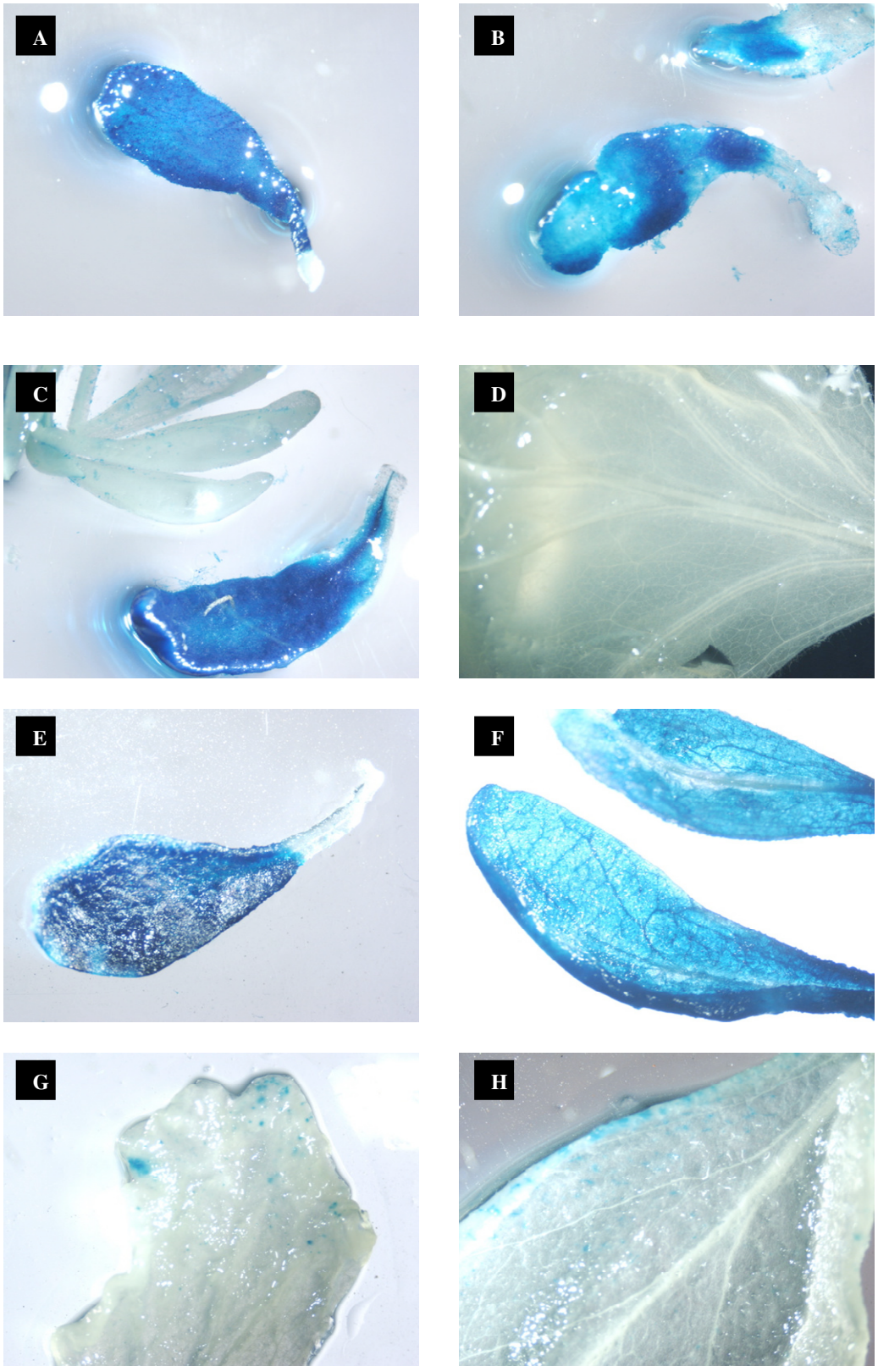

Figure 3.7 Photographs showing the histochemical detection of GUS in *N. benthamiana* shoots after 3 weeks of regeneration on MS2 medium. Both rooted (**A-D**) and unrooted (**E-H**) shoots were tested. In both cases, there were samples that tested positive (**A,B,C,E, F**), negative (**D**), and chimeras were also detected (**G,F**).

Table 3.1 Numbers of transformed, untransformed, and chimeric plants found in a population of randomly screened rooted and unrooted samples

	Transformed	Untransformed	Chimeric
Rooted	2	3	3
Unrooted	2	4	2

A sample size of eight rooted and unrooted samples, respectively, was used.

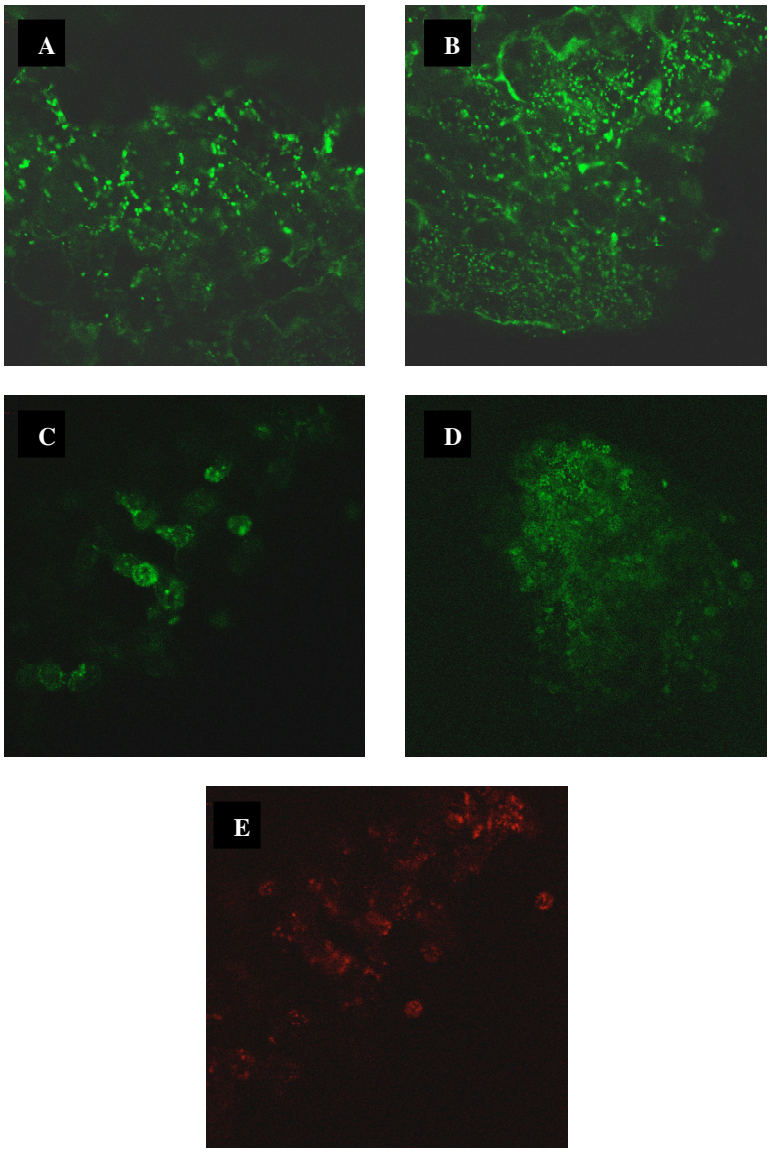

Figure 3.8 Confocal microscope observation of tissue sections cut from putatively transformed *N.benthamiana* leaf disks. GFP was clearly visible as bright green fluorescence in cells transformed with pBC1hpCAM (**A**-**C**). Green fluorescence was also detected in positive control samples transformed with pCAMBIA 1303 (**D**). No green fluorescence could be detected in negative control samples, and the red autofluorescence is shown here (**E**).

and all plant material relating to that study was discarded.

3.4.5 Acclimatization of putative transformants

Twenty one rooted plants, being either phenotypically normal or abnormal, were selected and acclimatized. After three weeks, all plants had died with the exception of two, both of which were phenotypically normal to begin with. The remainder of the plants were mostly atypical, and many died as a result of fungal growth in the peat pellets. Notably, the peat pellets of the surviving plants contained fungal growth as well, but in comparison to the abnormal plants, they were seemingly not severely affected by this.

3.4.6 Agroinfection of putative transformants.

All rooted plants that were acclimatized were also infected with SACMV after 1 week of acclimatization. Twenty three days later, the two surviving plants were highly symptomatic and seemingly had a severe SACMV infection (Fig 3.9). These plants were screened for the transgene by PCR, and quantitative real-time reverse-transcription PCR (RT-PCR) was done to determine the levels of BC1 transcript in the plants.

3.4.7 Screening for putative transformants by PCR amplification of *hptII*

It was noted that TNA extractions from phenotypically normal plants had a 4-10 fold higher yield of DNA in comparison to deformed plants. PCR amplification of a 200bp region of the *hptII* selectable marker gene, situated in the pCAMBIA 1303 T-DNA region, was done to screen putative transformants for the transgene cassette. The two infected acclimatized plants were found to be untransformed, as all attempts to amplify *hptII* were unsuccessful. Seven randomly picked rooted, and unrooted plants, respectively, were similarly screened for the transgene cassette by PCR. In all cases, a 200bp amplicon corresponding to the positive control, pCAMBIA1303, was produced, thereby indicating that all fourteen plants are transgenic (Fig 3.10.A, B). DNA extracts from wild-type tobacco did not amplify, and was used a negative control (Fig 3.10.B). Based on the PCR screening of a total of 21 putative transformants, a transformation efficiency of 86% was achieved in this study.

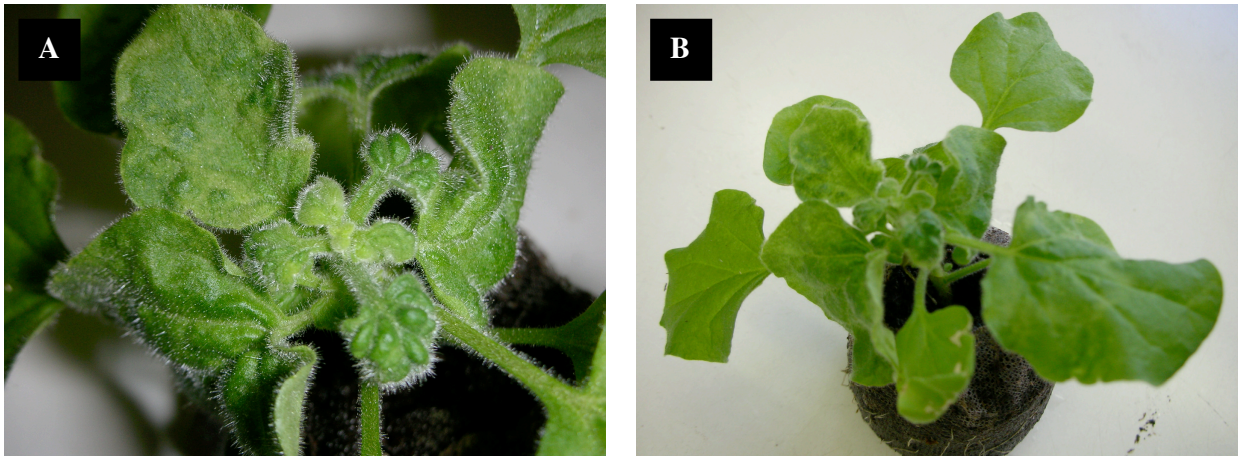

Figure 3.9 SACMV infected *N.benthamiana* plants at 23 dpi (**A** and **B**). Plants appeared highly symptomatic and the youngest tissues towards the uppermost node of the plant were most severly affected.

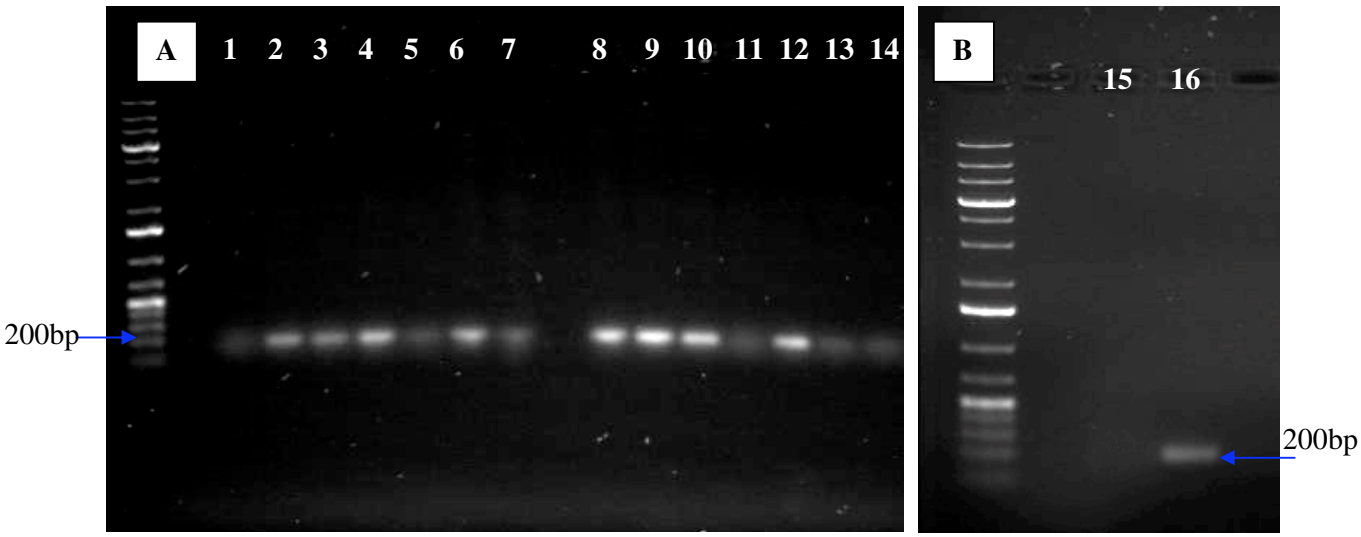

Figure 3.10 0.8% agarose gel electrophoresis was done to examine the amplification products of (**A**) random rooted and unrooted putative transgenic tobacco plants, and (**B**), positive and negative control reactions. It was found that all rooted (Lanes 1 – 7) and unrooted (Lanes 8-14) plants were transgenic, as a ~200bp amplicon was produced in all cases. Genomic DNA extracted from wild-type tobacco plants did not amplify, and was used as a negative control (Lane 15), whilst pCambia1303 was used as a positive control, and produced a 200bp amplicon (Lane 16). The size of amplicons were estimated in relation to an O'Generuler 1kb Ladder Plus (Fermentas)

All attempts to amplify the BC1 hairpin cassette from the genomic DNA of transformed plants, using the pART7(cassette) primers, were unsuccessful. Despite changing the concentrations of DMSO, $MgCl_2$, template DNA, and primers, no amplicons were produced.

3.4.8 Determining levels of BC1 transcript present in transgenic plants by quantitative real time RT-PCR.

A standard curve was constructed using known amounts of SACMV DNA-B (cloned into pBS). The concentrations of template DNA corresponds to a tenfold dilution series starting from $7.02x10^9$ to $7.02x10^5$ SACMV DNA-B molecules per reaction. The crossing points of amplification curves from the tenfold dilution series were equally spaced out, indicating a high level of precision in terms of aliquoting and experimental conditions (Fig 3.11). A trendline was fitted to the crossing point values of the curves (Fig 3.12). The equation of the graph, $y = (-3.360)(X) + (26.46)$ was used for subsequent calculations to determine the approximate amount (in picograms) of the BC1 transcript present in infected samples. Melting curve analyses showed a single peak, indicating that a single species of PCR product was produced. This was confirmed by agarose gel electrophoresis.

Seeing as the majority of rooted plants died during acclimatization, and the surviving plants were not transgenic, this work was done as a pilot study and optimization step for future work. RNA was extracted from the two surviving acclimatized plants after twenty three days post-infection (dpi) with SACMV. Unfortunately, 23dpi control plants had died during acclimatization, and 28dpi plants were kindly donated for use as controls by Ms Farhahna van Schalk. It was found that there was no substantial difference in the number of BC1 molecules present in the 28 dpi control samples as opposed to the 23 dpi samples that had been through the entire transformation procedure. Approximately $4,31x10^{13}$ BC1 transcript molecules were detected in the 23 dpi acclimatized samples, whereas approximately $2.59x10^{13}$ molecules were detected in the 28 dpi wild-type samples. These values were adjusted according to a 100pg standard sample that was amplified to normalize the data in terms of variation between runs. Analysis of the PCR products by melting curve and agarose gel electrophoresis confirmed the presence of a single species of PCR products.

In addition, we wanted to determine the differences between BC1 transcript levels in symptomatic as opposed to asymptotic infected leaf tissue of wild-type tobacco. As expected,

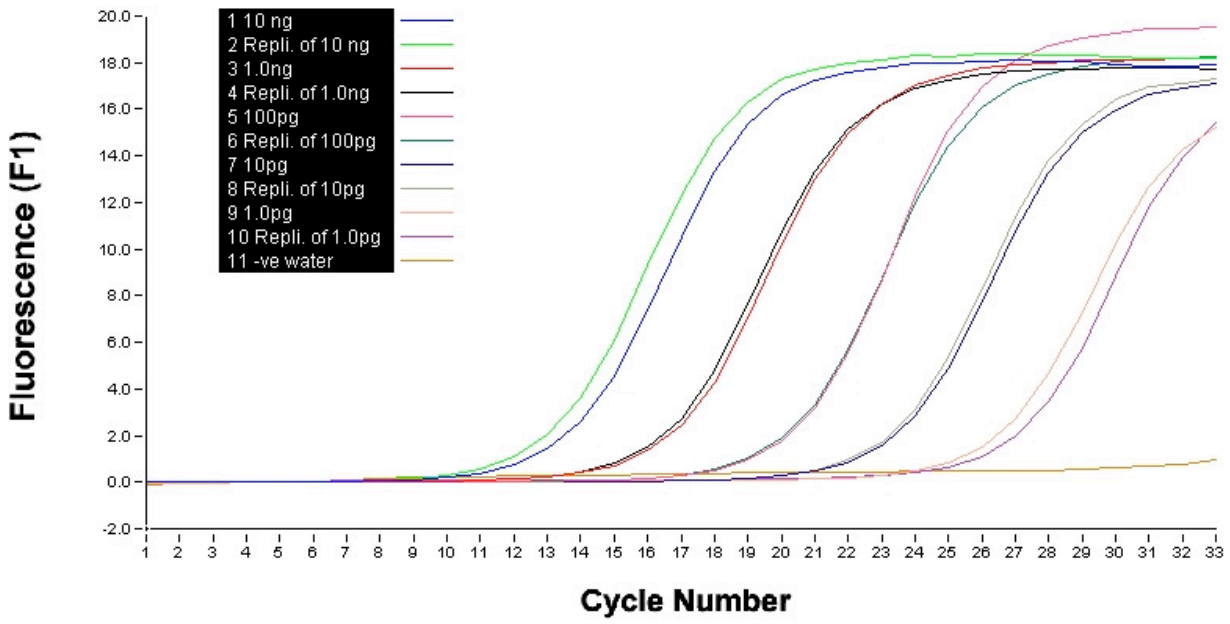

Figure 3.11 Amplification curves of tenfold dilutions made in duplicate from a standard DNA-B (in pBS) amount of 10ng. The crossing point where each sample entered the exponential phase of amplification was measured. The equal spacing between the crossing points is indicative of a precise dilution series.

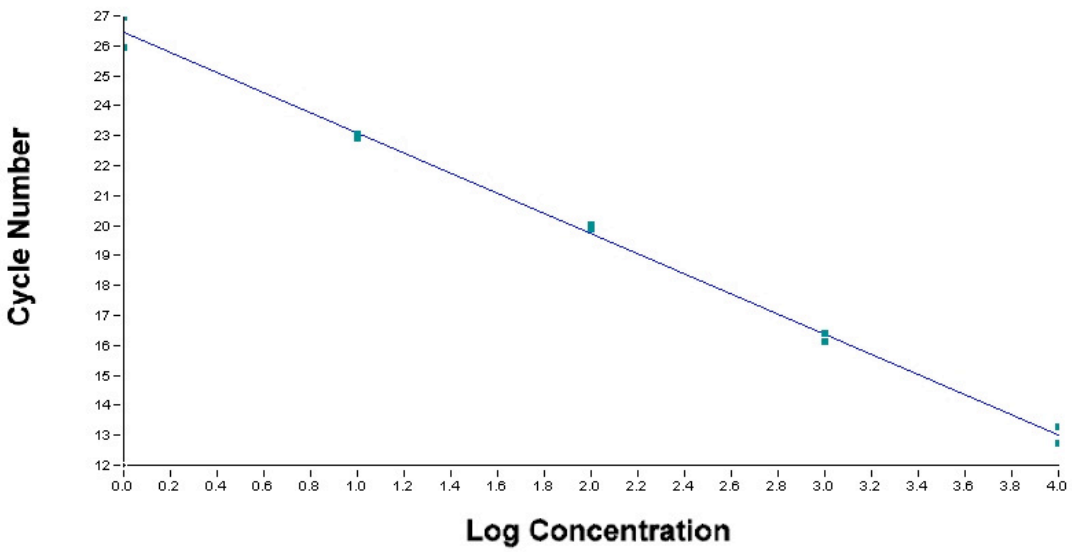

Figure 3.12 Crossing point values from the amplification curves were plotted on a standard curve. The cycle number at which a crossing point occurs can therefore be used to determine the starting concentration of target DNA present in future samples. A trendline was fitted to the data for linear regression of future samples. The trendline fitted the data with an error of 0.0925.

a substantial difference was observed in the number of BC1 transcript molecules detected in young symptomatic leaves as opposed to older asymptomatic leaves.

Approximately $3.54x10^{11}$ molecules were detected in symptomatic leaves, whereas only $8.01x10^{6}$ molecules of the BC1 transcript was detected in asymptomatic leaves. These values were adjusted according to a 100pg standard sample that was amplified to normalize the data in terms of variation amongst runs. Analysis of the PCR products by melting curve and agarose gel electrophoresis confirmed the presence of a single species of PCR products.

3.4.9 Treatment of vitrified plants for phenotype recovery

Seeing as the GUS assay and PCR results failed to relate the presence or expression of the transgene to the abnormal phenotypes and lack of rooting observed in the majority of plants, alternative explanations were sought. In addition, plants having normal phenotypes and roots would often revert to the abnormal phenotype once sub-cultured on fresh MS2 media.

An ethylene scrubber, potassium permanganate, was added to the tissue culture vessels housing freshly sub-cultured tobacco lines that were putatively transformed (Fig 3.13). Within one month, approximately 70-80% of previously deformed plants had returned to their normal phenotypes, and many of these had rooted. Plant tissues were no longer glassy and brittle, and most leaves had typical shapes and textures that were consistent with wild-type tobacco plants (Fig 3.13).

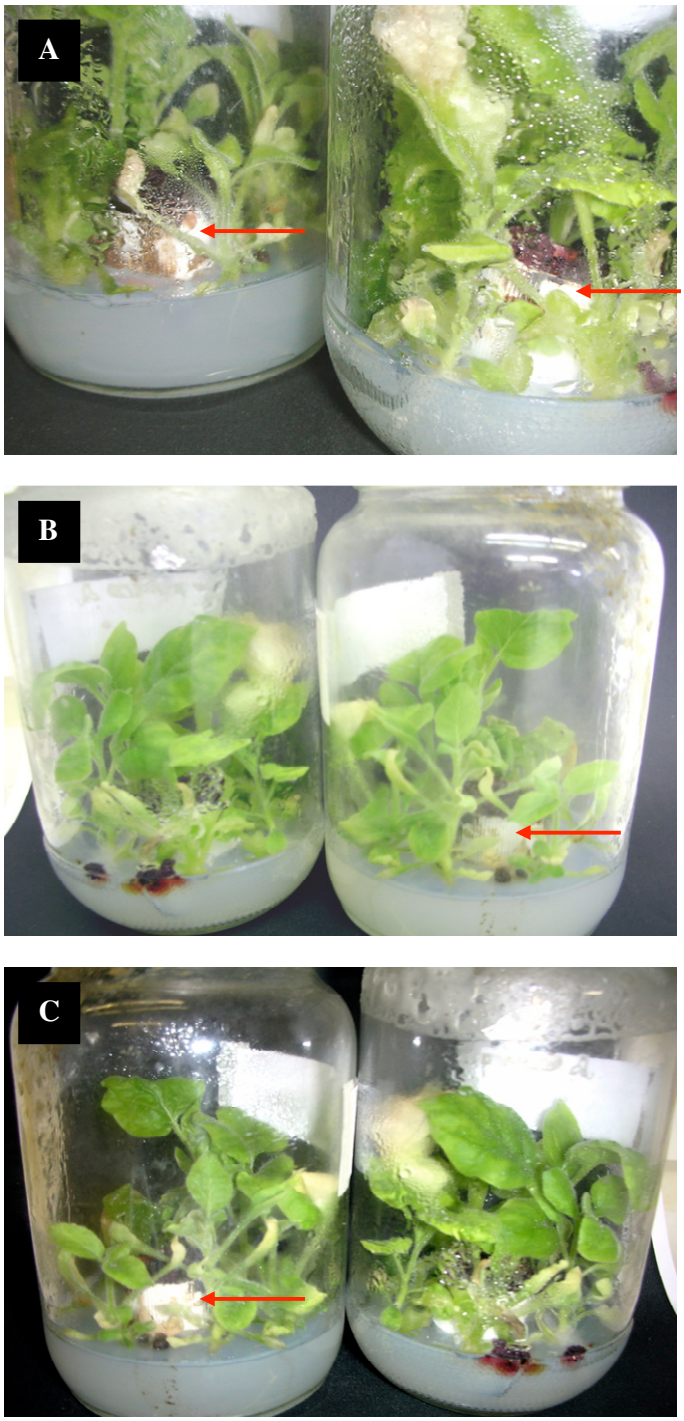

Figure 3.13 Putatively transformed *N.benthamiana* shoots grown on MS2 media for three weeks with an ethylene scrubber, potassium permanganate. The potassium permanganate cups were sterilized and placed inside the tissue culture vessels prior to sub-culturing, and are indicated by red arrows where visible. It was observed that 70-80% of previously deformed plants had regained their phenotype within 3 weeks of being incubated with the ethylene scrubber. In addition, the majority of recovered plants started rooting within 4 weeks.

3.5 Discussion

In this study, a protocol for the stable expression and screening of RNA silencing constructs in *Nicotiana benthamiana* was investigated and optimized. Particular obstacles that are routinely encountered in the regeneration of transgenic plants were resolved and an improved method for the rapid transformation, regeneration, and screening of tobacco is proposed.

Transformation of N.benthamiana

The transformation of tobacco leaf disks and auxiliary buds were attempted in this study, and contrary to what was expected, the leaf *disk* transformation protocol was found to be more efficient. A transformation efficiency of approximately 86% was achieved on leaf disk explants. In contrast, no transgenic auxiliary buds were produced. Based on GUS assays and GFP visualization, it appeared as if parental stem sections surrounding the auxiliary buds were susceptible to infiltration by *Agrobacterium*, however, the auxiliary buds themselves were never infiltrated or transformed. This is consistent with previous attempts at tobacco and cassava auxiliary bud transformation in our laboratory (unpublished data). It is suspected that the dense tissue morphology of the young auxiliary buds limit or prevent the movement of *Agrobacterium* in the intercellular spaces, thereby preventing gene transfer to the auxiliary bud. The successful transformation of tobacco auxiliary buds would have provided a very rapid transformation protocol, as auxiliary buds do not need to be regenerated from single cells into fully grown plants. It would theoretically have been possible to produce fully grown transgenic tobacco lines within one month.

In spite of the failed auxiliary bud transformations, numerous advances were made to improve the transformation and regeneration efficiency of tobacco leaf disks. Tobacco leaf disk transformation was pioneered by Horsch *et al.* (1985). The original protocol induced the formation of callus from transformed leaf disks, followed by indirect organogenesis of leafy shoots from callus. However, under suitable conditions, cells within an explant may start proliferating, thereby forming localized regions of cell division. These regions often become organized meristematic centers, eventually giving rise to new organs such as shoots or roots, depending on the stimulus (Brown and Thorpe, 1986). Direct organogenesis is therefore the process whereby these organs are produced directly from parental tissues such as leaf disks,

as opposed to indirect organogenesis where organs are produced from callus. The efficiency of direct organogenesis is influenced by the interactions between culture media and explants, and optimal conditions usually differ amongst diverse species of plants (Leifert, *et al.*, 1995). In cases of direct organogenesis, each meristem typically emerges from a single cell, and therefore represents a single transformation event or clonal process (Horsch, *et al.*, 1985). Chimeric plants may be produced in cases where meristems emerged from more than one parental cell, and these plants do not have a uniform genetic composition.

The phases of organogenesis witnessed in this study were similar to those in a study by Ramage and Williams (2003). During the first phase of organogenesis, explants increased in diameter. The leaf disks in our study are thought to have become hyperhydritic at this point, as the tissue became rigid, transparent, and expanded significantly as a result of the increased water content. Ramage and Williams reported the formation of callus around the cut edges of their leaf disks after 10 days. Callus formation was not observed at any time during our study. At the second phase of organogenesis, shoot meristem initiation was witnessed when discrete green lumps appeared around the cut edges of the leaf disks. Lastly, the third phase of organogenesis involved the differentiation and growth of leafy shoots on the leaf disks. In the study by Ramage and Williams, only one plant growth regulator, a cytokinin, was added to the culture media, and they were able to induce rapid organogenesis through a brief callus intermediate. In contrast, a combination of growth regulators, consisting of an auxin and a tenfold concentration of cytokinin, was used in this study and found to efficiently induce direct organogenesis.

Direct organogenesis of leafy shoots from tobacco leaf disks has previously been reported, however this was only efficiently achieved on MS2 media supplemented with nitrate, ammonia, and additional sucrose (Ramage, 2002). It was found that nitrate and ammonia affect shoot organogenesis synergistically, and that the ratio of nitrate to ammonia (70:30) was crucial for the efficient production of shoots from leaf disks. Interestingly, no additional nitrate, ammonia or sucrose was added to the MS2 media used in the current study, and a high efficiency of direct organogenesis was achieved. It is thought the hyperhydritic state of the leaf disks contributed to the efficiency of organogenesis witnessed in this study. The effects of hyperhydricity will be discussed thoroughly in a section to follow.

Regeneration of transformed shoots

In past studies, tobacco regeneration has reportedly been achieved without the use of plant growth regulators (Narvaez-Vasquez, *et al.*, 1992). This correlated with results from the current study, as a regeneration efficiency of approximately 17.5% was achieved for shoots placed on plain MS2 media. Attempts were also made to optimize the regeneration of tobacco on media containing growth regulators for the induction of rooting or elongation. The regeneration efficiency achieved in both cases was unsatisfactory. Shoots placed on rooting media dedifferentiated rapidly, forming large clumps of callus. Conversely, shoots placed on elongation media grew very rapidly to have long, unnaturally thin stems. These plants were so delicate that many of them died before being acclimatized. After being transferred from the leaf disks, all shoots placed on the rooting or elongation media had failed to root, and underwent dramatic morphological changes. Similarly, after 4 weeks of regeneration on plain MS2 media, approximately 93% of the shoots had grown into morphologically distorted plants that were no longer true to type. The rooting percentage on plain MS2 media was accordingly low. In addition, attempts to acclimatize rooted plants with an altered morphology were unsuccessful in all cases.

These results were unexpected, as growth regulators were specifically chosen to accelerate the rooting and/or elongation of the shoots. Auxin modulates the architecture of roots and shoots, vascular development, and tropic responses to light and gravity. In tissue culture, auxins are known to induce rooting from undifferentiated callus (Skoog and Miller, 1957). Auxins induce lateral root growth and the production of adventitious shoots (Zimmerman and Hitchcock, 1942). In this study, a synthetic auxin, 1-naphthalacetic acid (NAA), was used in the rooting media. This compound exerts auxin-like effects, and lateral root formation is usually induced when it is applied. Auxin rapidly induces the accumulation of at least 3 families of transcripts: *SMALLAUXIN-UP RNAs (SAURs)*, *GH3*-related transcripts, and *AUXIN/INDOLE3-ACETIC ACID (Aux/IAA)* family members. In addition to these, there is a large collection of other genes that are induced by auxin (Himanen, *et al.*, 2004). All of the auxin-induced genes appear to have an auxin-responsive element, *AuxRE*, which is a common sequence in their upstream regulatory regions.

Auxin and cytokinin levels are usually inversely proportional *in vivo*, and the application of auxin apparently inhibits cytokinin biosynthesis rapidly (Nordstrom, *et al.*, 2004). Accordingly, appropriate ratios of hormones were used in this study. Cytokinins are plant

hormones that promote cell division, differentiation, and the subsequent formation of meristematic tissues. The precise molecular mechanism and function of cytokinins remains unclear, but proposed cytokinin targets include genes affecting shoot meristem formation and genes involved in the regulation of the cell cycle (Jacqmard, *et al.*, 1994).

Gibberellins (GAs) are growth regulators that play a crucial role in plant development, and mutants that are deficient in GA are usually much shorter than wild-type plants (Hedden and Phillips, 2000). These growth regulators are not just involved in the elongation of stems, as was initially thought, but participate in the majority of plant developmental stages. GAs are present at exceptionally high levels in developing seeds of numerous species. In contrast, they are present at low concentrations in most vegetative and floral tissues. The signaling pathways involved in the regulation of GA biosynthesis have not been fully elucidated, but are thought to be highly complex due to the diverse roles of GAs in plant development.

Although the combinations of plant growth regulators used in this study have never been reported to have such negative effects on plant development or morphology, it is not fully understood how these hormones interact with one another or the plant. However, the development and morphology of regenerating plants was affected even when no growth regulators were added to the culture media. It was therefore concluded that the growth regulators may have contributed to the altered morphology of regenerating plants, but that they were not the source of the problem.

The stability of mismatched IR transgenes in Agrobacterium and N.benthamiana

Whilst the IR construct made in this study was efficiently propagated in *E.coli,* it was found that the growth rate of *Agrobacterium tumefaciens* was substantially reduced once it had been transformed with the pBC1hpCAM plasmid. It was previously concluded that the BC1 hairpin construct is stable in *E.coli* as a result of the mutations on the sense arm of the construct. However, if the secondary structure of the construct is stable in *E.coli*, it won't necessarily be equally stable in *Agrobacterium* or in plant cells. The conformation of a cruciform structure, formed as a result of an inverted repeat construct, depends on the surrounding ionic conditions (Shlyakhtenko, *et al.*, 1998). Cruciforms exist in two distinct conformations. The first has an extended conformation with an angle of approximately 180^{o} between the hairpin arms, and is known as the Y-conformation. The second, known as the X-conformation, is more compact with arms at acute angles to the main DNA strands

(Shlyakhtenko, *et al.*, 1998). The X-conformation is more stable, and its formation is reportedly favored in environments with a high ionic concentration.

Therefore, if *Agrobacterium* has a higher intracellular concentration of ions, relative to *E.coli,* the stability of cruciform structures will be increased. As a result, the destabilizing effect of the mismatched sense arm on the BC1hpCAM construct may be overcome to favor the formation of a cruciform structure in *Agrobacterium*. Cruciform structures are believed to stall DNA polymerases, which could account for the reduced growth rate of *Agrobacterium* on antibiotic media (Gebow, *et al.*, 2000). Nucleases in prokaryotes, such as SbcCD and Rus from *E.coli,* are involved in the degradation of hairpin DNA molecules like cruciforms (Sharples, *et al.*, 1994; Connelly, *et al.*, 1998). As a result, we were concerned that the inverted repeat construct had been deleted or rearranged by *Agrobacterium*. Nevertheless, results from PCR amplification and restriction digestion confirmed that the BC1 hairpin cassette construct was being propagated in *Agrobacterium,* and that the IR is intact. However, in contrast to the amplification reactions in *E.coli*, DMSO was required for successful amplification of the IR construct from *Agrobacterium.* This confirms that the internal conditions of *Agrobacterium* may counteract the stabilizing effect of the mismatches on the IR construct.

Concerns were also raised about the possible toxicity of the construct *in planta,* seeing as the BC1 hairpin cassette construct appeared to be marginally destabilized in *Agrobacterium.* Large DNA inverted repeats are known to cause genetic instability in prokaryotes and many lower eukaryotes (Gebow, *et al.*, 2000). The instability may lead to genetic rearrangements or deletions, and the full or partial deletion of inverted repeat constructs has been reported in transgenic plants (Meza, 2002).

However, if the mismatched IR constructs produced in this study are indeed stable *in planta*, the resulting siRNAs may induce off-target silencing of endogenous plant genes. If so, the off-target silencing may be responsible for the abnormal morphologies of transgenic plants encountered in this study. By comparing the genomes and transcriptomes of 25 plant species, it was recently predicted that approximately 50-70% of gene transcripts in plants could cause off-target silencing if they were used for the induction of PTGS (Xu, *et al.*, 2006). As a result, any off target silencing caused by the virus-derived BC1 hairpin construct could potentially affect numerous endogenous plant genes. The 56% cytosine to thymine mutations on the sense arm of the BC1 IR construct create a population of sense siRNAs that may be

complementary to host genes in regions where the original viral DNA was not. As a result, investigations were done to determine whether transgene integration and expression can be linked to the developmental and morphological defects encountered in this study.

Putative transformants with abnormal morphologies were randomly selected, and compared to putative transformants that were true to type. Similarly, the impact of the transgene on rooting was investigated by comparing rooted and unrooted plants. Samples were initially analyzed by doing GUS assays, and a fairly equal distribution of GUS positive, negative and chimeric plants were seen amongst the rooted and unrooted plants. Therefore, expression of the transgene cassette could not be linked to the morphology or the rooting status of the plants. Interestingly, PCR analyses on the same set of plants showed that all fourteen samples contained integrated copies of the transgene, despite being rooted, unrooted, true to type, or abnormal. Therefore, the transgene was present in all tested samples, but was not being expressed in all of the plants. This result was sufficient to rule out any contributions that the integrated transgene construct itself, or the expression thereof may have on the morphology or the rooting status of transformed plants. In addition, it was found in some instances that 'true to type' transformants would become morphologically deformed after sub-culturing on fresh media.

Seeing as it was conclusively shown that the altered morphology of the transformed plants was not caused by a genetic anomaly, the contribution of physiological conditions around the plants was investigated.

Ethylene, and its contribution to morphological defects in N.benthamiana

The morphological and developmental abnormalities encountered in this study were compared to a variety of morphological defects reported in recent literature. The morphology of our plants seemed to be consistent with that of severely hyperhydritic, or vitrified plants.

Hyperhydricity, or vitrification, is a physiological disorder that affects the morphology of plants grown *in vitro*. Characteristic features of hyperhydricity include thick, brittle stems and leaves with a glassy appearance, and generally a complete loss of the wild-type morphology (Park, *et al.*, 2004). Cells become over-engorged with water, which affects the intracellular ionic composition. Correspondingly, the chloroplast and protein contents within the vitrified tissues are reduced. The organization of leaf tissue is often severely disrupted, and palisade

cells may be completely absent whilst enlarged, vacuolated mesophyll cells are arranged around large intercellular spaces. It has also been reported that cellulose biosynthesis is reduced and disoriented, thereby contributing to the malfunction of guard cells and stomata. (Ziv, 1991). Hyperhydricity and leaf malfunction appears to be a stress response related to a high relative humidity, the use of rich culture media, hormone imbalances in the media, and generally unsuitable *in vitro* conditions (Ziv, 1991; Park, *et al.*, 2004). For example, the water potential of the medium, the relative humidity, as well as ammonia and calcium ions may contribute to either the induction or suppression of hyperhydricity (Ziv, 1991). The abnormal plant morphologies and physiological defects induced by hyperhydration can cause up to 80% losses of *in vitro* cultured plant tissues (Pacques, 1991).

Besides the physical abnormalities, the description of hyperhydricity correlates with several observations made in this study. For example, green fluorescence from GFP and red autofluorescence from chloroplasts could only be visualized under a confocal microscope, and were not visible under a high intensity ultraviolet beam. Similarly, the detection of GUS was very weak in severely hyperhydritic plants. These observations can be coupled to the reduced protein content and chloroplasts present in vitrified plants. The increased intracellular water content affects the osmolarity and electrolyte content within plant cells. Consequently, the altered intracellular ionic composition may stabilize cruciform structures (Shlyakhtenko, *et al.*, 1998). If this is the case, the mismatched IR constructs used in this study may not be stably expressed or maintained in the plant genome. In past studies, plants containing transgenes in an inverted repeat orientation have been reported to loose their transgenic phenotype due to the methylation and transcriptional inactivation of the transgene, or by the rearrangement or partial deletion if the IR (Meza, *et al.*, 2002). Therefore, for the successful application of this transformation technique as a screening tool for IR constructs, it was crucial to find the cause of hyperhydricity, and a means to prevent it from occurring during plant regeneration.

In past studies, it was suspected that ethylene may be a major inducer of hyperhydricity, as plants were observed to become vitrified at later stages of *in vitro* culture, when ethylene had accumulated excessively in the tissue culture vessels (Park, *et al.*, 2004). In a recent example, regenerating potato shoots were reportedly prone to severe vitrification. The effects of growing potato shoots in gas permeable, as opposed to sealed tissue culture vessels was investigated, and it was found that shoots grown in gas permeable vessels developed into morphologically normal plants, whereas those grown in sealed vessels became severely

vitrified (Park, *et al.* 2004). It was then proposed that ethylene accumulation in the tissue culture vessel may be responsible for the vitrification of micropropagated plant tissues. This was confirmed when potassium permanganate, an ethylene scrubber, was added to sealed tissue culture vessels. Subsequently, a low concentration of ethylene was detected inside the tissue culture vessels, and plants were observed to develop normally as a result.

These obsevations correspond to results in the current study. When incubated in sealed tissue culture vessels with potassium permanganate, the majority of transgenic tobacco shoots regained their natural morphology after 3-4 weeks. The rooting efficiency and overall regeneration procedure was significantly improved by the addition of the ethylene scrubber. It was therefore concluded that the accumulation of ethylene was responsible for the severe vitrification during the regeneration of *N.benthamiana*. Ethylene has previously been reported to have negative effects on the regeneration of various species of tobacco. For example, it was reported that ethylene reduced shoot regeneration in *Nicotiana plumbaginofolia,* and that the addition of silver nitrate, a substance used to reduce ethylene activity, correspondingly increased the efficiency of shoot regeneration (Purnhauser *et al.* 1987).

Ethylene is a gaseous hormone that affects plant development in numerous ways, ranging from the induction of fruit ripening, leaf expansion, seed germination, abscission of various organs, and senescence, to the induction or inhibition of flowering. It has been reported that ethylene production may be induced in response to environmental stresses such as wounding, flooding, or pathogen attack (Chang and Shockey, 1999). In addition, ethylene production is apparently promoted by *Agrobacterium* inoculation (Ezura, *et al.* 2000). Furthermore, increased levels of ethylene reportedly have a negative effect on the efficiency of gene transfer. Seeing as wild-type tobacco is routinely propagated on MS2 media without incidence, it is suspected that use of the supervirulent *Agrobacterium tumefaciens* strain AglI in this study may have contributed to the accumulation of ethylene in tissue culture vessels.

Seeing as ethylene is a gaseous phytohormone, it may regulate many aspects of plant morphogenesis. Depending on the plant species, ethylene has reportedly had either positive or negative effects on callus growth, shoot production, root production, and embryogenesis (Biddington 1992). Plant responses to hormones such as salicyclic acid, auxin, cytokinin, and abscisic acid may be controlled or influenced by ethylene (Guo and Ecker, 2004). The underlying interactions of ethylene with these hormones are poorly understood, and many effects of the intersecting biochemical pathways are still unknown. Reportedly, the

application of exogenous auxin enhances the production of ethylene (Morgan and Hall, 1962). Several connections between ethylene and auxin signaling pathways have been made, and there is evidence to suggest that ethylene may inhibit root growth by preventing lateral and basipetal transport of auxin (Morgan and Hall, 1962; Luschnig, *et al.*, 1998). In addition, basipetally transported auxin is required for this induction of GA_3 production (Wolfbang, *et al.*, 2004). Therefore, ethylene may affect the levels of gibberellins such as GA_3 in developing plant tissues. We can therefore deduce that the 0% rooting efficiency attained by placing transformed shoots on rooting media (containing auxin) or elongation media (containing GA_3), may have been a result of complex interactions between the growth regulators in the media and ethylene.

Potassium permanganate was successfully used to prevent ethylene accumulation. Potassium permanganate is a strong oxidizing agent, and in this study, mixed with absorptive perlite granules to ensure that a maximum surface area was covered in the saturated solution. When gaseous ethylene accumulates in the tissue culture vessel, it is readily oxidized by potassium permanganate to form ethylene oxide. This, in turn, serves as an intermediate compound, as it will react with the water in the tissue culture vessel to yield ethylene glycol. Therefore, this strategy serves to prevent the accumulation of ethylene whilst simultaneously reducing the relative humidity within a sealed tissue culture vessel.

Quantification of BC1 transcription in infected N.benthamiana

Real time quantitative RT-PCR was successfully used in this study to estimate levels of BC1 transcription in SACMV-infected tissues. In the future, this assay can be used to determine BC1 knockdown levels in transgenic *N.benthamiana*.

As expected, the pilot study on BC1 distribution showed that BC1 was transcribed at high levels in very young symptomatic leaves. This is because of meristematic tissues have cells that are rapidly growing and replicating, which is conducive to the efficient multiplication of the virus. It was encouraging however, to detect BC1 transcription in older asymptomatic tissues that were not located immediately next to a site of infection. It proves that the viral infection was initially spread systemically throughout the plant and is present in tissues that are not symptomatic. The BC1 gene product, MP (long distance movement protein), is therefore believed to be required for the efficient infection of a host plant by SACMV. The exact molecular mechanism employed by Geminiviruses to facilitate the symplastic transport

of their nucleic acids has not been fully elucidated. However, recent studies have correlated with the "double skating model" (Frischmuth, *et al.* 2007). In this model, the BV1 gene product, NSP (nuclear shuttle protein), forms a complex with the viral DNA in the nucleus, and facilitates its exportation into the cytoplasm. Once out of the nucleus, it is thought that the BC1 gene product, MP, is added onto the NSP-DNA complex as a membrane adapter for the movement into adjacent cells (Hehnle *et al.* 2004).

If efficient knockdown of BC1 is achieved by use of the constructs made in this study, they may be used to produce cassava with a high level of resistance to SACMV.

CHAPTER 4

Conclusions and Future studies

4.1 Mismatched IR constructs - present and future prospects

In the current study, mismatched inverted repeat constructs were successfully created, and they were acceptably stable in *E.coli* and *Agrobacterium*. Studies are currently underway to screen transformed *N. benthamiana* plants for stably integrated IRs. We successfully showed that the T-DNA from *Agrobacterium* was present in stably transformed plants, however this does not necessarily mean that the IR is present. Southern blotting and PCR analyses are being done in an attempt to detect the BC1 IRs. In addition, PAGE Northern blotting is going to be done in hopes of detecting siRNAs derived from the transgene. If siRNAs are being produced, it will serve as conclusive evidence that these novel mismatched IR constructs are effective alternatives to the currently available matched IR or intron-spliced hairpin systems. Whilst this study was mostly aimed at optimizing construct design and cloning, future studies will be aimed at developing an easier vector system for the fast construction of mismatched IR constructs. Numerous cloning and screening steps were necessary during this study, which increases the amount of time an expense required to produce completed constructs. Once the efficacy of the mismatched IR constructs has been conclusively proven, a two-step vector system will be designed to reduce the number of cloning and screening steps required.

Lastly, *N. benthamiana* plants containing stably integrated copies of the BC1 hairpin cassette will be challenged with SACMV. The knockdown efficiency of BC1 will be an indication as to whether the design principles outlined this study were successfully applied. If this is the case, hybrid constructs will be made against several species of cassava-infecting begomoviruses, or several ORFs of a single virus. This combinatorial RNAi strategy will facilitate the engineering of cassava with widespread resistance to begomoviruses, irrespective of the location in Africa.

CHAPTER 5

References

- Akbergenov, R. Si-Ammour, A., Blevins, T., Amin, I., Kutter, C., Vanderschuren, H., Zhang, P., Gruissem, W., Meins Jr, F. Hohn, T., Poogin, M.M. 2006. Molecular characterization of geminivirus-derived small RNAs in different plant species. Nucleic Acids Research 34: 462-471

- Allawi H.T., SantaLucia, J.Jr. 1997. Thermodynamics and NMR of Internal G,T Mismatches in DNA. Biochemistry 36:, 10581-10594

- Allem, A.C. 2002. The origins and taxonomy of cassava. In: R.J. Hillocks, J.M. Tres, and A.C. Bellotti (Eds.), Cassava: Biology, Production and Utilization. CABI Publishing, pp. 1–16.

- Argüello-Astorga, G.R., Ruiz-Medrano, R. 2001. An iteron-related domain is associated to Motif 1 in the replication proteins of geminiviruses: identification of potential interacting amino acid-base pairs by a comparative approach. Arch Virol 146: 1465–1485

- Arias-Garzon, D.I., Sayre, R.T. 2000. Genetic engineering approaches to reducing cyanide toxicity in cassava (Manihot esculenta Crantz). In: L. Carvalho, A.M. Thro and A.D. Vilarinhos (Eds.) Proceedings of the IV International Scientific Meeting Cassava Biotechnology Network (3–7 November 1998, Salvador, Brazil), EMBRAPA, Brazilia, pp. 213–221.

- Ballas, N., Citovsky, V. 1997. Nuclear localization signal binding protein from Arabidopsis mediates nuclear import of Agrobacterium VirD2 protein. Proc. Natl. Acad. Sci. USA 94:10723–10728. 43.

- Berrie, L.C., Palmer, K.E., Rybicki, E.P., Rey, M.E.C. 1998. Molecular characterisation of a distinct South African cassava infecting geminivirus. Arch Virol 143: 2253–2260

- Berrie, L.C., Rybicki, E.P., Rey, M.E.C. 2001. Complete nucleotide sequence and

host range of South African cassava mosaic virus : further evidence for recombination amongst begomoviruses. Journal of General Virology 82: 53–58.

- Berry, S., Rey, M.E.C. 2001. Molecular evidence for diverse populations of cassava-infecting begomoviruses in southern Africa. Arch Virol 146: 1795–1802

- Berstein, E., Caudy, A.A., Hammond, S.M., Hannon, G.J. 2001. Role for a bidentate ribonuclease in the intiation step of RNA interference. Nature 409: 363-364

- Biddington NL (1992) The influence of ethylene in plant tissue culture. Plant Growth Regul 11:173–187

- Briddon, R.W., Pinner, M.S., Stanley, J. and Markham, P.G. 1990. Geminivirus coat protein gene replacement alters insect specificity. Virology 177: 88–94

- Brigenti, G., Voinnet, O., Li., W.X., Ji., J.H.. 1998. Viral pathogenicity determinants are suppressors of transgene silencing in Nicotiana benthamiana. EMBO J. 17: 6739-46

- Brodersen, P., Voinnet, O. The diversity of RNA silencing pathways in plants. Trends in Genetics 22: 268-280

- Brown D.C.W., Thorpe T.A. (1986) Plant regeneration by organogenesis. In: Vasil IK (ed) Cell culture and somatic cell genetics of plants, vol 3. Academic, New York, pp 49–65

- Ceballos, H., Iglesias, C.A., Perez, J.C., Dixon, A.G.O. 2004. Cassava breeding: opportunities and challenges. Plant Molecular Biology 56: 503–516

- Cerutti, L., Mian, N., Bateman, A. 2000. Domains in gene

- Chang, C., Shockey, J.A. 1999. The ethylene-response pathway: signal perception to gene regulation. Current Opinion in Plant Biology 2: 352–358

- Chellappan, P., Masona, M.V., Vanitharani, R., Taylor, N.J., Fauquet, C.M. 2004. Broad Spectrum Resistance to ssDNA Viruses Associated with Transgene-Induced Gene Silencing in Cassava. Plant Molecular Biology 56: 601–611

- Chellappan, P., Vanitharani, R., Fauquet, C.M. 2004. Short Interfering RNA Accumulation Correlates with Host Recovery in DNA Virus-Infected Hosts, and Gene Silencing Targets Specific Viral Sequences. Journal of Virology 78: 7465–7477

- Chengguo, D., Chunhan, W., Huishan, G. 2006. Regulation of microRNA on plant development and viral infection. Chinese Science Bulletin 51: 269-278

- Chilton, M.-D., M. H. Drummond, D. J. Merlo, D. Sciaky, A. L. Montoya, M. P. Gordon, and E. W. Nester. 1977. Stable incorporation of plasmid DNA into higher plant cells: the molecular basis of crown gall tumorigenesis. Cell 11:263–271.

- Chuang, C.F., Meyerowits, E.M. 2000. Specific and heritable genetic interference by double-stranded RNA in Arabidopsis thaliana. PNAS 97: 4985-90

- Cogoni, C., Macino, G., 1999. Gene silencing in Neurospora crassa requires a protein homologous to RNA-dependent RNA polymerase. Nature 399: 166-169

- Connelly, J.C., Kirkham, L.A., Leach, D.R.F. 1998. The SbcCD nuclease of Escherichia coli is a structural maintenance of chromosomes (SMC) family protein that cleaves hairpin DNA. Proc. Natl . Acad. Sci . USA 95: 7969-7974

- Dalmay, T., Hamilton, A., Rudd, S., Angell, S., Baulcombe, D.C. 2000. An RNA-Dependent RNA Polymerase Gene in Arabidopsis Is Required for Posttranscriptional Gene Silencing Mediated by a Transgene but Not by a Virus. Cell 101: 543-553

- Dogar, A.M. 2006. RNAi dependent epigenetic marks on a geminivirus promoter. Virology Journal 3(5): 1-4

- Doyle, J.J., Doyle, J.L.1987. A rapid isolation procedure for small quantities of fresh

leaf tissue. Phytochemical Bulletin 19:11-15.

- Duckett, D.R., Murchie A.I.H., Diekmann, S., von Kitzing, E., Kemper, B., Lilley, D.M.J. 1988. The Structure of the Holliday Junction, and Its Resolution. Cell: 55, 79-89

- Eichman, B.F.,Vargason, J.M.,Mooers B.H.M., Ho, P.S. 2000. The Holliday junction in an inverted repeat DNA sequence: Sequence effects on the structure of four-way junctions. PNAS 97: 3971-3976

- El-Sharkawy, M.A. 2004. Cassava biology and physiology. Plant Molecular Biology 56: 481–501

- Escobar, R.H., Hernandez, C.M., Larrahondo, N., Ospina, G., Restrepo, J., Mun, O.Z., Tohme, J., Roca, W.M. 2005. 2005. Tissue culture for farmers: Participatory adaptation of low-input cassava propagation in Colombia. Expl. Agric. 42: 103–120

- Fagard, M., Boutet, S., Morel, J.B., Bellini, C. Vaucheret, H. (2000) AGO1, QDE-2, and RDE-1 are related proteins required for post-transcriptional gene silencing in plants, quelling in fungi, and RNA interference in animals. PNAS 97: 11651-6

- Fauquet, C.M. 2004. Editorial: The Global Cassava Partnership for Genetic Improvement. Plant Molecular Biology 56: v–x

- Fauquet, C.M.2003 Revision of taxonomic criteria for species demarcation in the family Geminiviridae, and an updated list of begomovirus species. Arch. Virol. 148, 405–421

- Fauquet, C.M., Stanley, J. 2005. Revising the way we conceive and name viruses below the species level: A review of geminivirus taxonomy calls for new standardized isolate descriptors. Arch Virol 150: 2151–2179

- Fauquet, C.M., Tohme, J. 2000. Editorial: The Global Cassava Partnership for Genetic

Improvement. Plant Molecular Biology 56: v-x

- Fire, A., Albertson, D., Harrison, S., Moerman, D. 1991. Production of antisense RNA leads to effective and specific inhibition of gene expression in C. elegans muscle. Development 113, 503–514

- Fire, A., Xu, S., Montgomery, M.K., Kostas, S.A., Driver, S.E., Mello, C.C. Potent and specific genetic interference by double-stranded RNA in Caenorhabditis elegans. Nature 391: 806-11

- Fofana, I.B.F., Sangare, A., Collier, R., Taylor, C., Fauquet, C.M. 2004. A geminivirus-induced gene silencing system for gene function validation in cassava.

- Fondong, V.N., Pita, J.S., Rey, M.E.C., de Kochko, A, Beachy, R.N., Fauquet, C.M. 2000. Evidence of synergism between African cassava mosaic virus and a new double-recombinant geminivirus infecting cassava in Cameroon. Journal of General Virology 81: 287–297

- Fontes, E.P., Eagle, P.A., Sipe, P.S., Luckow, V.A. and Hanley-Bowdoin, L. 1994. Interaction between a geminivirus replication protein and origin DNA is essential for viral replication. J. Biol. Chem. 269: 8459–8465.

- Frey, P.M., Shrarer-Hernandez, N.G., Futterer, K., Potrykus, I., Puontikaerlas, J. 2001. Simultaneous Analysis of the Bidirectional African Cassava Mosaic Virus Promoter Activity Using Two Different Luciferase Genes. Virus Genes 22: 231-242

- Frischmuth, S., Wege, C., Hulser, D., Jeske, H. 2007. The movement protein BC1 promotes redirection of the nuclear shuttle protein BV1 of Abutilon mosaic geminivirus to the plasma membrane in fission yeast. Protoplasma 230: 117–123

- Gebow, D., Miselis, N., Liber, H.L. 2000. Homologous and Nonhomologous Recombination Resulting in Deletion: Effects of p53 Status, Microhomology, and Repetitive DNA Length and Orientation. Molecular and Cellular Biology: 4028–4035

- Gevin, S.B. 2003. Agrobacterium-Mediated Plant Transformation: the Biology behind the “Gene-Jockeying” Tool. Microbiology and Molecular Biology reviews 67: 16-37

- Gevin, S.B. 2003. Improving plant genetic engineering by manipulating the host. TRENDS in Biotechnology 21: 96-98

- Giese, M.R., Betschart, K., Dale, T., Riley, C.K., Rowan, C., Sprouse, K.J., Serra, M.J. 1998. Stability of RNA Hairpins Closed by Wobble Base Pairs. Biochemistry 37 : 1094-1100

- Gleave, A.P. 1992. A versatile binary vector system with a T-DNA organisational structure conductive to efficient integration of cloned DNA into the plant genome. Plant Molecular Biology 20 : 1203-1207

- Gniadkowski, M., Hemmings-Mieszczak, M., Klahre, U., Liu, H., Filipowicz, W. 1996. Characterisation of intronic uridine-rich sequence elements acting as possible targets for nuclear proteins during pre-mRNA splicing in Nicotiana plumbaginifolia. Nucleic Acids Research 24: 619–627

- Gonzalez de-Schopke, A.E., Schopke, C., Taylor, N.J., Beachy, R.N. and Fauquet, C.M. 1998. Regeneration of transgenic plants (Manihot esculenta Crantz) through Agrobacterium- mediated transformation of embryogenic suspension cultures. Plant Cell Rep. 17: 827–831.

- Gordenin, D.A., Lobachev, K.S., Degtyareva, N.P., Malkova, A.L., Perkins, E., Resnick, M.A. 1993. Inverted DNA Repeats: a Source of Eukaryotic Genomic Instability. Molecular and Cellular Biology 13 : 5315-5322

- Gough, G. W., Sullivan, K. M., and Lilley, D. M. J. 1986. The structure of cruciforms in supercoiled DNA: probing the single-stranded charac- ter of nucleotide bases with bisulphite. EMBO J. 5, 191196.

- Grishok, A., Pasquinelli, A.E., Conte, D., Li, N., Parrish, S., Ha, L., Baillie, D.L.,

Fire, A., Ruvkun, G., Mello, C.C. Genes and Mechanisms Related to RNA Interference Regulate Expression of the Small Temporal RNAs that Control C. elegans Developmental Timing

- Guo, H., Ecker, J.R. 2004. The ethylene signaling pathway: new insights. Current Opinion in Plant Biology 7: 40–49

- Hanley-Bowdoin, L., Settlage, S. B., Orozoo, B. M., Nagar, S., and Robertson, D. 1999. Geminiviruses: Models for Plant DNA Replication, Transcription, and Cell Cycle Regulation. Crit. Rev. Plant Sci. 18: 71–106.

- Hannon, G. J. 2002. RNA Interference. Nature 418 : 244-251

- Harrison, B. D. 1985. Advances in geminivirus research. Annu. Rev. Phytopathol. 23: 55–82.

- Harrison, B.D., Zhou, X., Otim-Nape, G.W., Liu, Y. and Robinson, D.J. 1997. Role of a novel type of double infection in the geminivirus-induced epidemic of severe cassava mosaic in Uganda. Ann. Appl. Biol. 131: 437–448.

- Hebsgaard, S.M., Korning, P.G., Tolstrup, N., Engelbrecht, J., Rouzé, P., Brunak, S. 1996. Splice site prediction in Arabidopsis thaliana pre-mRNA by combining local and global sequence information. Nucleic Acids Research 24: 3439–3452

- Hedden, P., Phillips, A.L. 2000. Gibberellin metabolism: new insights revealed by the genes. Trends in Plant Science 5: 523- 530

- Hehnle S, Wege C, Jeske H (2004) The interaction of DNA with the movement proteins of geminiviruses revisited. J Virol 78: 7698–7706

- Helliwell, C., Waterhouse, P. 2003. Constructs and methods for high-throughput gene silencing in plants. Methods 30: 289–295

- Henderson, S.T., Petes, T.D., 1993. Instability of a Plasmid-Borne Inverted Repeat in Saccharomyces cerevisiae. Genetics 133: 57-62

- Himanen K, Vuylsteke M, Vanneste S, Vercruysse S, Boucheron E, Alard P, Chriqui D, Van Montagu M, Inze´ D, Beeckman T. 2004. Transcript profiling of early lateral root initiation. Proceedings of the National Academy of Science of the USA 101: 5146–5151.

- Holsters M., De Waele D., Depicker A., Messens E., Van Montagu M., Schell J. 1978. Transfection and transformation of Agrobacterium tumefaciens. Mol Gen Genet 163: 181–187

- Hood, E. E., Fraley, R. T., Chilton, M.-D. 1987. Virulence of Agrobacterium tumefaciens strain A281 on legumes. Plant Physiol. 83:529–534.

- Horsch, R. B., Fry, J. E., Hoffmann, N. L., Eichholtz, D., Rogers, S.G., Fraley, R.T. 1985. A Simple and General Method for Transferring Genes into Plants. Science, New Series, 227: 1229-1231

- Howard, E. A., B. A. Winsor, G. De Vos, and P. Zambryski. 1989. Activation of the T-DNA transfer process in Agrobacterium results in the generation of a T-strand-protein complex: tight association of VirD2 with the 5`T-strands. Proc. Natl. Acad. Sci. USA 86:4017–4021.

- Hutvagner, Gyorgy, Zamore, P.D. 2002. RNAi: nature abhors a double strand. Current Opinion in Genetics and Development 12 : 225-232

- Jacobsen, S.E., Running, M.P., Meyerowitz, E.M. 1999.Disruption of an RNA helicase/RNAse III gene in Arabidopsiscauses unregulated cell division in floral meristems. Development 126: 5231-5243

- Jacqmard A, Houssa C, Bernier G. 1994. Regulation of the cell cycle by cytokinins. In: Mok DWS, Mok MC (eds) Cytokinins—Chemistry, Activity, and Function. Boca

Raton: CRC Press. pp. 197–215

- Jarchow, E., Grimsley, N. H., Hohn, B. 1991. virF, the host-range- determining virulence gene of Agrobacterium tumefaciens, affects T-DNA transfer to Zea mays. Proc. Natl. Acad. Sci. USA 88:10426–10430.

- Jeske, H., Lutgemeier, M., and Preiss, W. 2001. Distinct DNA forms indicate rolling circle and recombination-dependent replication of Abutilon mosaic geminivirus. EMBO J. 20: 6158–6167.

- Jha, A.K., Dahleen, Suttle, J.C. 2007. Ethylene influences green plant regeneration from barley callus. Plant Cell Rep 26: 285–290

- Jin, S., Prusti, R. K., Roitsch, T.R., Ankenbauer, G., Nester, E. W. 1990. Phosphorylation of the VirG protein of Agrobacterium tumefaciens by the autophosphorylated VirA protein: essential role in biological activity of VirG. J. Bacteriol. 172:4945–4950.

- Jones, A. L., E.-M. Lai, K. Shirasu, and C. I. Kado. 1996. VirB2 is a processed pilin-like protein encoded by the Agrobacterium tumefaciens Ti plasmid. J. Bacteriol. 178:5706–5711.

- Jouanin, L., Bouchez, D., Drong, R. F., Tepfer, D., Slightom, J. L. 1989. Analysis of TR-DNA/plant junctions in the genome of a Convolvulus arvensis clone transformed by Agrobacterum rhizogenes strain A4. Plant Mol. Biol. 12:75–85.

- Kerschen, A., Napoli, C.A., Jorgensen, R.A., Muller, A.E. 2004. Effectiveness of RNA interference in transgenic plants. FEBS Letters 566 : 223-228

- Khvorova, A., Reynolds, A. & Jayasena, S. D. 2003. Functional siRNAs and miRNAs exhibit strand bias. Cell, 115, 209–216.27.

- Kong, L.J., Orozco, B.M., Roe, J.L., Nagar, S., Ou, S., Feiler, H.S., Durfee, T., Miller,

A.B., Gruissem, W., Robertson, D. and Hanley-Bowdoin, L. 2000. A geminivirus replication protein interacts with the retinoblastoma protein through a novel domain to determine symptoms and tissue specificity of infection in plants. EMBO J. 19: 3485–3495.

- Kunik, T., Tzfira, T., Kapulnik, Y., Gafni, Y., Dingwall, C., and Citovsky V. 2001. Genetic transformation of HeLa cells by Agrobacterium. Proc.Natl. Acad. Sci. U.S.A. 98:1871-1876.

- Lacroix, B., Vaidya, M., Tzfira, T., Citovsky, V. 2005. The VirE3 protein of Agrobacterium mimics a host cell function required for plant genetic transformation. EMBO J. 24 : 428–437

- Leach, D.R. 1994. Long DNA palindromes, cruciform structures, genetic instability and secondary structure repair. Bioessays 16:893-900

- Legg, J.P., Fauquet, C.M. 2004. Cassava mosaic geminiviruses in Africa. Plant Molecular Biology 56: 585–599

- Leifert C., Murphy K.P., Lumsden P.J. (1995) Mineral and carbohydrate nutrition of plant cell and tissue cultures. CRC Crit Rev Plant Sci 14:83–109

- Li, H.Q., Sautter, C., Potrykus, I. and Pounti-Kaerlas J. 1996. Genetic transformation of cassava (Manihot esculenta Crantz). Nature Biotech. 14: 736–740.

- Lily, D.M.J., Norman, D.G. 1999. The Holliday junction is finally seen with crystal clarity. Nature Structural Biology 6: 897-900

- Lindbo, J.A., Silva-Rosales, L., Proebsting, W.M., Dougherty, W.G. lnduction of a Highly Specific Antiviral State in Transgenic Plants: lmplications for Regulation of Gene Expression and Virus Resistance. The Plant Cell 5: 1749- 1759

- Lu, S., Shi, R., Tsao, C.C., Yi, X., Li, L., Chiang, V.L. 2004. RNA silencing in plants

by the expression of siRNA duplexes. Nucleic Acids Research 32 (21): e171

- Luschnig C, Gaxiola RA, Grisafi P, Fink GR: EIR1, a root-specific protein involved in auxin transport, is required for gravitropism in Arabidopsis thaliana. Genes Dev 1998, 12:2175-2187.

- Makunga, N.P., Jager, A.K., van Staden, J. 2006. Improved in vitro rooting and hyperhydricity in regenerating tissues of Thapsia garganica L. Plant Cell Tiss Organ Cult 86 : 77–86

- Maruthi, M.N., Colvin, J., Seal, S., Gibson, G. and Cooper, J. 2002. Co-adaptation between cassava mosaic geminiviruses and their local vector populations. Virus Res. 86: 71–85

- Matzke, M., Matzke, A.J.M., Kooter, J.M. 2001. RNA: Guiding Gene Silencing. SCIENCE 293: 1080-1083

- Mok, D.W.S., Mok, M. 2001. Cytokinin Metabolism and Action. Annu. Rev. Plant Physiol. Plant Mol. Biol. 52: 89–118

- Montgomery, M.K., Fire, A. 1998. Double-stranded RNA as a mediator in sequence-specific genetic silencing and co-suppression. TIG 14: 255-9

- Morgan PW, Hall WC. 1962. Effect of 2,4-dichlorophenoxyacetic acid on the production of ethylene by cotton and grain sorghum. Physiologia Plantarum 15: 420–427.

- Mourrain, P., Beclin, C., Elmayan, T., Feuerbach, F., Arabidopsis SGS2 and SGS3 Genes Are Required for Posttranscriptional Gene Silencing and Natural Virus Resistance. Cell 101: 533-542

- Murashige, T., Skoog, F. 1962. A revised medium for rapid growth and bioassays with tobacco tissue cultures. Physiol. Plant. 15, 473–497.

- Nakatsuka, T., Abe, Y., Kakizaki., Yamamura, S., Nishihara, M. 2007. Production of red-flowered plants by genetic engineering of multiple flavonoid biosynthetic genes. Plant Cell Rep : DOI 10.1007/s00299-007-0401-0

- Napoli, C., Lemieux, C., Jorgensen, R. lntroduction of a Chimeric Chalcone Synthase Gene into Petunia Results in ReversibleHomologous Genes Ín trans. The Plant Cell 2: 279-289

- Narváez-Vásquez, J., Orozco-Cárdenas, M.L., and Ryan, C.A. 1992. Differential expression of a chimeric CaMV-tomato proteinase inhibitor I gene in leaves of transformed nightshade, tobacco and alfalfa plants. Plant Mol. Biol. 20,1149-1157.

- Nordstrom A, Tarkowski P, Tarkowska D, Norbaek R, A°stot C, Dolezal K, Sandberg G. 2004. Auxin regulation of cytokinin biosynthesis in Arabidopsis thaliana: a factor of potential importance for auxin-cytokinin-regulated development. Proceedings of the National Academy of Science of the USA 101: 8039–8044.

- Pacques, M. (1991) Vitrification and micropropagation: causes, remedies and prospects. Acta Hort 289:293–290

- Padidam, M., Beachy, R. N., and Fauquet, C. M. 1996. The role of AV2 (“Pre- coat”) and coat protein in viral replication and movement in tomato leaf curl geminivirus. Virology 224: 390–404.

- Padidam, M., Sawyer, S. and Fauquet, C.M. 1999. Possible emergence of new geminiviruses by frequent recombination. Virology 265: 218–225.

- Park, S.W., Jeon, J.H., Kim, H.S., Park, Y.M., Aswath, C., Joung, H. 2004. Effect of sealed and vented gaseous microenvironments on the hyperhydricity of potato shoots in vitro.

- Pasquinelli, A.E., Reinhert, B.J., Slack, F. 2000. Conservation of the sequence and

temporal expression of let-7 heterochronic regulatory RNA. Nature 408: 86-90

- Peralta, E. G., Ream, L. W. 1985. T-DNA border sequences required for crown gall tumorigenesis. Proc. Natl. Acad. Sci. USA 82:5112–5116.

- Pilartz, M., Jeske,H. 2003 Mapping of abutilon mosaic geminivirus minichromosomes. J. Virol., 77, 10808–10818.

- Pita, J.S., Fondong, V.N., Sangare, A., Otim-Nape, G.W., Ogwal, S. and Fauquet, C.M. 2001a. Recombination, pseudorecombination and synergism of geminiviruses are determinant keys to the epidemic of severe cassava mosaic disease in Uganda. J. Gen. Virol. 82: 655–665.

- Pooggin, M.M, Hohn, T. 2004. Fighting geminiviruses by RNAi and vice versa. Plant Molecular Biology 55: 149–152

- Pooggin, M.M. 2003. RNAi targeting of DNA virus in plants. Nature Biotechnology 21 : 131-132

- Preiss, W., Jeske, H. 2003. Multitasking in Replication Is Common among Geminiviruses. Journal of Virology 77: 2972–2980

- Pruss, G., Ge, X., Shi, X.M., Carrington, J.C., Vance, V.B 1997. Plant Vira1 Synergism: The Potyviral Genome Encodes a Broad-Range Pathogenicity Enhancer That Transactivates Replication of Heterologous Viruses. The Plant Cell 9: 859-868

- Purnhauser L, Medgyesy P, Czako M, Dix PH, Marton L (1987) Stimulation of shoot regeneration in Triticum aestivum and Nicotiana plumbaginofolia tissue cultures using the ethylene inhibitor AgNO3 . Plant Cell Rep 6:1–4

- Ramage, C.M, Williams, R.R. 2002. Inorganic nitrogen requirements during shoot organogenesis in tobacco leaf disks. Journal of Experimental Botany 53: 1437-1443

- Ramage, C.M, Williams, R.R. 2003. Mineral uptake in tobacco leaf discs during different developmental stages of shoot organogenesis. Plant Cell Rep 21:1047–1053

- Ratcliff, F., Harrison, B.D., Baulcombe, D.C. A Similarity Between Viral Defense and Gene Silencing in Plants. Science 276: 1558-1560

- Ratcliff, F., Martin-Hernandez, A.M. and Baulcombe, D.C. (2001) Tobacco rattle virus as a vector for analysis of gene function by silencing. Plant J. 25, 237–245.

- Ratcliff, F.G., MacFarlane, S.A., Baulcombe, D.C. 1999. Gene Silencing without DNA: RNA-Mediated Cross-Protection between Viruses. 1999. The Plant Cell 11: 1207-1215

- Regensburg-Tuink, A. J. G., Hooykaas, P. J. J. 1993. Transgenic N. glauca plants expressing bacterial virulence gene virF are converted into hosts for nopaline strains of A. tumefaciens. Nature 363:69–71.

- Rothenstein, D. Haible, D., Dasgupta, I., Dutt, N., Patil, B.L., Jeske, H. 2006. Biodiversity and recombination of cassava-infecting begomoviruses from southern India. Arch Virol 151: 55–69

- Rubin, R. A. 1986. Genetic studies on the role of octopine T-DNA border regions in crown gall tumor formation. Mol. Gen. Genet. 202:312–320.

- Saher, S., Piqueras, A., Hellin, E., Olmos, E. 2005. Prevention of hyperhydricity in micropropagated carnation shoots by bottom cooling: implications of oxidative stress. Plant Cell, Tissue and Organ Culture 81:149–158

- Sambrook, J., Russel, D.W. 2001. Molecular cloning: A laboratory manual, the third edition, Cold Spring Harbor Laboratory Press, Cold Spring Harbor, New York, 16-42.

- Sanderfoot, A.A.,Lazarowitz, S.G. 1995. Cooperation in viral movement: the geminivirus BL1 movement protein interacts with BR1 and redirects it from the

nucleus to the cell periphery. Plant Cell 7: 1185–1194.

- Schattat, M.H., Klosgen, R.B., Marques, J.P. 2004. A Novel Vector for Efficient Gene Silencing in Plants. Plant Molecular Biology Reporter 22: 145–153

- Schroeder, S., Kim, J., Turner, D.H. 1996. GA and UU Mismatches Can Stabilize RNA Internal Loops of Three Nucleotides. Biochemistry 35: 16105-16109

- Schubert, S., Grunweller, A., Erdmenn, V.A., Kurreck, J. Local RNA Target Structure Influences siRNA Efficacy: Systematic Analysis of Intentionally Designed Binding Regions. J. Mol. Biol. 348: 883–893

- Scott, G.J., Rosegrant, M.W. and Ringler, C. 2000. Roots and tubers for the 21st century. Trends, projections, and policy options. International Food Policy Research Institute (IF- PRI)/Centro Internacional de la papa (CIP), Washington, USA, 64 pp.

- Seal, S.E. 2006. Factors Influencing Begomovirus Evolution and Their Increasing Global Significance: Implications for Sustainable Control. Critical Reviews in Plant Sciences 25: 23–46

- Semizarov, D., Kroeger, P., Fesik, S. 2004. siRNA-mediated gene silencing: a global genome view. Nucleic Acids Research 32: 3836-3845

- Serra, M.J., Barnes, T.W., Betschart, K., Gutierrez, M.J., Sprouse, K.J., Riley, C.K., Stewart, L., Temel, R.E. 1997. Improved Parameters for the Prediction of RNA Hairpin Stability. Biochemistry 36: 4844-4851

- Shapiro, R., Weisgras, J.M. 1970. Bisulfite-catalyzed transamination of cytosine and cytidine. Biochemical and Biophysical Research Communications 40 : 839-843

- Sharples, G.J., Chan, S.N., Mahdi, A.A., Whitby, M.C., Lloyed, R.G. 1994. Processing of intermediates in recombination and DNA repair: identification of a new endonuclease that specifically cleaves Holliday junctions. EMBO J. 13: 6133-6142

- Shlyakhtenko, L.S., Potaman, V.N., Sinden, R.R., Lyubchenko, Y.L. 1998. Structure and dynamics of supercoil-stabilized DNA cruciforms. J.Mol.Biol. 280: 61-72

- silencing and cell differentiation proteins: the novel PAZ domain and redefinition of the Piwi domain. TIBS 25: 481-482

- Siritunga, D. and Sayre, R.T. 2003. Generation of cyanogen-free transgenic cassava. Planta 217: 367–373.

- Skoog F, Miller CO. 1957. Chemical regulation of growth and organ forma- tion in plant tissues cultured in vitro. Symposia of the Society for Experimental Biology 11: 118–131.

- Smith, N.A., Singh, S.P., Wang, M.B., Stoutjesdijk, P.A., Green, A.G., Waterhouse, P.M. 2000. Total silencing by intronspliced hairpin RNAs. Nature 407: 319-320

- Smith, T. 1999. Holliday model of recombination. Nature Structural Biology 6: 908-909

- Stachel, S. E., Timmerman, B., Zambryski, P. 1986. Generation of single-stranded T-DNA molecules during the initial stages of T-DNA transfer from Agrobacterium tumefaciens to plant cells. Nature 322:706–712.

- Stam, M., Mol, J.N.M., Kooter, J.M. 1997. The Silence of Genes in Transgenic Plants. Annals of Botany 79 : 3–12

- Stam, M., Mol, J.N.M., Viterbo, A., Kooter, J.M. 1998. Position-Dependent Methylation and Transcriptional Silencing of Transgenes in Inverted T-DNA Repeats: Implications for Posttranscriptional Silencing of Homologous Host Genes in Plants. Moleculer and Cellular Biology 18: 6165-6177

- Stanley, J., Markham, P.G., Callis, R.J. and Pinner, M.S. 1986. The nucleotide sequence of an infectious clone of the geminivirus beet curly top virus. EMBO J. 5:

1761–1767.

- Sunter, G., Bisaro, M. 1992. Transactivation of geminivirus AR1 and BR1 gene expression by the viral AL2 gene product occurs at the level of transcription. Plant Cell 4: 1321–1331.

- Sunter, G., Hartitz, M.D., Hormudzi, S.G., Brough, C.L. and Bisaro, D.M. 1990. Genetic analysis of tomato golden mosaic virus: ORF AL2 is required for coat protein accumulation while ORF AL3 is necessary for efficient DNA replication. Virology 179: 69–77

- Tabara, H., Sarkissian, M., Kelly, W.G., Fleenor, J., Grishok, A., Timmons, L., Fire, A., Mello, C.C. 1999. The rde-1 Gene, RNA Interference, and Transposon Silencing in C. elegans. Cell 99: 123-132

- Tanaka, H., Tapscott, S.J., Trask B.J., Yao, M.C. 2002. Short inverted repeats initiate gene amplification through the formation of a large DNA palindrome in mammalian cells. PNAS 99: 8772-8777

- Taylor, N., Chavarriaga, P., Raemakers, K., Siritunga, D., Zhang, P. 2004. Development and application of transgenic technologies in cassava. Plant Molecular Biology 56: 671–688

- Thomas, C.L., Jones, L., Baulcombe, D.C., Maule, A.J. 2001. Size constraints for targeting post-transcriptional gene silencing and for RNA-directed methylation in Nicotiana benthamiana using a potato virus X vector. The Plant Journal 25: 417-425

- Thomashow, M. F., Panagopoulos, C. G.,Gordon, M. P., Nester, E.W. 1980. Host range of Agrobacterium tumefaciens is determined by the Ti plasmid. 283:794–796.339.

- Tijsterman, M., Ketting, R.F., Plasterk, R.H.A. 2002. The Genetics of RNA silencing. Annu. Rev. Genet 36: 489–519

- Tinland, B., Hohn, B., Puchta., H. 1994. Agrobacterium tumefaciens transfers single-stranded transferred DNA (T-DNA) into the plant cell nucleus. Proc. Natl. Acad. Sci. USA 91:8000–8004.

- Trench T.N, Martin M.M. 1985 An assessment of cassava African mosaic disease in South Africa and Swaziland. S Afr J Plant Soil 2: 169–170

- Trinks, D., Rajeswaran, R., Shivaprasad, P.V., Akbergenov, R., Oakeley, E.J., Veluthambi, K., Hohn, T., Pooggin, M.M. 2005. Suppression of RNA Silencing by a Geminivirus Nuclear Protein, AC2, Correlates with Transactivation of Host Genes. JOURNAL OF VIROLOGY 79: 2517–2527

- Van Nguyen, T., Thu, T.T., Claeys, M., Angenon, G. 2007. Agrobacterium-mediated transformation of sorghum (Sorghum bicolor (L.) Moench) using an improved in vitro regeneration system. Plant Cell Tiss Organ Cult : DOI 10.1007/s11240-007-9228-1

- Vanitharani, R., Chellappan, P., Fauquet, C.M. 2005. Geminiviruses and RNA silencing. TRENDS in Plant Science 10: 144-151

- Vanitharani, R., Chellappan, P., Pita, J.S., Fauquet, C.M. 2004. Differential Roles of AC2 and AC4 of Cassava Geminiviruses in Mediating Synergism and Suppression of Posttranscriptional Gene Silencing. Journal of Virology 78: 9487–9498

- Vargason, J.M., Ho, P.S. 2002. The effect of cytosine methylation on the structure and geometry of the Holliday junction: The structure of d(CCGGTACm5CGG) at 1.5 Å resolution. The American Society for Biochemistry and Molecular Biology. Article in press.

- Vecenie, C.J., Morrow, C.V., Zyra, A., Serra, M.L. 2006. Sequence Dependence of the Stability of RNA Hairpin Molecules with Six Nucleotide Loops. Biochemistry 45: 1400-1407

- Vecenie, C.J., Serra, M.L. 2004. Stability of RNA Hairpin Loops Closed by AU Base

Pairs. Biochemistry 43: 11813-11817

- Vergunst, A. C., B. Schrammeijer, A. den Dulk-Ras, C. M. T. de Vlaam, T. J. G. Regensburg-Tuink, and P. J. J. Hooykaas. 2000. VirB/D4-dependent protein translocation from Agrobacterium into plant cells. Science 290:979–982.

- Voinett, O. 2005. Induction and suppression of RNA silencing: Insights from viral infections. Nature Reviews Genetics 6: 206-220

- Voinnet, O., Baulcombe, D.C., Lederer, C. A Viral Movement Protein Prevents Spread of the Gene Silencing Signal in Nicotiana benthamiana. Cell 103: 157-167

- Voinnet, O., Pinto, Y.M., Baulcombe, D.C. 1999. Suppression of gene silencing: A general strategy used by diverse DNA and RNA viruses of plants. PNAS 96: 14147-52

- Voinnet, O., Vain, P., Angell, S., Baulcombe, D.C. 1998. Systemic Spread of Sequence-Specific Transgene RNA Degradation in Plants Is Initiated by Localized Introduction of Ectopic Promoterless DNA. Cell 95: 177-187

- Wang, M.B., Abbott, D., Waterhouse, P.M. 2000. A single copy of a virus-derived transgene encoding hairpin RNA gives immunity to barley yellow dwarf virus. Molecular Plant Pathology 1: 347-356

- Wang, M.B., Metzlaff, M. 2005. RNA silencing and antiviral defense in plants. Current Opinion in Plant Biology 8 : 216-222

- Wang, M.B., Waterhouse, P.M. 2001. Application of gene silencing in plants. Current Opinion in Plant Biology 5 : 146-150

- Wasseneger, M. 2000. RNA-Directed DNA Methylation. Plant Molecular Biology 43: 203-220

- Wassenegger, M. 2002. Gene silencing-based disease resistance. Transgenic research 11 : 639-653

- Waterhouse, P.M. Graham, M.W., Wang., M.B.1998. Virus resistance and gene silencing in plants can be induced by simultaneous expression of sense and antisense RNA. Proc. Natl. Acad. Sci. USA 95: 13959-13964

- Waterhouse, P.M., Helliwell, C.A. 2003. Exploring plant genomes by RNA-induced gene silencing. Nature Reviews Genetics 4: 29-38

- Waterhouse, P.M., Wang, M.B., Lough, T. 2001. Gene silencing as an adaptive defence against viruses. NATURE 411, 834-842

- Watson, J.M, Fusaro, A.F., Wang, M., Waterhouse, P.M. 2005. RNA silencing platforms in plants. FEBS Letters 579: 5982–5987

- Watson, J.M., Fusaro, A.F., Wang, M.B., Waterhouse, P.M. 2005. RNA silencing platforms in plants. FEBS Letters 579 : 5982–5987

- Wesley, S.V., Helliwell, C.A., Smith, N.A., Wang, M.B., Rouse, D.T., Liu, Q., Gooding P.S., Singh, S.P., Abbott, D., Stoutjesdijk, P.A., Robinson, S.P., Gleave A.P., Green, A.G., Waterhouse, P.M. 2001. Construct design for effcient, effective and high throughput gene silencing in plants. The Plant Journal 27: 581-590

- Wolbang CM, Chandler PM, Smith JJ, Ross JJ. 2004. Auxin from the developing inflorescence is required for the biosynthesis of active gibberellins in barley stems. Plant Physiology 134: 769–776.

- Woodward, A.W., Bartel, B. 2005. Auxin: Regulation, Action, and Interaction. Annals of Botany 95: 707–735

- Xu, P., Zhang, Y., Kang, Li., Roossinck, M.J., Mysore, K.S. 2006. Computational Estimation and Experimental Verification of Off-Target Silencing during

Posttranscriptional Gene Silencing in Plants. Plant Physiology 142 : 429–440

- Yanofsky, M. F., Nester E.W. 1986. Molecular characterization of a host-range-determining locus from Agrobacterium tumefaciens. J. Bacteriol. 168:244–250.

- Zamore, P.D., Tuschl, T., Sharp, P., Bartel, D.P. 2000. RNAi: Double Stranded RNA Directs the ATP-Dependent Cleavage of mRNA at 21 to 23 Nucleotide Intervals. Cell 101: 25-33

- Zhang, P., Potrykus, I. and Pounti-Kaerlas, J. 2000. Efficient production of transgenic cassava using negative and positive selection. Plant Cell Rep. 9: 405–415.

- Zhang, P., Vanderschuren, H., Fütterer, J., Gruissem, W. 2005. Resistance to cassava mosaic disease in transgenic cassava expressing antisense RNAs targeting virus replication genes. Plant Biotechnology Journal 3 : 385–397

- Zhao, M.M., An, D.R., Zhao, J., Huang, G.H., He, Z.H., Chen, J.Y. 2006. Transiently Expressed Short Hairpin RNA Targeting 126 kDa Protein of Tobacco Mosaic Virus Interferes with Virus Infection. Acta Biochim Biophys Sin 38: 22-28

- Ziv, M. 1991. Quality of micropropagated plants—Vitrification. In Vitro Cellular & Developmental Biology - Plant 27: 64-69

- Zuker, M. 2003. Mfold web server for nucleic acid folding and hybridization prediction. Nucleic Acids Research 31: 3406-15